APPENDIX J
HYDROLOGY

SPRINGBANK OFF-STREAM RESERVOIR PROJECT Environmental Impact Assessment

Volume 4: Appendices
Appendix J: Hydrology

Hydrology Technical Data Report

Prepared for:
Alberta Transportation

Prepared by:
Stantec Consulting Ltd.

March 2018

Table of Contents

LIST OF TABLES

LIST OF FIGURES

Abbreviations

AEP	Alberta Environment and Parks
AOI	area of interest
ASTM	American Society for Testing and Materials
DEM	digital elevation model
EC	electrical conductivity
FDC	flow duration curve
GPS	global positioning system
GSD	grain size distribution
HD	hydrodynamic
HEC-HMS	Hydrologic Engineering Center Hydrological Modeling System
HI	hysteresis index
HRU	hydrological response unit
HYFRAN+	Hydrologic Frequency Analysis Plus
LAA	local assessment area
LiDAR	Light Detection and Ranging
LWD	large woody debris
m asl	metres above sea level
MT	mud transport
PDA	project development area
PMF	probably maximum flood
PRISM	Parameter Regression of Independent Slopes Model

PSD	particle size distribution
RAA	regional assessment area
RL	rising limb
RTK	real time kinematic
SL	falling limb
SSC	suspended sediment concentration
ST	sediment transport
SWE	snow water equivalent
TDL	temporary diversion license
TDS	total dissolved solids
the City	City of Calgary
the Project	Springbank Off-stream Reservoir Project
TOR	terms of reference
TR1	Tributary One
TSS	total suspended sediment
VEC	valued ecology component
WSC	Water Survey of Canada

1.0 INTRODUCTION

This appendix includes information on hydrology that supports the environmental assessment for the Springbank Off-stream Reservoir Project (the Project). Specifically, the appendix:

- identifies methods used to assess potential effects of the project on hydrology
- lists data sources (e.g., historical records, field data, and relevant statistics for hydrological variables)
- describes model inputs and parameters
- explains how data was analyzed and assumptions made
- presents results of these analyses

2.0 METHODS

2.1 STUDY AREAS

Study areas for hydrology were selected at both regional and local scales to examine the potential cumulative changes to watercourses resulting from the Project and other development in the watershed. The local assessment area (LAA) extends from the diversion structure to the inlet of the Glenmore Reservoir. The LAA also encompasses the water quality modelling domain. The regional assessment area (RAA) is the Elbow River watershed, including Glenmore Reservoir (Figure 2-1). The RAA is further subdivided into two zones to better reflect the transition from the broad, low gradient Alberta Plains to the high gradient, high elevation Front Ranges of the Rocky Mountains that form the headwaters of the Elbow River. The delineation is based on the approximate location of the geological transition from the Alberta syncline to the Foothills of the eastern margin of the Cordillera (Figure 2-2).

Data collected at five key locations are used in this Appendix to characterize the hydrology of the RAA and LAA (Figure 2-2 and Table 2-1). These locations reflect key sites representative of the to the Project footprint and long-term data collection points used by the Water Survey of Canada, the City of Calgary and Alberta Environment and Parks in the Elbow River. As such, the key locations have been used to divide the Elbow River into three major sections, based primarily on the location of bridge structures that artificially control hydraulic geometry (Table 2-1). As a result, the three sections form the base measurement units for examining existing conditions and the effects of the Project on hydrology and sediment transport. Further detail on each of the key locations and the data products used/generated is provided in the following sections.

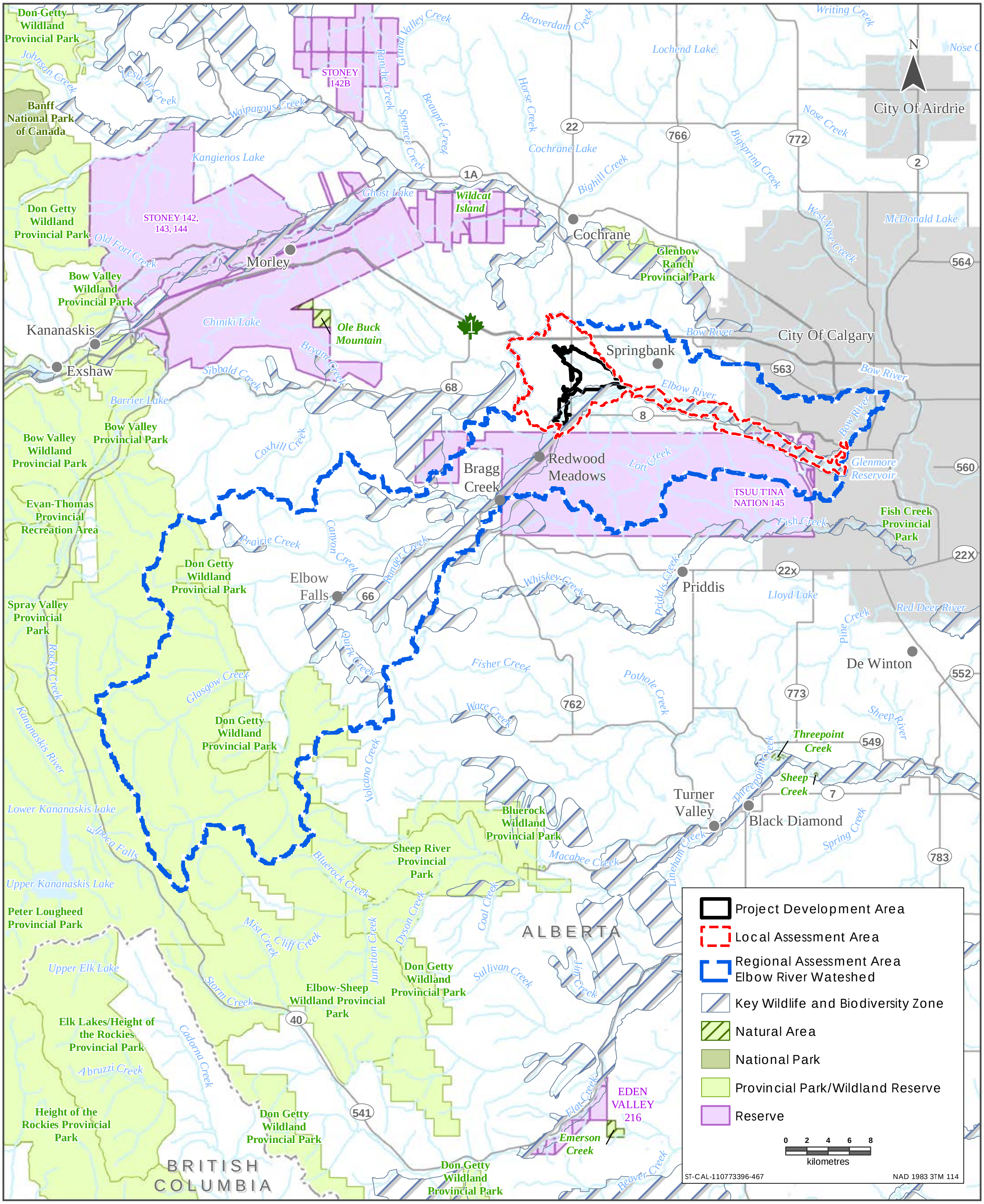

Sources: Base Data - ESRI, Natural Earth, Government of Alberta, Government of Canada
Thematic Data - ERBC, Government of Alberta, Stantec Ltd

Regional and Local Assessment Areas

Stantec

Figure 2-1

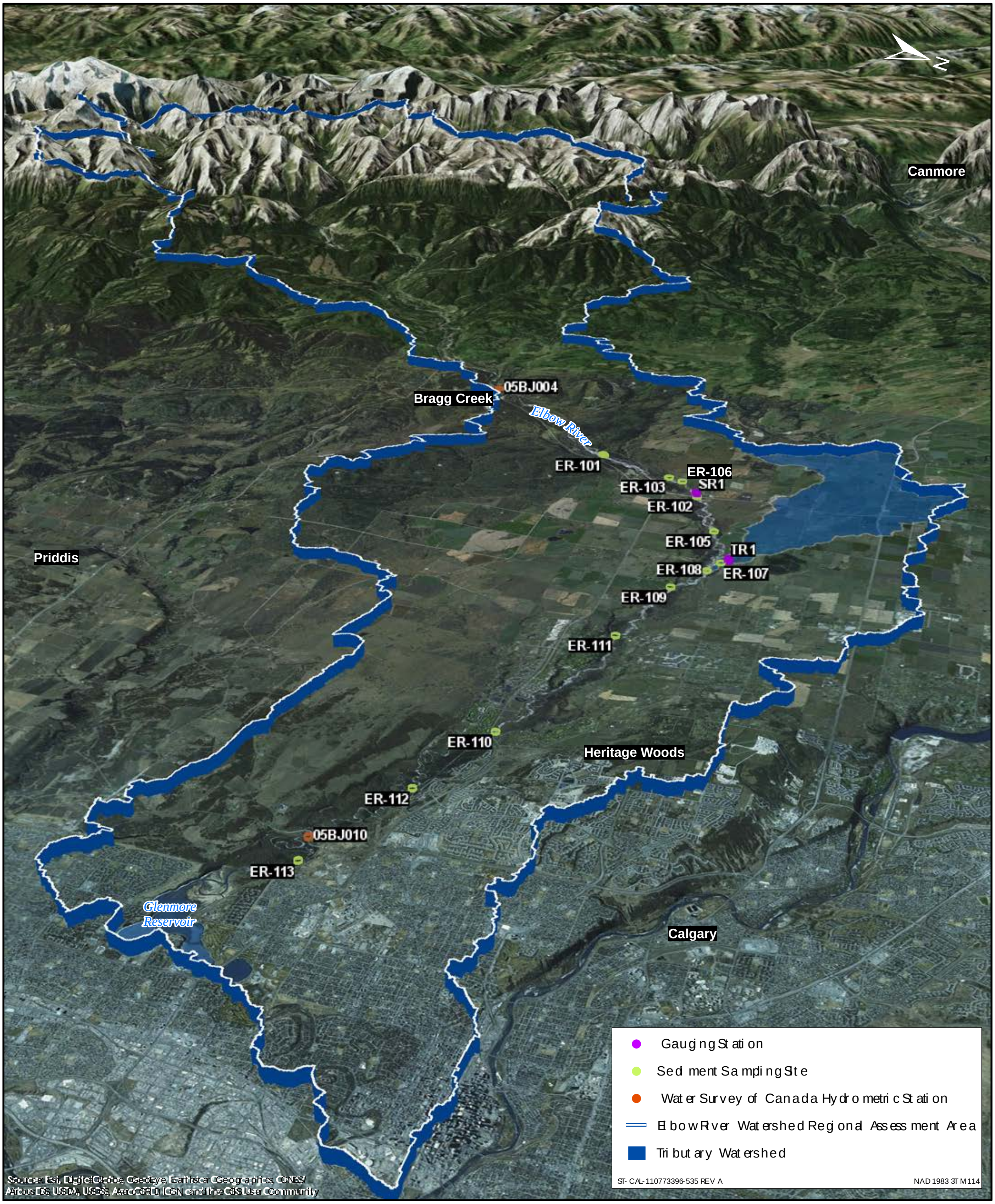

Sources: Esri, DigitalGlobe, GeoEye, Earthstar Geographics, CNES/Airbus DS, USDA, USGS, AeroGRID, IGN, and the GIS User Community

Sources: Base Data - ESRI, Natural Earth. Thematic Data - ERBC, Stantec

Elbow River Watershed Overview

Figure 2-2

Table 2-1 Summary of Sections and Key Data Collection Points in the RAA and LAA

Section	Key Site No.	Site IDs	Names	Location	Data Type	Purpose	Source
BRAGG CREEK to HIGHWAY 22 BRIDGE	1	05BJ004	Elbow River at Bragg Creek	RAA	Hydrometric Data	Hydrology	Water Survey of Canada
		N/A	Elbow River above Bragg Creek	RAA	Suspended Sediment Concentrations	Sediment Transport	City of Calgary
		AB05BJ0115	Elbow River upstream of Bragg Creek RDB	RAA	Suspended Sediment Concentrations	Sediment Transport	Alberta Environment and Parks
HIGHWAY 22 BRIDGE to TWIN BRIDGES	2	N/A	Elbow River at Highway 22 Bridge	LAA	Suspended Sediment Concentrations	Sediment Transport	City of Calgary
		SR1	Elbow River at Highway 22 Bridge	LAA	Hydrometric Data Water Quality	Hydrology Sediment Transport	Stantec
		AB05BJ0170	Elbow River at Highway 22	LAA	Suspended Sediment Concentrations	Sediment Transport	Alberta Environment and Parks
	3	TR1	Low-level outlet channel	LAA	Hydrometric Data Water Quality	Hydrology Sediment Transport	Stantec
	4	AB05BJ0290	Elbow River upstream of Twin Bridges at Highway 8	LAA	Suspended Sediment Concentrations	Sediment Transport	Alberta Environment and Parks
		N/A	Elbow River at Twin Bridges	LAA	Suspended Sediment Concentrations	Sediment Transport	City of Calgary
		AB05BJ0295	Elbow River downstream of Twin Bridges	LAA	Suspended Sediment Concentrations	Sediment Transport	Alberta Environment and Parks
TWIN BRIDGES AT HIGHWAY 8 to SARCEE BRIDGE	5	05BJ010	Elbow River at Sarcee Bridge	LAA/ RAA	Hydrometric Data	Hydrology	Water Survey of Canada
		N/A	Elbow River at Sarcee Bridge	LAA	Suspended Sediment Concentrations	Sediment Transport	City of Calgary
		AB05BJ0300	Elbow River at Sarcee Bridge	LAA	Suspended Sediment Concentrations	Sediment Transport	Alberta Environment and Parks

2.2 DESKTOP DATA

Assessing the potential effects of the Project on hydrology requires an understanding of not only flow dynamics and sediment transport but also the primary driving forces that modulate precipitation inputs and generate runoff within the Elbow River watershed. The driving forces include climate and the physical nature of the Elbow River watershed. The physical aspects include physiography, surficial geology, geological history and landcover. Included in these physical aspects is the generation and availability of sediment for fluvial sediment transport. The transfer of sediment in watersheds like the Elbow River varies in space and time and assuming connectivity, transport is a function the capacity and competency of the Elbow River and its tributaries to move sediment from sources to sinks. An understanding of sediment generation and potential dynamics is important because the Project is for flood mitigation, and diversion will affect sediment transport in the Elbow River and could result in downstream changes to morphology and sediment yield. The following sections include methods used to better understand the physical nature of the Elbow River watershed.

2.2.1 Geological Setting

Description on the geological setting of the RAA and LAA was based on published literature.

2.2.2 Climate

Two primary data sets were used to characterize general climate patterns in the RAA, using the most recent climate normal period of 1981 to 2010 as a time reference. The first data set was sourced from Alberta Environment and Parks and Environment Canada meteorological stations (Table 2-2). These data cover different time periods due to data gaps prior to 2001 for the Evan Thomas Creek and Canada Olympic Park meteorological stations. As a result, the most recent climate normal period of 1981-2010 is not covered at these stations. Spatial representativeness of meteorological stations is also difficult to assess, especially in mountainous areas. As a meteorological station represents a specific point, data recorded at that site may not be representative of the wider area due to orographic and aspect controls on precipitation distribution. These effects are important at the RAA scale given the elevation changes associated with the transition from the low gradient Plains to the high gradient topography of Elbow River headwaters. To account for this difference, the Elbow River watershed was divided into an upper and lower watershed, reflecting differences between the high gradients of the Front Ranges and the low gradient of the Plains. The demarcation between the two zones is approximately at Maclean Creek where gradients start to increase. The upper watershed having an area of approximately 812 km^2 and the lower watershed, 425 km^2.

Data on elevation influenced climate normal precipitation and air temperature data was generated using the ClimateWNA software. This software combines interpolation and elevation adjustment to downscale precipitation and air temperature data, scale free, to points of interest using a high resolution Digital Elevation Model (DEM) within the model and a Parameter Regression of Independent Slopes Model (PRISM) (Wang et al. 2006; Daly et al. 2008; Wang et al. 2012; Hamann et al. 2013). Climate data is generated from 20,000 climate surfaces of monthly, seasonal and annual climate variables from 1901 to 2009. The output from ClimateWNA has been validated against 3,353 weather stations in western North America (Wang et al. 2012).

The spatial variability in precipitation and air temperature was mapped by generating a 1 km^2 grid for the upper and lower watershed. A total of 3244 points were generated for the upper watershed and 1707 for the lower watershed. Precipitation and air temperature data were then extracted for each point using ClimateWNA. The values were then mapped and a surface fitted with the 1981-2010 climate normal monthly averages calculated using all data points in the upper and lower watershed.

Table 2-2 Key Climate Stations Relevant to the RAA and LAA

Name/Operator	Station ID	Elevation (m asl)	Latitude	Longitude	Primary Parameters	Record Length Used
Evan Thomas Creek/AEP[1]	3052D82	1,341	50.7922	-115.0522	Air temperature, precipitation	2001-2016
Little Elbow Summit/AEP	305LRKB	2,120	50.822	-114.9889	Precipitation, snow water equivalent (SWE)	1984-2016
Canada Olympic Park – Upper/EC[2]	3031875	1,235	51.0833	-114.2167	Air temperature, precipitation	2001-2016
Springbank Airport[2]	303F0PP	1,200	51.1	-114.37	Air temperature, precipitation	1981-2010[3]
Calgary International Airport/EC	3031093	1,084	51.1139	-114.0203	Air temperature, precipitation	1981-2010[4]

NOTES:

[1] Alberta Environment and Parks

[2] Environment Canada

[3] Total record length is 1961-2017. Record length used reflects the most recent climate normal period. 1981-2010

[4] Total record length is 1881-2017. Record length used reflects the most recent climate normal period. 1981-2010

Potential evaporation rates for the PDA were estimated using the Hargreaves method. This method is based on air temperature and extra-terrestrial radiation as input data. he equation for this method is given as follows (Maidment 1993):

$$E_t = a + b.\frac{1}{\lambda}.0.0023.\left(\frac{T_{max}+T_{min}}{2} + 17.8\right).\sqrt{T_{max} - T_{min}}.R_a \tag{1}$$

where T_{max} is the maximum daily air temperature in °*C*, T_{min} is the minimum daily air temperature in °*C*, R_a is the extra-terrestrial solar radiation in MJ/m^2.day. Coefficients a, and b are assumed to be 0 and 1 respectively. The extra-terrestrial solar radiation (in mm/day) for each day was estimated as follows

$$R_a = 15.392 \cdot d_r(\omega \cdot sin\phi \cdot sin\delta + cos\phi \cdot cos\delta \cdot sin\omega) \tag{2}$$

where ω is the sunset hour angle and calculated as

$$\omega = arccos(-tan\phi \cdot tan\delta) \tag{3}$$

φ (in radians) is the latitude of the gage
δ (in radians) is the solar declination angle for each day of the year, and calculated as follows

$$\delta = 0.4093 \cdot sin\left(\frac{2\pi}{365}J - 1.405\right) \tag{4}$$

where *J* is the Julian Day
and d_r is the relative distance between the Earth and the Sun given as,

$$d_r = 1 + 0.033 \cdot cos\left(\frac{2\pi \cdot J}{365}\right) \tag{5}$$

The R_a value calculated based on Equation (2) was in mm/day which was multiplied by a factor of 2.45 to convert into MJ /m^2.day (FAO 1998).

$$\lambda = 2.501 - 0.002361T_s \tag{6}$$

Where λ is latent heat of vaporization and T_s is temperature of the water surface.

Daily climate data from the Calgary International Airport was used to estimate the potential evaporation. Historical mean monthly shallow lake evaporation values calculated for Calgary International Airport were sourced from those published by the Alberta Government (2013). A ratio was created between the reported monthly values and estimated monthly. These ratios were then applied to estimate the daily evaporation values for the Project DA.

2.2.3 Basin Characteristics

The topography of the RAA was based on a combination of DEM of different spatial resolutions and data types. These DEM products were used to delineate watershed and sub-watershed boundaries; generate drainage networks; generate watershed and sub-watershed slopes and to provide the topography for the hydrodynamic and sediment transport modeling. The choice of DEM resolution was driven in part by data requirements and part by data availability. The DEM products used, resolution, source, and application are summarized in Table 2-3.

Table 2-3 Topographic Source, Data Type, Resolution/Accuracy, and Application

Source	Data Type	Resolution/Accuracy	Application	Notes
AltaLIS	LiDAR	15.0 m Bare Earth. Accuracy of 0.3 m vertical, 0.5 m horizontal	RAA/LAA, Hydrodynamic Model Domain	Used for slope characterization and watershed delineation
Government of Alberta	LiDAR	1.0 m Bare Earth	RAA/LAA, Hydrodynamic Model Domain	Flown Fall 2015
Government of Alberta	DEM	1:20 000 scale derived from photogrammetry. Relative accuracy of ± 5 m	RAA/LAA	Processed to ESRI geodatabase feature classes, exported as a 15m DEM with matching cell positions to the 15 m resolution AltaLIS LiDAR
River Forecasting Center, Government of Alberta	LiDAR	0.5 m Bare Earth. RMSEz of ± 0.088 m	Hydrodynamic Model Domain	Flown Oct 2015
Stantec	Real Time Kinematic (RTK) Survey	< 0.001 m	Improvement of elevation model in Project area	
Tarin	LiDAR	1.0 m Bare Earth, Full Feature	LAA	Flown Sept 2013/Oct-Nov 2015

The RAA encompasses the Elbow River watershed upstream from its confluence with Bow River using the Alberta Government 1:20,000 DEM as input. Upon receipt of the 15 m resolution LiDAR for a large portion of the RAA, the RAA topography was updated using a combined DEM. In the combined DEM, the 1:20 000 DEM data are used upstream of the Project and the 15 m resolution LiDAR data is used for the project area and the area downstream. The 0.5 m resolution LiDAR received from the River Forecasting Center was used primarily for the hydrodynamic and sediment transport modeling domains, where this level of accuracy was required (see Section 2.4). A 2 km buffer is imposed beyond the boundaries of the hydrology RAA and this is the revised RAA used for modelling.

A breakdown of landcover within the RAA used a hydrological response unit (HRU) analysis. This type of analysis provides context for understanding the relative influence of catchment structure on runoff response (Buttle 2006; Jensco and McGlynn 2011). HRUs are landscape units that have a similar hydrological response to a climatic input, for example, a rainfall event (Devito et al. 2005). These landscape units are defined as a combination of slope, surficial geology, and land cover because these components largely determine the magnitude and timing of the hydrological response of a watershed to precipitation or snow (Devito et al. 2005; Jensco and McGlynn 2011). Although HRU classifications can be used to statistically evaluate hydrological controls (Jensco and McGlynn 2011) or group watersheds using clustering approaches (Wilcock et al. 2004), they are presented here to identify potential runoff constraints in the RAA and LAA.

Given the high number of potential combinations of different types of surficial geology, slope and land cover, it is necessary to reduce the number of possible classifications (Table 2-4). The surficial geology was classified into specific groupings based on mapping produced by Alberta Geological Survey and the Geological Survey of Canada at scales of 1:50 000 to 1:500 000. Surficial geology was classified into three main groups: coarse, fine and bedrock. Coarse material, such as glaciofluvial material tend to have higher infiltration capacity and fine, such as glaciolacustrine, typically have reduced infiltration capacity and thus, potentially higher runoff potential.

Two categories were used to classify slope using the combined 1:20,000 and 15 m LiDAR DEM described above: greater than 10% slope and less than 10% slope. Research suggests that for greater than 10% slope, gravitational and cryogenic processes dominate, and for less than 10% slope, fluvial processes dominate (Church and Ryder 2010).

Landcover was classified into four main groups using data from the Alberta Boreal Monitoring Institute Wall-to-Wall Landcover (ABMI 2010), Alberta Boreal Monitoring Institute Human Footprint (ABMI 2012) and the Alberta Merged Wetland Inventory database (AESRD 2012). The four main groups are: alpine, forest, disturbance (includes forestry, agriculture, and urbanized areas), wetland (further divided into: bog; fen and swamp; marsh); barren land and open water.

The surficial geology, slope and landcover groups were mapped as unique HRUs and expressed as a percentage of the watershed area. For example, a unique HRU would be: Forest/Coarse Surficial Material/ Slope less than 10%.

Table 2-4 Hydrological Response Unit Classification

Category	Sub-Category	Description	Hydrological Characteristics
Surficial geology	coarse	colluvial deposits; fluvial deposits; fluted moraine; glaciofluvial deposits; ice-thrust moraine; preglacial fluvial deposits; stagnant ice moraine	Coarse-grained material typically has a high infiltration capacity that reduces surface runoff potential until that capacity is exceeded. Some fluvial and glaciogenic units will have fine material present that will reduce infiltration capacity.
	fine	eolian deposits; glaciolacustrine deposits; lacustrine deposits; organic deposits	Fine-grained surficial material has a low infiltration capacity resulting in a higher potential for surface runoff.
Slope	> 10%	slopes greater than 10% are typically dominated by gravitational and cryogenic processes	Lower infiltration capacity. High potential for surface runoff where impervious areas exist (e.g., bedrock). Rapid response to precipitation due to low depression storage.
	< 10%	slopes less than 10% are typically fluvial dominated	Moderate to higher infiltration capacity, with higher seasonal storage capacity in depression. Moderate capacity for surface runoff depending on surface depression storage capacity. Attenuated response to precipitation as determined by antecedent conditions.
Land cover: alpine	-	limited vegetation cover of trees, shrubs, and grasses. Significant areas of talus slopes (rubble), bare rock, glacial ice and snow	Moderate to high potential for surface runoff due to lower infiltration capacity. Low to moderate capacity for surface runoff depending on surface depression storage capacity
Land cover: forest	-	vegetated land cover including trees and shrubs.	Moderate to high infiltration capacity, high interception and seasonal storage capacity. Low to moderate capacity for surface runoff depending on surface depression storage capacity. Connectivity with shallow groundwater.
Land cover: disturbed	-	industrial activities, disturbance, developed cultivated, and urban land	Moderate to high potential for surface runoff due to lower infiltration capacity. Potential for altered drainage patterns affecting flow timing and magnitude.

Table 2-4 Hydrological Response Unit Classification

Category	Sub-Category	Description	Hydrological Characteristics
Land cover: wetland[a]	bog	Peat shrubby or forested wetlands raised above surrounding landscape	High water table, limited hydrologic connectivity and interflow.
	swamp/fen	Mineral and peat wetlands with sedges, shrubs and forest cover	High water tables and periodic inundation by standing or seasonal/permanent slowly moving water. Slow internal drainage by seepage. Subsurface flow may be present (shallow groundwater).
	marsh	Mineral wetlands with emergent graminoid and herbaceous vegetation	Periodically inundated by standing or slowly moving water. Subsurface flow may be present (shallow groundwater).
Barren and open water	barren	Barren areas include bedrock	High potential for surface runoff where impervious areas exist (e.g., bedrock). Low infiltration capacity.
	open water	Waterbodies	Open water has high evaporation potential and can attenuate high flow peaks. High storage capacity depending on antecedent conditions.

NOTE:

[a] Descriptions and hydrological characteristics are based on AESRD (2012)

2.2.4 Hydrology

Long term records exist for currently active Water Survey of Canada (WSC) hydrometric stations on the Elbow River and are summarized in Table 2-5. In addition to the mean daily flow for each station, hourly flow and water level (stage) data for the Bragg Creek station was obtained from the WSC for the period January 1999 to December 2016 and for March 2006 to December 2016 for the Sarcee Bridge station (Lazowski 2016, pers. comm.). Flow and stage data for 2014, 2015 and 2016 is provisional and subject to change.

Table 2-5 Active Water Survey of Canada Stations on Elbow River

Station ID	Watershed Area (km²)	Mean Daily Flow Record		Instantaneous Peak Flow Record		Hourly Flow/Stage Record		15-min Flow/Stage Record		Record
		From	To	From	To	From	To	From	To	
05BJ004 Elbow River at Bragg Creek	790.8	May 1935	Dec 2016[1]	June 1950	June 2012	Jan 1999	Oct 2016[1]	Jan 2013[1]	Dec 2013[1]	Partial
05BJ010 Elbow River at Sarcee Bridge	1189.3	April 1979	Dec 2016[1]	May 1979	June 2012	Mar 2006	Oct 2016[1]	-		Partial

NOTE:

[1] Discharge and stage data is provisional for 2014, 2015 and 2016 and subject to change

The mean daily and hourly discharge data were used to generate different hydrological metrics. For historical monthly flow volumes and variance, the mean daily flow data was used. This data was also used to generate Flow Duration Curves (FDC) for the Elbow River at Bragg Creek and Sarcee Bridge stations. An FDC is a cumulative frequency curve that shows the percent of time a specified discharge is equaled or exceeded for a given time period, in this case the period of record (Searcy 1959; Vogel and Fennessey 1995). Differences in the shape of the curve have been used to interpret the influence of basin geology/land cover on flow generation and flow characteristics (Searcy 1959). For example, the Q_{50} (discharge at the 50th percentile) represents the median flow and the ratio of the Q_{95}/Q_{50} has been used as a baseflow index (Caissie and Robichaud 2009).

Hourly resolution discharge values were used to generate suspended sediment-discharge rating curves and in the hydrodynamic sediment transport modeling. Hourly flow records are not available for Sites 2 (Highway 22) and Site 4 (Twin Bridges). As a result, hourly discharge was estimated by scaling from Bragg Creek and Sarcee Bridge stations, respectively. Scaling was applied using the single station method of Watt et al. (1989). Although this method is typically used for scaling floods, the method was applied to the hourly data on the assumption that the short transfer distances between Bragg Creek and Highway 22 (approximately 12 km) and between Sarcee Bridge and Twin Bridges (4 km) are unlikely to result in significant lag times. Comparison of the scaled data with measured data for 2015 and 2016 at Highway 22 supports this assumption as no significant lag effect was observed. Additionally, there are no significant tributary inputs with the two scaled sections. The single station scaling method of Watt et al. (1989) is calculated as:

$$x_{Tu} = x_{Tg}\left(A_u/A_g\right)^n$$

Where: x_{Tu} = the ungauged site
x_{Tg} = the gauged site
A_u = the area of the ungauged watershed
A_g= the area of the gauged watershed.

This relationship is restricted to rivers where the ratio A_u/A_g is between 0.5 and 2.0 (Watt et al. 1989). Area ratios are 1.08 and 0.89 for Bragg Creek/Highway 22 and Sarcee Bridge/Twin Bridges, respectively. The exponent n was initially estimated as 0.92 using a log-log regression between corresponding return period floods. However, this exponent resulted in overestimation of flows when compared with the measured data at Sarcee Bridge. Variations of exponents between 0.6 and 9.0 resulted in an exponent 0.8 providing the best fit between the measured data at Bragg Creek and at Sarcee Bridge, as validated by measured data at Highway 22 for 2015 and 2016.

A detailed flood frequency analysis was undertaken using peak instantaneous flows at the Bragg Creek Station for the period 1934 to 2013 and for the period 1908 to 2013 for downstream stations by Stantec (2015b) (Table 2-6). Data from the downstream stations was amalgamated into a Combined Station on the basis of minor differences in watershed area and distances between stations (Stantec 2015b). Data gaps each Bragg Creek and the Combined Station annual maximum daily and peak instantaneous flow record were infilled, where possible, using a linear or power curve relationships between annual maximum flow and peak instantaneous flow. This infilling was done either within or between the two datasets (Stantec 2015b). This approach allowed a peak instantaneous flow record to be developed for Bragg Creek and the Combined Station for the period 1908 to 2013 for use in the flood frequency analysis.

Table 2-6 Hydrometric Station Data used for Flood Frequency Analysis

Station ID	Station Name	Watershed Area (km²)	Period of Record		Percent Missing Data	Years of Acceptable Flow Data	Type of Flow
			From	To			
05BJ004	Elbow River at Bragg Creek	790.8	1934	2013	25%	59	Natural
05BJ010[1]	Elbow River at Sarcee Bridge	1189.3	1979	2013	37%	20	Natural
05BJ005[1]	Elbow River above Glenmore Dam	1220	1933	1977	0%	45	Natural
05BJ001[1]	Elbow River below Glenmore Dam	1235.7	1908	2011	2%	102	Unregulated (1908 – 1932)/ Regulated

NOTE:

[1] Downstream stations

Initial flood peak and volumetric analyses on the data for Bragg Creek and the Combined Station followed the Frequency Analysis Procedure for Stormwater Design developed by the City of Calgary (AMEC 2014). Analyses were done using10 different probability distributions fitted using the Hydrologic Frequency Analysis Plus (HYFRAN+) software with statistical testing for randomness, stationarity, homogeneity, independence, and outliers performs using the City of Calgary procedure (Stantec 2015b). Plotting of the instantaneous peak, 7-day and 56-day flow volumes on log-log paper with best fit lines fitted showed that for recurrence intervals of less than 10 years, a logarithmic equation provided the best fit and for greater than 10 years, a power curve.

2.2.5 Water Quality

Relevant water quality data for the Elbow River were sourced from Alberta Environment and Parks (AEP) water quality database and the City of Calgary (the City) water quality database (Table 2-7). Two parameters were selected were focused on: total suspended sediment (TSS) in mg/L and Total Dissolved Solids (TDS) in mg/L for the Elbow River only. TSS values of less than 5 mg/L were discarded due to detection. Other water quality parameters and sampling locations are discussed in Appendix D5 Surface Water Quality.

The TSS and TDS concentrations were used to generate TSS or TDS – discharge rating curves. These rating curves were then used to estimate long term continuous TSS and TDS concentration dataset based on available hourly or mean daily discharge records. In turn, the long-term concentration datasets were used to estimate suspended sediment and TDS sediment yields in the Elbow River watershed.

Table 2-7 Relevant Water Quality Data for the Regional Assessment Area

Site ID	Site Name	Source	Longitude	Latitude	First Year	Last Year
Elbow River Mainstem Sites						
N/A	Elbow River above Bragg Creek[a]	City of Calgary	-114.581043	50.943478	1998	2013
AB05BJ0115	Elbow River upstream of Bragg Creek RDB[a]	AEP	-114.343000	50.946390	1999	2002
N/A	Elbow River at Highway 22 Bridge[b]	City of Calgary	-114.466077	51.032861	1998	2013
SR1	Elbow River at Highway 22 Bridge	Stantec	-114.466669	51.032943	2015	2016
AB05BJ0170	Elbow River at Highway 22[b]	AEP	-114.280500	51.031940	1979	2002
AB05BJ0290	Elbow River upstream of Twin Bridges at Highway 8[c]	AEP	-114.142500	51.016670	1979	2009
N/A	Elbow River at Twin Bridges[c]	City of Calgary	-114.237602	51.013748	1982	2013
AB05BJ0295	Elbow River downstream of Twin Bridges[c]	AEP	-114.141200	51.014030	1999	2008
N/A	Elbow River at Sarcee Bridge[d]	City of Calgary	-144.165348	50.995597	1981	2015
AB05BJ0300	Elbow River at Sarcee Bridge[d]	AEP	-114.095500	50.995000	1988	1999
AB05BJ0320	Elbow River at Weaselhead Bridge[e]	AEP	-114.085000	50.991670	1999	2002
N/A	Elbow River at Weaselhead Foot Bridge[e]	City of Calgary	-114.147664	50.992120	1991	2013
Elbow River Tributary Sites						
TR1	Low-level outlet channel (unnamed tributary)	Stantec	-114.394953	51.046729	2016	2016

NOTES:

[a] Data for AEP site AB05BJ0115 Elbow River upstream of Bragg Creek RDB and the City site Elbow River above Bragg Creek were combined because the locations are close and water quality is assumed to be the same or very similar between the two sites.

[b] Data for AEP site AB05BJ0170 Elbow River at Highway 22, the Elbow River at Highway 22 Bridge, and Stantec data for the Elbow River at Highway 22 (ER H22) were combined because the locations are close and water quality is assumed to be the same or very similar between the three sites.

[c] Data for AEP site AB05BJ0290 Elbow River upstream of Twin Bridges at Highway 8, site AB05BJ0295 Elbow River downstream of Twin Bridges and the City site Elbow River at Twin Bridges were combined because the locations are close and water quality is assumed to be the same or very similar between the three sites.

[d] Data for AEP site AB05BJ0300 Elbow River at Sarcee Bridge and Elbow River at Sarcee Bridge were combined because the locations are close and water quality is assumed to be the same or very similar between the two sites.

[e] Data for AEP site AB05BJ0320 Elbow River at Weaselhead Bridge and Elbow River at Weaselhead Foot Bridge were combined because the locations are close and water quality is assumed to be the same or very similar between the two sites.

2.2.6 Sediment Yield

2.2.6.1 Suspended Sediment and Total Dissolved Solids

Suspended sediment yields were estimated using site specific suspended sediment concentration (SSC)-discharge rating curves. This approach is widely used where continuous discharge data exists but continuous SSC data does not (Gray and Simões 2008; Araujo et al. 2012). These transport curve relationships are typically defined as a power curve:

$$Q_s = aQ_w{}^{b}$$

Where

Q_s = suspended-sediment discharge in kg or tons

Q_w= water discharge in m^3/s

a = the intercept; and

b = the slope

Typical values for the slope, b, are between 1 and 2 (Knighton 1998).

Generating suspended sediment yields using a transport curve approach assumes a direct, and constant, relationship between discharge and SSC. However, this assumption is not often met due complex hysteresis relationships between SSC and discharge (Araujo et al. 2012). Hysteresis can result from activation of sediment sources at different times during a transport event; sediment exhaustion on the rising limb of an event; random bank collapse; seasonality and downstream variability in storage and release of sediment (Beel et al. 2011). As a result, SSC-discharge rating curves derived typically have considerable scatter which can result in under- and over-estimation of suspended sediment yields. It has also been demonstrated that when these curves are generated with logarithmic transformations to linearize the fit, suspended sediment yields are often underestimated (Ferguson 1986; Walling et al. 1992; Gray and Simōe 2008). In recognition of these types of biases, Ferguson (1986) proposed a bias correction factor based on the standard error of the regression equation, However, subsequent work has demonstrated that this bias correction can cause over-estimation of yields (Cohn et al. 1989). Given the lack of consensus in the literature over the validity of bias correction, none was applied in this study.

The methods used to sample suspended sediment in natural flows may also affect the concentrations measured, and subsequently the sediment yield estimates (Ashmore and Day 1988a,b). For example, the WSC standard practice is to collect a depth integrated sample and then to adjust that value to a cross-section average (Ashmore and Day 1988b). The measured value is plotted against stage and a curve fitted. The resulting curve is used to estimate a mean daily concentration which is then multiplied by the mean daily flow to generate a daily suspended sediment load. In this study, it is unknown if the samples collect by AEP and the City of Calgary were depth-integrated and/or averaged across the section. As a result, the suspended sediment concentration data is presented on the assumption that they are point sampled and that the concentrations are representative of a fully mixed cross section due to turbulence during transport events (Gurnell 1987).

The reliability of transport curve generated sediment yields is strongly influenced by the range of discharges over which suspended sediment samples are collected. Often regular suspended sediment samples collected as part of routine monitoring programs tend to reflect non-flood flows (Gray and Simões 2008). As a result, a high number of samples at low concentrations and low discharges can skew the slope and intercept of a fitted line, particularly if the variance in the samples collected is high. This skewness can result in a wide range of concentration estimates at higher discharges that may also skew interpretation of the resulting data series (Orwin at al. 2010).

In this study, we applied a group-averaging approach to minimize the influence of higher numbers of samples at low flows on the slope and intercept of the fitted curves. In this method, the arithmetic mean of all suspended sediment samples is calculated for a small range of discharge (Glysson 1987). The average of the sediment discharge is then plotted against the average observed discharge for that range and a curve fitted in logarithmic space. Discharge ranges were determined by applying the Jenks natural breaks classification method to the hourly discharge data for each site. This classification is a data clustering method designed to minimize the variance within classes and maximize the variance between classes.

Two types of suspended sediment transport curves were generated in this study using the SSC data collected by AEP and the City. The first was used to generate continuous, instantaneous suspended sediment concentrations and the second to estimate daily suspended sediment yields (tons) as a function of mean daily flow. These data were used in the sediment transport modeling and to characterize historical monthly average suspended sediment yields as well as to establish the effective discharge range for suspended sediment in the Elbow River at Sites 1,2, and 4.

The same approach was used to estimate TDS yields. TDS data was only available at Highway 22 and Twin Bridges.

2.2.6.2 Bedload

Estimates of bedload transport were based on a literature review of historic bedload measurements taken in the Elbow River near Bragg Creek.

2.2.6.3 Effective Discharge

Effective discharge is based on the concept that the amount of sediment transported by a given flow magnitude depends on the relationship between discharge and sediment load and the discharge frequency distribution (Wolman and Miller 1960; Ashmore and Day 1988b). The effective discharge is thus the frequency of the flow that cumulatively transports the highest amount of sediment load. This flow is often at a higher magnitude but is not typically associated with extreme flood flows. Although extreme flows transport significant quantities of sediment, they occur infrequently to have a significant cumulative effect on sediment yields (Knighton 1998). Thus, the effective discharge can be used to indicate under what range of flow conditions the greatest amount of sediment transport may occur.

The effective discharge has been linked to bankfull discharge which has a recurrence interval of between 1 and 2 years (Knighton 1998). This link has also been used to equate the bankfull discharge with the dominant discharge for controlling channel morphology (Andrews 1980). Wolman and Miller (1960) defined the dominant discharge as the flow that performs the most work, i.e. sediment transport, over the long term. However, as noted by Ashmore and Day (1988b), there is considerable variability in the effective discharge for sediment transport where the effective discharge for transport may not always correspond to the dominant discharge for channel morphology (Bunte et al. 2014). This discrepancy is controlled in part by hydrological conditions, flood history and difference in sediment transport thresholds. Thus, the effective discharge for bedload is often at higher magnitudes than those for suspended sediment.

Despite the debate over the links between effective discharge and dominant discharge, calculation of effective discharge, and its duration, provides useful data on streamflow regime and the nature of the sediment load (Ashmore and Day 1988b). This type of analysis is directly relevant to the proposed project during construction, dry operation and when diversion and release of flow may directly affect suspended sediment transport patterns. As a result, the effective discharge analysis was applied to the suspended sediment record for three primary reasons. First, there is a long-term data record of discrete suspended samples from the four site, second, as is it is of direct relevance to water quality and fisheries VECs and third, suspended sediment has been previously shown to dominate sediment yield in the Elbow River (Hudson 1983).

2.2.7 Surface Water Withdrawals

Data on registered surface water withdrawal licenses in the RAA was obtained from AEP in April 2017 (Yan 2017, pers. comm.). The licenses are divided into short-term (less than one year) temporary diversion licenses (TDLs) and permanent Water Act licences. Licensed volumes are not necessarily used in their entirety. The allocations were used to estimate water withdrawals within the LAA.

2.3 FIELD DATA

2.3.1 Hydrology and Water Quality

Two hydrometric monitoring locations were selected to characterize the hydrology of the LAA. One site was installed on the Elbow River at the Highway 22 bridge as this was the closest stable cross-section downstream of the proposed diversion Inlet. This site was run from April 2015 to May 2017. The second station, TR1, was installed on the low-level outlet channel to characterize the flow regime of small Alberta Plains based tributaries in the RAA. The TR1 station was located approximately 200 m upstream of the low-level outlet channel's confluence with the Elbow River. This location was chosen to minimize any potential backwater effects on stage from the Elbow River on stage if high flows were experienced during the monitoring period. The TR1 site was operational from June 2016 to May 2017.

The hydrometric installation, instrumentation, surveys and flow measurements followed federal and provincial guidelines (AENV 2006; BC MoE 2009) and industry recommended best practice (Orwin and de Pennart 2013). Water level (stage), water temperature, turbidity and electrical conductivity sensors were installed at each site. All instrumentation was connected to a Campbell Scientific CR800 or CR300 datalogger programmed to take readings every 60 s. Those values were averaged and stored every 15 minutes. Data was transmitted by to a central database hourly via cellular telemetry using Raven XT modems. Power supply for the dataloggers and modems was provided by sealed lead-acid 12V batteries recharged by solar panel.

2.3.2 Water Level and Discharge

OTT™ PLS vented pressure transducers were used to measure water level fluctuations and water temperature. These freeze-proof, vented instruments have an accuracy of 0.05% full scale (0.002 m) for water level over a range of 0-4 m and an accuracy of 0.1°C for water temperature, per accepted standards (Orwin and de Pennart 2013). The continuous water levels were converted to elevations using surveyed water levels relative to three benchmarks at each site. The benchmarks were installed according to accepted standards (Orwin and de Pennart 2013). The acceptable margin of error for benchmark elevations was ± 0.002 m and for water elevations the margin of error was ± 0.005 m. The manual water level elevations were used to adjust the continuous water levels, where necessary, to account for instrument drift. Maximum drift at the SR1 station was 0.004 m and 0.001 m for TR1. Benchmark elevation error over the field period did not exceed 0.002 m at either site. Water level relative to the benchmarks were measured contemporaneously with discharge measurements.

For flows less than 12 m^3/s, discharge was calculated using the mid-section method. Velocities were measured using a SonTek™ FlowTracker Acoustic Doppler Velocimeter. A minimum of 20 panels per cross section were used with a maximum of 10% of the total flow contained within each panel was required as a minimum standard for discharge calculation. For flows > 12 m^3/s, a River Surveyor Acoustic Doppler Current Profiler was used to calculate discharge. Compass calibration and moving bed tests were completed as per manufacturer instructions. Between 10 and 20 profiles were used to generate the average discharge during each site visit. Field visits were timed to capture as wide a range of flows at each site as possible. All field-collected discharge data were graded according to accepted standards (Orwin and de Pennart 2013).

Calculated discharge and surveyed water surface elevations were used to develop stage-discharge rating curve equations using the AQUARIUS rating curve toolbox. The rating curve equations were applied to water levels from the continuous data record to develop a continuous record of discharge. Knee bend and truss shifts were applied where necessary to account for changes in hydraulic controls during low and medium flows. These shifts reflect changes to water levels exerted by section control shifts (e.g., minor aggradation/degradation of gravel). These time transient effects have a greater impact on the stage-discharge relationship at lower flows than at high flows which are typically channel controlled. A total of 16 flow measurements were used to establish the rating curve for the SR1 station and six for TR1. Typically, a minimum of 10 flow measurements across a range of flows are required to establish a stable stage-discharge relationship, assuming stable hydraulic conditions (BC MoE 2009; Orwin and de Pennart 2013). A total of 15 manual measurements over a range of 2.5 to 24 m^3/s were used to generate the rating curve for the SR1 station and six manual measurements over a range of 0.001 to 0.581 m^3/s for TR1. All measurements were taken during 2016.

2.3.3 Bed Sediment Characteristics

A surface and sub-surface sediment sampling program was undertaken from Bragg Creek to the Weaselhead Bridge to quantify bed material gradation. This data was used to inform the hydrodynamic modeling of sediment transport, geomorphic changes and to provide information on the current particle size distribution and longitudinal variability in the Elbow River. Particle size ranges were based on Wentworth (1922) and associated stream classification on Bunte and Abt (2001) (Table 2-8).

Table 2-8 Particle Size Ranges

Particle Description		Particle Size Range (mm)	Stream Classification
GRAVEL	Boulder	256 - 4096	Boulder-bed Stream
	Cobble	64 - 256	Cobble-bed Stream
	Pebble	4 - 64	Gravel-bed Stream
	Granule	2.00 - 4	
SAND	Very Coarse Sand	1.00 - 2.00	Sand-bed Stream
	Coarse Sand	0.5 - 1.00	
	Medium Sand	0.25 - 0.5	
	Fine Sand	0.125 - 0.25	
	Very Fine Sand	0.0625 - 0.125	
SILT	Coarse Silt	0.031 - 0.0625	-
	Medium Silt	0.0158 - 0.031	
	Fine Silt	0.0078 - 0.0158	
	Very Fine Silt	0.0039 - 0.0078	
MUD	Clay	0.001-0.0039	

A number of approaches exist to sampling bed-material for particle size distribution (PSD) (Bunte and Abt 2001). In large part, the choice of sampling approach is driven by the dominant particle size where, for example, sampling in a gravel-bed stream requires both surface and sub-surface samples as the surface is often coarser than the sub-surface (Bunte and Abt 2001). Sampling these sediments can also be done using different methods including pebble counts (Wolman 1954), bulk volumetric or mass sampling (Church et al. 1987) or surface photo sieving (Detert and Weitbrecht 2013). In this study, sediment samples were sampled using bulk mass sampling for surface and sub-surface material and surface material photo sieving.

Samples were taken from 14 sites (Figure 2-2). Determination of sampling sites was based on the location of fisheries in-stream sampling for habitat (see Volume 4, Appendix M, Aquatic Ecology). However, the focus in this analysis was bar sediment as previous studies have suggested that bedload in the Elbow River, as represented by the particle size distribution of the subsurface sediment, is typically mobilized from gravel bars rather than the channel itself (Hudson 1988).

Due to logistical constraints, the sample mass to be sampled at each site was based on the D_{dom}. As sediment supply to the Elbow River is dominated by supply from mountain tributaries (Hudson 1983), the D_{dom} is approximately equivalent to the D_{90} and is typically the largest bedload size transported during more frequent flood flows (Bunte and Abt 2001). The D_{95} may be used to represent the D_{max}, particularly in uncoupled streams. The D_{max} equates to approximately the largest transportable size class (Bunte and Abt 2001). Note that the D_{max} is not the absolute largest particle size found within a reach. However, detail on the D_{95} for the Elbow River was not available prior to field work so the D_{dom} was used as a guide for minimum sample mass at each site.

The D_{dom} was determined based on a D_{90} of 78 and 68 mm for surface and sub-surface sediment, respectively. These values were based on average values from three sites upstream of Glenmore Reservoir, sampled for the City of Calgary by Klohn Crippen Berger (2016). Minimum sample mass required at each site was estimated using American Society for Testing and Materials (ASTM) C136-71 standards. The estimated minimum sample size required for a rounded surface D_{dom} of 80 mm was approximately 59 kg for surface samples and for a rounded sub-surface D_{dom} of 70 mm, 48 kg. Based on Church et al. (1987), these sample sizes indicate that the largest particle in the sample represents approximately 1-2% of the total sample. Using a sediment density of 2650 kg/m^3, volumetrically a minimum of 22 and 18 L of material was required at each site with sampling depths of approximately 16 and 14 cm for surface and sub-surface samples, respectively (Bunte and Abt 2001).

Surface and sub-surface samples were taken from each site using an approximately 1 m^2 grid. Representative sample sites at each site were determined visually before sampling. As a result, there may be operator bias towards finer fractions (Bunte and Abt 2001). All sediment was removed by hand or using a shovel. Removal of the armour layer was primarily by hand to minimize inclusion of sub-surface material. Samples were weighed and sieved on-site using 100, 63, 31.5, 16, 8 and 4 mm sieves. For sub-surface samples, the fraction less than 4 mm was retained and sent to the laboratory for further analysis using ASTM standard test methods for: Sieve Analysis for Fine and Coarse Aggregates (ASTM C136); Materials Finer than 75 µm (ASTM C117), and Particle Size Analysis of Soils (ASTM D422). All analyses were done in Stantec's Calgary geotechnical laboratory.

Photo sieving was used at each sediment sample site to augment the sieved surface sample data and to remove some of the operator bias in the manual samples by increasing the sample size. Photo sieving is a technique is based on automatic extraction of areal river bed particle size distributions from digital imagery (Graham et al. 2005; Graham et al. 2010; Strom et al. 2010). Advances in image processing algorithms and semi- and fully-automated classification approaches has resulted in photo sieving methods being as precise as traditional field methods (Graham et al. 2010). If sample areas are between 50 and 200 times that of the largest particle, percentile errors of less than 10% can be achieved (Graham et al. 2010). The automated extraction software used in this report to estimate additional grain size distributions was BASEGRAIN (v. 2.2.04) (Detert and Weitbrecht 2012; Detert and Weitbrecht 2013).

BASEGRAIN is built around a MATLAB based image processing to detect and measure grain area and related dimensions from vertical (top-view) digital photographs. The core detection algorithm automatically separates interstices from grain areas using a series of five detection steps. These steps include double grey threshold detection, gradient filtering, watershed bridging to detect edges and ellipse fitting (Detert and Weitbrecht 2012; Detert and Weitbrecht 2013). As photo sieving techniques cannot detect fine fractions (< 10 mm), these are estimated using the approach of Fehr (1987) and are user adjustable. Grain size distributions are output from the software as both Fehr's (1987) line-by-number and area-by-weight. Field/laboratory data can be input into the software for comparison. No adjustments were made to the BASEGRAIN generated grain size distributions for comparison to the field sieved data, as per Stähly et al. (2017); Kellerhals and Bray (1971), Graham et al. (2005). Images were acquired using a Nikon D7000 with a 35-mm lens and each image contained a survey stadia rod for scale. Three images were obtained at each sample location with analysis area being approximately 1 m^2. Images were processed as 10 megabyte jpegs.

2.3.4 Turbidity and Suspended Sediment Concentrations

High-frequency records of turbidity were used to provide a more detailed record of suspended sediment transfer patterns at the SR1 and TR1 stations. The OBS-3+ instruments operate in the infrared spectrum and have a backscatter geometry of between 140° and 160° (Downing 1991). Laboratory testing has shown that the OBS-3+ has a maximum sensitivity to silt and coarse clay size fractions, with reduced sensitivity to very fine and fine sands and clays (Orwin and Smart 2005) (Figure 2-3). Silt and coarse clay size fractions generally dominate the re-mobilization of glaciolacustrine and glaciofluvial source material (Gurnell 1987).

Manual grab sample of suspended sediment during different flows was used to convert the OBS-3+ turbidity data to suspended sediment concentrations. The laboratory testing of Orwin and Smart (2005) also suggests that the OBS-3+ sensor are likely to have a linear response up to approximately 2000 mg/L. However, the sensor response to sediment suspended in the water column is also determined by particle shape, colour and changing particle sizes under different flows. For example, under higher flows an increase in sand transport would result in a reduced signal from the turbidimeter relative to an apparent increase in concentration owing to the increased mass. These effects introduce error when converting turbidity to suspended sediment concentrations and when combined with discharge measurement, may lead to under- and under-estimation of suspended sediment yields (Gurnell and Warburton 1990; Ferguson 1987; Minella et al. 2008). However, the benefits of continuous data on transfer dynamics outweigh these errors (Orwin et al. 2010).

Suspended sediment yields were estimated from the converted turbidity data and discharge data. The products for the 15-minute discharge and derived concentrations were used to calculate instantaneous suspended sediment flux rates. Suspended sediment yields were given by:

$$Yield_{SS} = \sum_{i=1}^{T/\delta t} C_i \, Q_i \delta t$$

Where $Yield_{SS}$ is the total suspended yield, C_i is the estimated suspended sediment concentration (g/m^3), Q_i is discharge (m^3/s) and T and δt is time (seconds) (Ferguson 1987).

In addition to the generation of suspended sediment yields for the study period, the continuous suspended sediment concentration data was used to gain an understanding of sediment sources. During a high flow, suspended sediment being transferred through the channel will reflect a combination of sediment mobilized from the channel bed and from sediment input from extra-channel sources (Beel et al. 2011). The relative contribution will vary in time and space throughout the high flow and, as a result, the changes in relationship between suspended sediment concentration and discharge can be used to infer sediment sources (Oerung et al. 2010). This inference is made using a hysteresis analysis.

Plots of suspended sediment concentration versus discharge typically show two types of hysteresis, clockwise and anti-clockwise. Clockwise hysteresis occurs when the concentration on the ascending discharge limb is higher than for the same discharge on the descending limb. Anti-clockwise is the opposite. Clockwise hysteresis has been used to infer near field sediment sources where there is rapid depletion of sediment stored in the channel (Beel et al. 2011) or sediment mobilized from sources close to channel banks (Navratil et al. 2010). Anti-clockwise has commonly been interpreted as indicating delayed sediment input from upstream slopes (McDonald and Lamoureux 2009; Duvert et al. 2010; Beel et al. 2011). More complex hysteresis loops in a “figure-of-eight” are related to initial exhaustion followed be renewed supply later in the flow. Characterizing the direction and relative strength of hysteresis can be done using a simple hysteresis index (HI) approach.

The HI method of Lawler et al. (2006) was applied to identify the dominant hysteresis direction. This index is dimensionless and based on the ratio of a pair of SSC on the rising limb (RL) and falling limb (SL) for a standardized discharge. Two standardized discharges were used at 50% (0.5) and 75% (0.75). The great the HI value, the stronger the hysteresis. Clockwise hysteresis strength is calculated as:

$$HI = \left(\frac{SSC_{RL}}{SSC_{FL}}\right) - 1$$

For anti-clockwise, the strength is calculated as:

$$HI = \left(\frac{-1}{SSC_{RL}/SSC_{FL}}\right) + 1$$

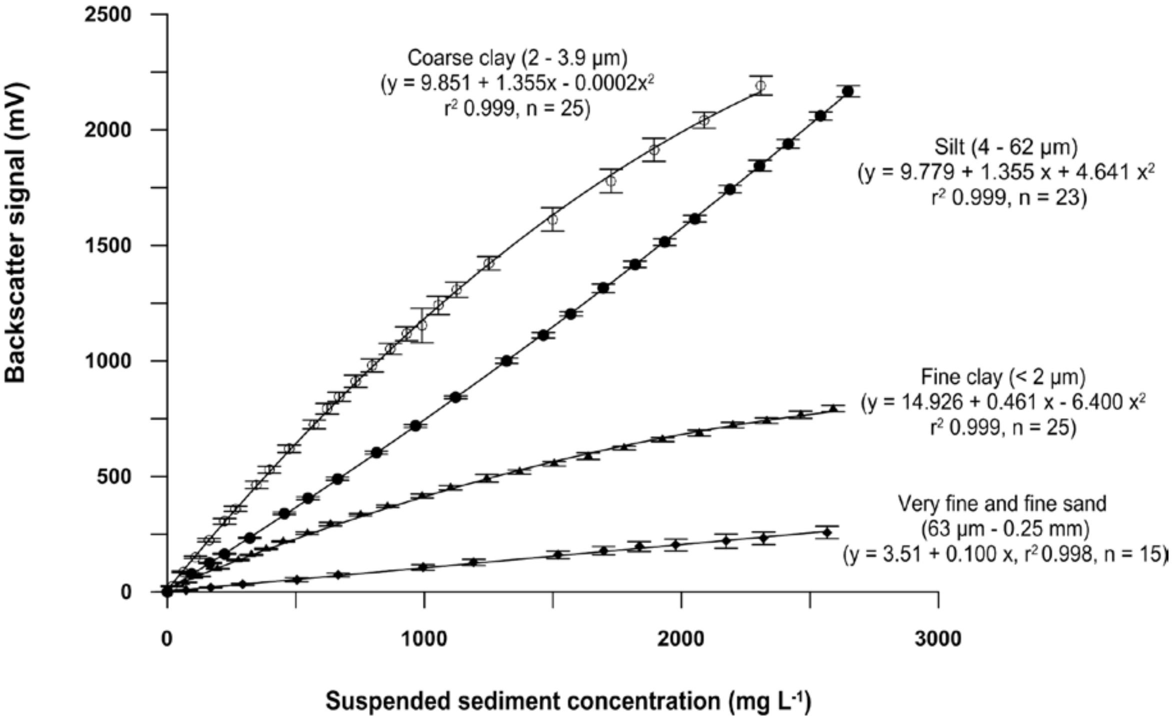

Figure 2-3 Response of the OBS-3 Turbidimeter to Different Particle Sizes

2.3.5 Electrical Conductivity and Total Dissolved Solids

Electrical conductivity (EC) was measured at both sites using a Campbell Scientific CS547A sensor. These sensors have a conductivity range of ~0.005 to 7 mS/cm and a water temperature range of 0 °C to 50 °C. Accuracy of the conductivity sensor is ±5% of the reading over a range of 0.44 to 7 mS/c. Temperature accuracy is typically less than 0.1 °C. Conductivity was measured as specific conductivity, temperature compensated to 25 °C, in µS/cm. Total dissolved solids (TDS) in mg/L was estimated by applying a multiplier of 0.55 to the EC values, as per the manufacturer's recommendation.

All logger collected data were within the AQUARIUS™ hydrometric software environment. AQUARIUS is a standalone water data management and analysis tool used by the Water Survey of Canada and the U.S. Geological Survey for their respective national hydrology monitoring programs. The software provides secure data storage and robust analytical and data correction capabilities. This software was used throughout the data production process, including the development of stage-discharge rating curves. Statistical analyses and composite data production (e.g., suspended sediment yields) were undertaken using custom coding and packages within the *R*Studio® environment.

2.3.6 Ice Dynamics

Current ice dynamics in unmodified and modified sections of the Elbow River was assessed using a semi-quantitative approach. This data was used to assess the potential for ice jam effects post-construction of the Project elevating upstream water levels, as compared to unmodified sections. The assessment is semi-quantitative as it is based on limited field observations with no modeling undertaken due to lack of available data.

The primary basis of the ice dynamics assessment was repeat surveys of selected cross sections. Three cross sections were chosen for ice thickness monitoring over the course of the 2016/2017 winter. One cross section was surveyed at the proposed diversion site. This cross-section is currently unmodified. The remaining two cross-sections were located immediately upstream of the Highway 22 bridge. The Highway 22 bridge abutment influences these two cross-sections by confining the main channel of the Elbow River between the northern abutment and the middle bridge pier. Thus, the Highway 22 cross sections were assumed as an analog for the proposed project structures. The bottom bathymetry of each cross section was surveyed in December 2016, immediately prior to freeze-up. Point spacing was approximately 0.3 – 0.4 m. Top-of-ice and through augered holes bottom-of-ice measurements were repeat surveyed in January, February and March of 2017. The winter survey points were within ± 0.05 m of the original bathymetry coordinates. A Trimble R10 dome with a TSC3 controller global positioning system (GPS) was used for all surveys. This setup gives horizontal accuracies of 0.014-0.060 m and vertical accuracies of 0.018-0.070 m. All data was corrected to the HPN ASCM 425603 control point.

Supplementary data on the timing of ice formation and decay was also used in the assessment. Continuous pressure transducer measurements from the SR1 station hydrometric station provide a record of water levels under the ice cover. A remote camera installed underneath the Highway 22 bridge provided visual data on ice dynamics during freeze-up and breakup. Images were taken hourly from 0700 h to 1800 h.

2.4 HYDRODYNAMIC MODELLING APPROACH

Modelling contemporaneous hydrodynamics and sediment transport is a computationally complex process that involves the numerical solution of one or more equations of continuity, momentum, and energy of fluids as well as sediment continuity (Papanicolaou et al. 2008). The choice of model reflects the primary problem or question being asked, knowledge of the system and data availability (Simões and Yang 2006). The model itself should capture all the dominant processes occurring in the system to be modeled, as balanced by model complexity, processing times and data availability. It should be recognized that there is no universal model and all models have specific strengths and limitations (Simões and Yang 2006). In the context of this assessment, the model output also needs to satisfy data and informational requirements of other Valued Ecology Components (VECs). These VECs include hydrogeology, water quality, aquatics and vegetation. These requirement place limitations on suitable modeling approaches and platforms.

As the focus of this assessment is on the spatial and temporal changes in the flows and water levels and changes in sediment erosion, suspension, transport, and deposition of multiple size fractions in different aquatic environments, a 2D modeling approach was applied. In this application, 2D modeling has several advantages over a 1D model. As a 2D model is mesh based, the mesh network, if based on, for example, LiDAR, better represents large spatial areas and subtleties in floodplain topography than surveyed cross-sections used in 1D models. As a result, 2D models can simulate complex flow structures and recirculating zones (Benjankar et al. 2015). Representing this complexity is important as both flow and transport of cohesive and non-cohesive sediment in river, canal and reservoir environments is required for this assessment.

DHI Water and Environment’s software, MIKE21™, a 2D hydrodynamic numerical model that simulates vertically homogenous flow and sediment transport was used to assess the potential changes in flow and sediment transport due to the Project operation. MIKE21 is based around several modules that are used to simulate hydrodynamic and sediment transport processes within different aquatic systems. Although originally design for coastal environments, MIKE21 can also be applied to river, reservoir and lake systems (DHI 2005; Morianou et al. 2016). The ability to simulate multiple aquatic environments is key in this assessment as both riverine systems and a reservoir require contemporaneous modeling. This diversion of flow and sediment from a river to a reservoir introduces additional complexity where simultaneous transport of non-cohesive and cohesive sediment, current dynamics and deposition within the diversion canal and the reservoir need to be modeled whilst maintaining non-diverted flow downstream. A flexible mesh system is required to better define the hydraulic structures, sand bars, back channels, and shoreline features. As a result, specialist river hydraulics and morphology modules, such as MIKE21C, would not provide the required flexibility in this context. The proposed MIKE 21 model for the hydrology assessment was based on coupling of the Hydrodynamic (HD), Mud Transport (MT) and Sediment Transport (ST) modules.

The HD module simulates unsteady flow considering density variations, bathymetry and external forcings in rivers, lakes, estuaries and coastal areas. The modelling system is based on the numerical solution of 2D incompressible Reynolds averaged Navier-Stokes equations subject to the assumptions of Boussinesq and of hydrostatic pressure. Thus, the model consists of continuity, momentum, temperature, salinity and density equations and it is closed by a turbulent closure scheme. The HD module features with modelling hydraulic structures which are usually smaller in dimension than the element sizes, including weir, culvert, dike, gate, pier and turbine. The HD module is the basic computational component of the MIKE modelling system and can be extended to simulate reciprocal interactions among flows, sediment transport and particle dispersion by coupling with the other modules in an add-on manner.

The MT module simulates the erosion, transport, settling and deposition of cohesive sediment (silts and clays) in marine, brackish and freshwater environments. The MT module also takes into account fine-grained non-cohesive material (sand/gravel). The MT module is an add-on module to the HD module. The main features of the MT module are multiple sediment fractions, multiple bed layers, flocculation, hindered settling, inclusion of non-cohesive sediments, bed shear stress, consolidation, morphological update of bed and tracking sediment spills. A major advantage of the MT module is the ability to model transport, dispersion and settling of three sediment size fractions, in this application silt, sand and gravel. Although this ability introduces additional computational complexity, it does provide a more realistic estimate of sediment transport patterns. As a result, the primary application of the MT module was to estimate the transport patterns of primarily silt and sand size fractions in the Elbow River, the diversion channel, through the reservoir into the low-level outlet channel and back into Elbow River. Sediment depth and extent of deposition in the reservoir is estimated using this module. The governing equations of the MT module are based on Mehta's method (Mehta et al., 1989)

The ST module simulates the sediment transport capacity, initial rates of bed-level changes and the morphological changes of non-cohesive sediment (sand and gravels). Like the MT module, the ST module is an add-on to the HD module. The primary advantage of the ST module is its ability to track, with full dynamism, bed level changes by adjusting for changes in shear stress from the mean flow using helical flow (DHI 2007). This ability allows for calculation of morphological changes at each time step based on sediment transport rates. In this application, the Meyer-Peter and Müller (1948) bedload transport equation was used. The dimensionless bed-load transport rate, Φ_b, is calculated as (DHI 2007):

$$\Phi_b = 8(\theta' - \theta_c)^{1.5}$$

with

$$\Phi_b = \frac{q_b}{\sqrt{(s-1)gd^3}}$$

where θ' is the Shields parameter related to skin friction and θ_c, is its critical value, s is the relative density of the bed sediment, g is acceleration due to gravity and d is grain size. In the model in the application here, d was defined as the median grain size (d_{50}) based on measurements collected from the Elbow River in 2016.

The combination of the MT and ST modules provides the necessary flexibility required to estimate project effects on sediment transport. This model module combination also provides data on estimated geomorphic changes in river bed(s) due to project implementation. The application of this modelling approach also allows generation of data to address stakeholder concerns on sedimentation distribution and depths in the reservoir. However, modelling the bed morphology changes in Elbow River, low-level outlet channel simultaneously with suspended sediment transport in Elbow River, reservoir and low-level outlet channel is constrained by data availability and computational limitations within each of the MT and ST modules.

The MIKE 21 coupled model was implemented using a flexible mesh (FM), which breaks down the Elbow River domain into discrete cells of finite volume, within which flow and transport equations are independently calculated. Specifically, in the horizontal plane, an unstructured grid is used, comprised of triangular and quadrilateral elements. The FM was based on a combination of elevation products but with a primary reliance on two LiDAR derived bare earth data flown in the fall of 2015 (see Section 2.2 for more detail). As a result, the combined DEM used to generate the FM and upon which the hydrodynamic and sediment transport modeling was applied represent the active floodplain topography of the Elbow River after the 2013 flood. Thus, the locations of sediment erosion and deposition and water extents will differ from that immediately observed after the 2013 flood. To maximize computational efficiency, the spatial density of the FM was also varied, depending on the necessity for higher, or lower, resolution within the modeling domains.

2.4.1 Modeling Domains

The overall model domain includes an approximately 37-km reach of Elbow River from Bragg Creek to Glenmore Reservoir and the entire Glenmore Reservoir. The upstream boundary is defined by the WSC Station 07BJ004 Elbow River at Bragg Creek and the downstream boundary at the hydraulic control outlet structures of Glenmore Dam. To facilitate the modeling, the overall domain was divided into three sub-domains:

- Elbow River

  The mesh arrangement was optimized to establish smooth boundaries and higher resolutions in areas of interest. Small elements were typically used in areas more detail is required, while larger elements were used in flat and open areas. The resolution of the model in space and time was selected with respect to numerical stability, and the mesh was optimized based on the level of details required and the amount of computational time necessary to run the model. This model domain generated contains 12,388 nodes and 20,579 elements, with mesh resolution varying from meters to tens of meters where fine meshes were applied in the surrounding areas of hydraulic structures and the areas of interests.

- diversion control structure and channel, reservoir and dam outlet

  This model domain contains 6,542 nodes and 11,183 elements, with similar mesh resolution settings as in the Elbow River domain.

- low-level outlet channel

  This model domain contains 9,858 nodes and 18,897 elements. To better describe the presence of low-level outlet channel, finer meshes in order of 2 m to 3 m were applied along the length.

Flow and sediment transport data output from each sub-domain was used as input into other sub-domains. For example, output from the Elbow River sub-domain was used as the input into the diversion canal and output from this sub-domain at the low-level outlet is used as the input into the low-level outlet channel sub-domain and back into the Elbow River sub-domain. Cumulative computational time for the three sub-domains was a total of four months from May 1 to August 31. The combination of input-output data from the three domains was generated for three floods.

2.4.2 Modelled Floods

Three floods are modelled: 1:10 year, the 1:100 year and the design floods. The 1:10 flood is the minimum flow that the Project can actively divert and the design flood is based on the 2013 flood (Stantec 2015). It is important to note here that the conceptual design flood that was used to estimate water retention volumes is based directly on volumes derived from the estimated hydrograph at Glenmore Reservoir, not at Bragg Creek. The estimated hydrograph at Glenmore Reservoir was the only data available at the time of the conceptual design (Stantec 2015a). However, to maximize realism for the floods used in this modelling, the hydrographs recorded by the WSC at Bragg Creek are used as the upstream boundary condition, where possible.

To further maximize the accuracy and dynamism of the model, hourly data is required to provide enough temporal resolution to capture the full detail of flow fluctuations during high flows. Capturing flow fluctuations at this resolution reduces the effect of under- or over-estimation of sediment transport if, for example, mean daily values were used (Orwin et al. 2010). The high flow hydrographs used in each flood are based on hourly discharge and water level data collected by the WSC for station 07BJ004 Elbow River at Bragg Creek and station 07BJ010 Elbow River at Sarcee Bridge. The hourly data was available for the period 1999 – 2016 for the Bragg Creek Station and the period 2006 – 2016 for the Sarcee Bridge station. The discharge data supplied by the WSC for 2014 – 2016 period is currently provisional and subject to change (Lazowski 2016, pers. comm.). To maintain consistency, the discharge and water level data used in each flood was sourced from the common period of record, 2006 – 2016.

Using the flood frequency analysis results presented by Stantec (2015b), peak flows at the proposed diversion site were estimated at approximately 200 m^3/s, 765 m^3/s and 1,150 m^3/s for the 1:10 year flood, 1:100 year flood and design flood, respectively. Using the hourly flow data from the WSC Bragg Creek station, a single peaked, high flow in 2008 had an hourly peak of approximately 202 m^3/s at 2100 h on May 24th with the instantaneous peak of approximately 204 m^3/s at 2130 h. The 2013 design flood had an hourly peak of approximately 1159 m^3/s at 1200 h on June 20th with the instantaneous peak of approximately 1170 m^3/s at 1116 h at Bragg Creek. Based on available estimates, a peak flow at Bragg Creek of 1150 m^3/s has a recurrence interval of approximately 230 years (Stantec 2015b). As a result, the hourly hydrographs from these floods were used as the best representation of the approximate 1:10 year flood and the 2013 flood in the model. However, the 1:100 year flood peak flow of 765 m^3/s has not occurred within the common data period or in the 1999 – 2016 hourly data set for Bragg Creek.

The initial hourly hydrographs for the 1:100 year flood at Bragg Creek and Sarcee Bridge were generated using the Hydrologic Engineering Center Hydrological Modeling System (HEC-HMS) model designed by the US Army Corps of Engineers. HEC-HMS computes runoff excess through estimating the amount of rainfall lost to infiltration and subtracting these values from precipitation. The HEC-HMS model was originally built and calibrated for the entire natural Elbow River watershed as part of a probably maximum flood analysis (PMF) by Stantec (2015c).

In the PMF analysis, the Elbow River watershed was divided into 11 sub-watersheds based on topography, landcover, geology and watercourse length/gradient (Stantec 2015c). Initial loss of 20 mm was applied to all sub-watersheds with a constant loss rate of 6 mm/hour. Transformation of the runoff excess to a volumetric time series was based on a unit hydrograph approach, with lags estimated for each sub-watershed. The resulting volumes were routed through channels using a kinematic wave method for smaller tributaries and the Muskingum method for between Bragg Creek and Glenmore Reservoir (Stantec 2015c). Baseflows were estimated as either 1 m^3/s or 27 m^3/s, depending on sub-watershed size.

Estimated precipitation for the 1:100 year flood, 24-hr antecedent rainfall event was used to generate the 1:100 year hydrographs for Bragg Creek and Sarcee Bridge (Stantec 2015c). The resulting hydrographs approximated the peak and 7-day volume estimated through flood frequency analysis (Stantec 2015b). The underlying assumption of this runoff generation approach is that the precipitation is uniform across all sub-watersheds. The resulting hourly estimates were then extended by blending the recession curve with the 1:10 (2008) data to provide a dataset that extended through both the diversion and release of water from the reservoir and provided an approximate match to the 56-day volume estimated through flood frequency analysis (Stantec 2015a,b). No further rainfall floods are assumed in the extension of the 1:100 year flood and no tributary input.

The HEC-HMS PMF model was also used to estimate tributary inflows between Bragg Creek and Sarcee Bridge for the design flood and 1:10 year flood. These flow inputs were generated using measured or estimated rainfall data applied to all watersheds with input hydrographs extracted for each sub-watersheds. These three sub-watersheds represent discharge input to the Elbow River between the upstream and downstream boundaries of the model. Tributary flow inputs were estimated for the 1:10 year flood over the Elbow River watershed using Thiessen polygon interpolation from 11 climate stations with rainfall data during 2008. Precipitation for the design flood was based on a gridded dataset developed as part of the PMF study. The timing/lag of discharge input into the Elbow River was maintained within the MIKE21 model. Validation of the modeled tributary inputs was based on the increase in total volume between measured data at the WSC Bragg Creek and Sarcee Bridge stations over 7 and 56 day periods, where possible.

The resulting hydrographs for the 1:10 year, 1:100 year and design floods modeled for diversion are shown in Figure 2-4.

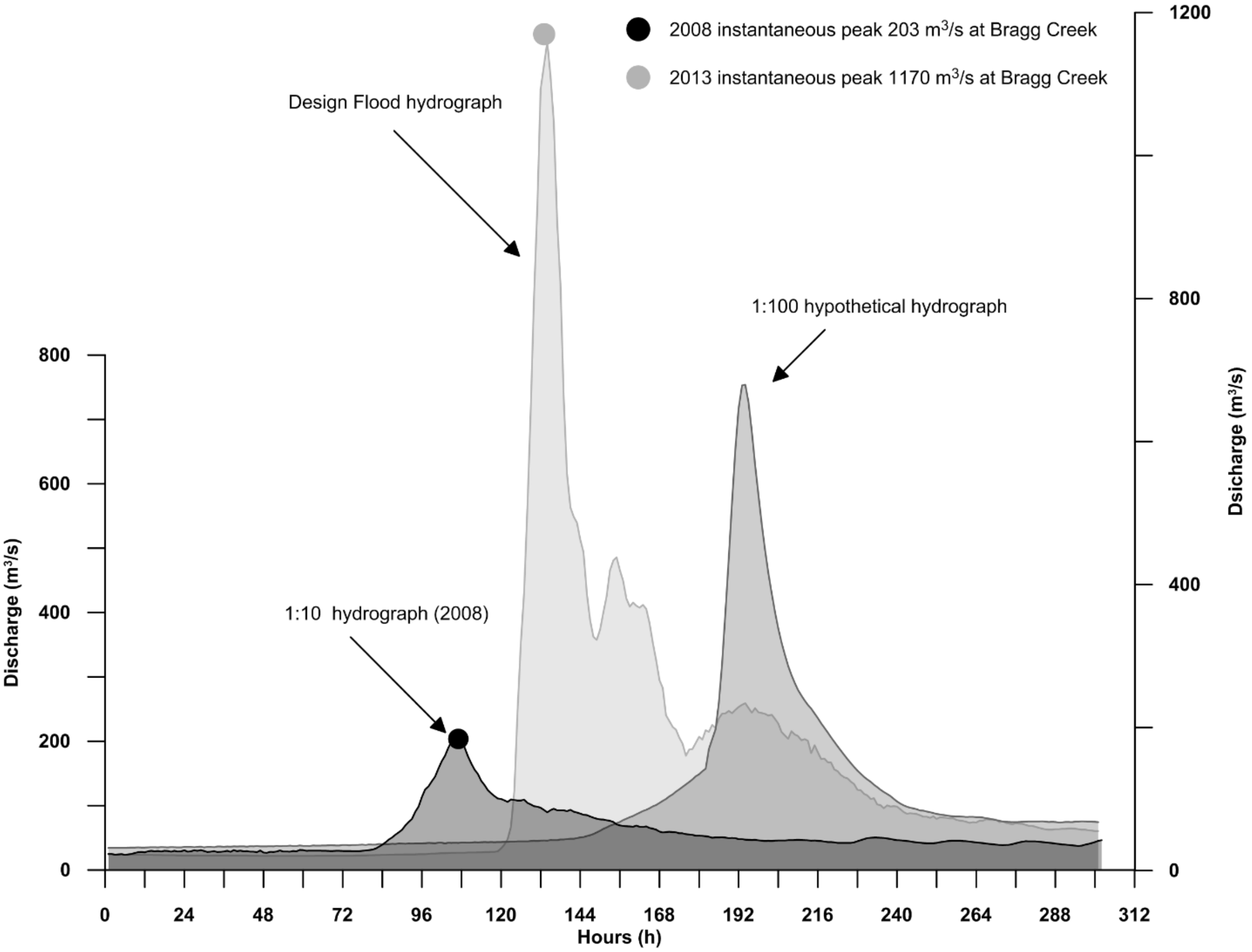

Figure 2-4 1:10 Year, 1:100 Year and Design Flood Hydrographs used in Modelling

A comparison between the peak instantaneous flows, 7- and 56-day volumes used in the floods and the flood frequency estimates are summarized in Table 2-9.

Table 2-9 Flow and Volume Estimates at Bragg Creek and Sarcee Bridge for Modelled Floods

Flood	peak flow (m^3/s)	7-day volume (dam^3)	56-day volume (dam^3)	FFA peak flow (m^3/s)	FFA 7-day volume (dam^3)	FFA 56-day volume (dam^3)	peak flow (%)	7-day volume (%)	56-day volume (%)
1:10 year, Bragg Creek	205 [1]	44,829 [1]	172,600 [1]	200	52,700	199,000	2.4	-17.6	-15.3
1:100 year, Bragg Creek	754	105024	281763	755	105,000	282,000	-0.1	0.0	-0.1
Design flood, Bragg Creek	1,159 [1]	140,000 [1]	NA	1,150	138,600	NA	0.8	1.0	NA
1:10 Sarcee Bridge	200 [1]	54,800 [1]	205,100 [1]	205	59,700	238,000	-2.5	-8.9	-16.0
1:100 Sarcee Bridge	820	118937	320047	820	119,000	321,000	0.0	-0.1	-0.3
Design Flood Sarcee Bridge	1,240 [2]	153,200 [2]	NA	1,240	149,600	NA	0.0	2.3	NA

NOTES:

[1] Measured data provided by the Water Survey of Canada for 2008 at Bragg Creek and Sarcee Bridge, 2013 at Bragg Creek only

[2] Modeled data provided by the City of Calgary based on level pool routing in Glenmore Reservoir

NA: data not available

Modeling of each flood is based on the diversion operational parameters, which are based on the design flood hydrograph at Sarcee Bridge (Stantec 2015a).

The primary goal of the Project is to maintain 160 m^3/s in the Elbow River. Flows less than 160 m^3/s are not diverted. This flow rate threshold, as a mean daily flow, is equaled or exceeded less than 0.05% of the time at Bragg Creek and less than 0.12% at Sarcee Bridge. Diversion starts when flows exceed 160 m^3/s with increasing diversion occurring until flows in the diversion canal reach a maximum of 600 m^3/s. Any flow remaining in the Elbow River above 760 m^3/s (160 m^3/s plus 600 m^3/s) is allowed to pass downstream whilst 600 m^3/s is continuously diverted into the diversion canal.

For example, if the flow in the Elbow River is 805 m^3/s, a maximum of 600 m^3/s can be diverted leaving 205 m^3/s in the Elbow River (160 m^3/s maintained plus the excess above 760 m^3/s of 45 m^3/s). Hydrographs showing the effect of the operational rules for the design flood, 1:100 year flood, and 1:10 year flood are shown in Figure 2-5 to Figure 2-7.

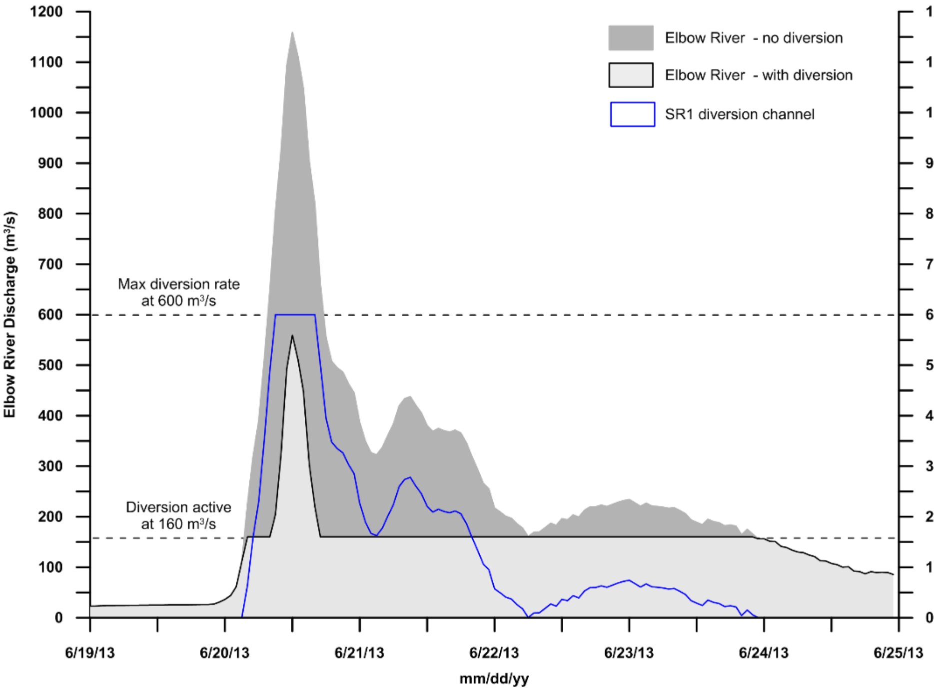

Figure 2-5 Design Flood using Bragg Creek 2013 Data

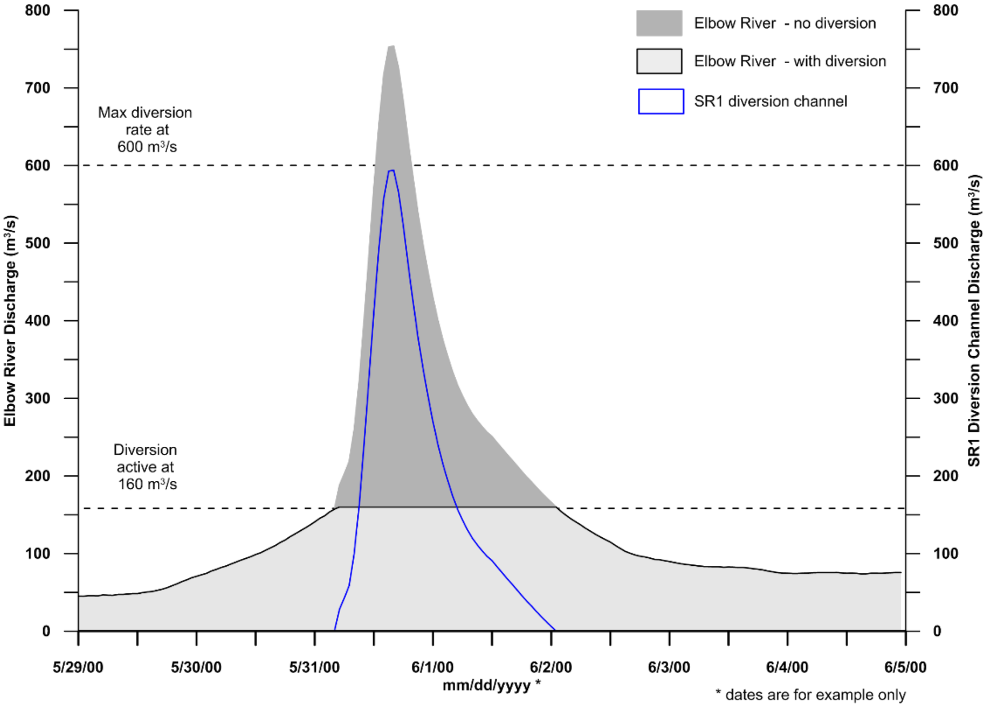

Figure 2-6 1:100 Year Flood

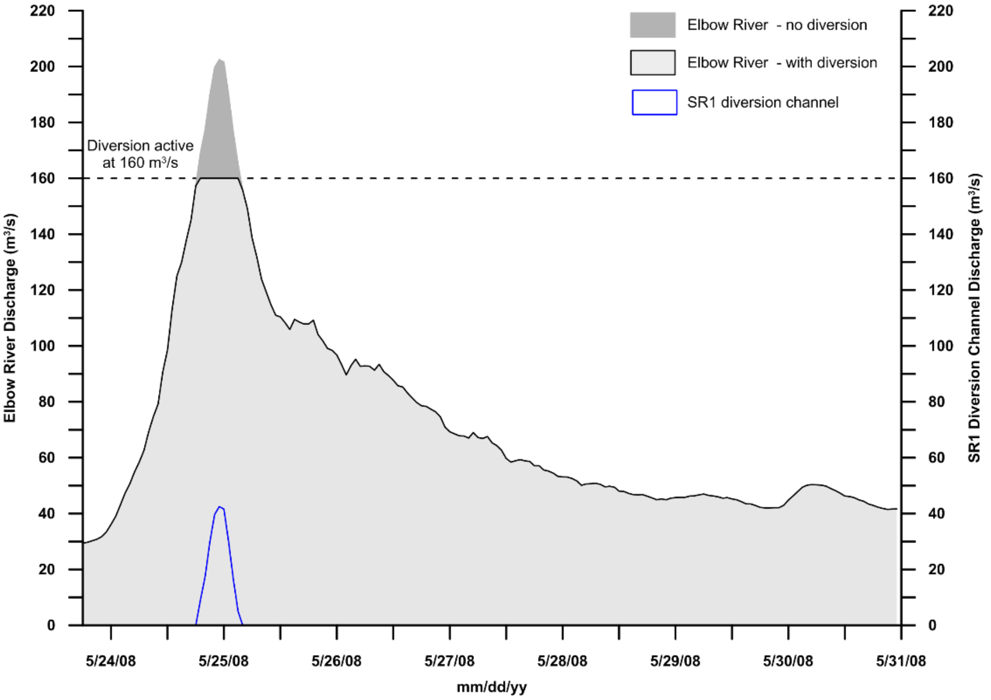

Figure 2-7 1:10 Year Flood Using Bragg Creek 2008 Data

Modeling of sediment transport was based on a combination of field collected data and site specific mathematical relationships between discharge and the

The timing of release of diverted water from the reservoir for the three floods is based on two criteria. The first criterion was that flows in the Elbow River needed to be less than 20 m^3/s before release could occur. This threshold was based on a maximum design release rate of 27 m^3/s and the effective discharge for suspended sediment transport of between 35 and 50 m^3/s (see Volume 4 Appendix J Hydrology for more detail). Remobilization of sediment would occur if the combined discharge from the reservoir release and the existing discharge in the Elbow River were sufficient to impart boundary shear stresses high enough to re-initiate sediment transport. This mobilization applies to both suspended sediment and bedload. To reduce this possibility, water is assumed to be held in the reservoir until the flow in the Elbow River would be less than the suspended sediment effective discharge rate when combined with the released flow. The suspended sediment effective discharge was used as the threshold as shear stresses to mobilize suspended sediment are typically lower than that for bedload (Bunte et al. 2014; Knighton 1998).

The second criterion is based on the length of time to drain the reservoir using the engineering design full service volume of approximately 84,500 dam^3. Under this volume, the length of time to drain the reservoir is estimated at approximately 42.4 days. Initial drawdown curves were established based on engineering design and discharge rates estimated. However, variance in the generation of these curves resulted in differences in the length of drawdown within the model environment. As a result, the diverted flows have drawdowns that range between 30 to 40 days (Figure 2-8). It is important to note the actual operational release rate from the reservoir will be varied depending on circumstances at the time of diversion and release. For example, release rates may be varied in order to minimize mobilization of sediment in the low-level outlet channel and remobilization of sediment in Elbow River downstream of its confluence with the low-level outlet.

Large woody debris (LWD) deposits are present throughout the Elbow River floodplain. The presence of LWD, including log jams, may influence channel morphology through localized changes in roughness increasing sediment deposition, thus changing longitudinal channel profiles. The presence of LWD has been demonstrated to play a significant role in small to medium sized river channel morphology by altering lateral channel migration, planforms and sediment storage and release (e.g., debris flows) (Benda et al. 2005; Wohl 2017). The role of LWD in large rivers is still poorly understood (Faustini and Jones 2003; Wohl 2017). However, their effects on channel morphology, grain size distributions, bedforms and sediment transport rates in larger river systems is likely overprinted by spatio-temporal variation in sediment erosion and deposition during floods (Faustini and Jones 2003). As a result, the potential effect of LWD on sediment transport and channel morphology in the three floods are not assessed.

Modeling was conducted in unsteady flow and the model run was for approximately four months of simulation period to allow for dispersion, decay, settling of suspended substances.

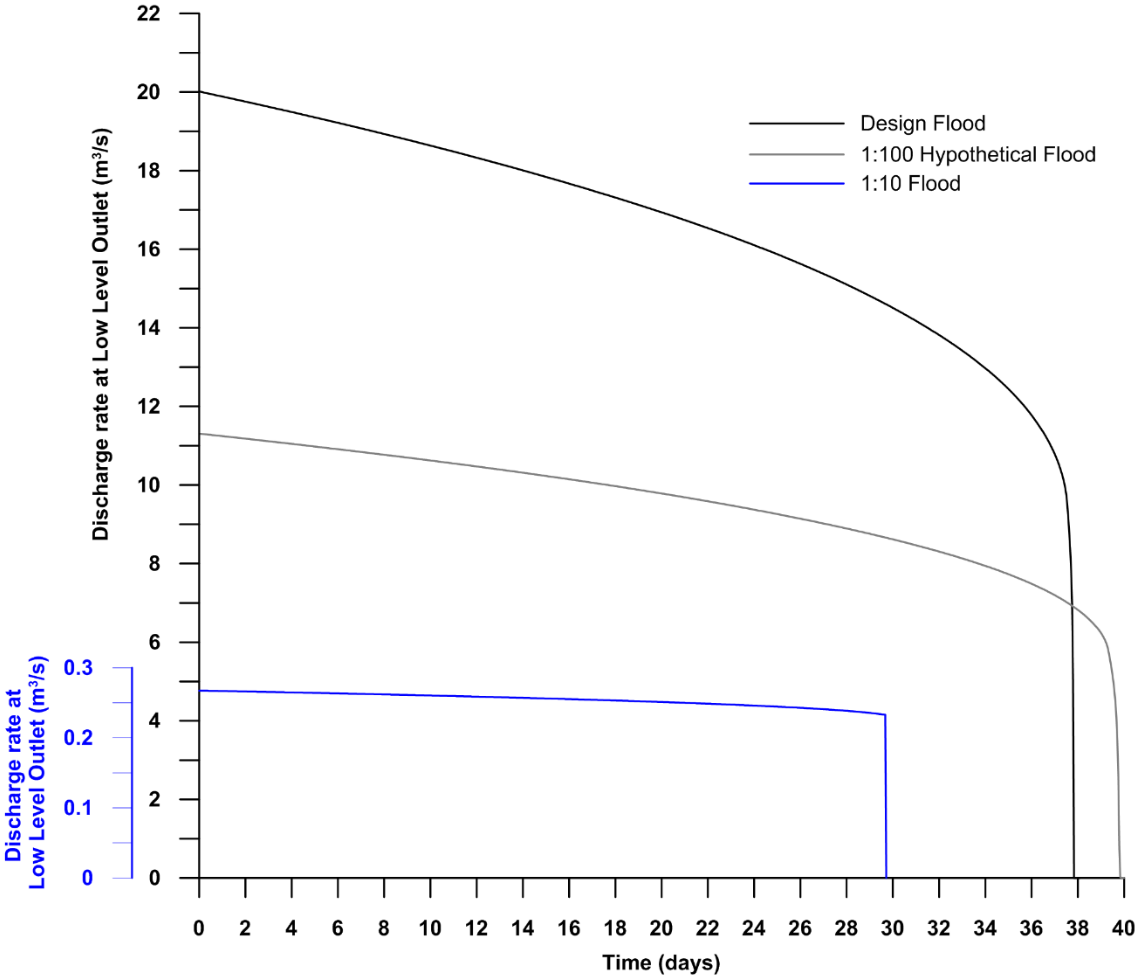

Figure 2-8 Modelled Floods Release Rates from the Reservoir

2.4.3 Model Calibration, Uncertainties, and Assumptions

Models were firstly calibrated using the existing available hydrographic data from historical observations and project field measurements, and then applied to project specific modelling.

Uncertainties are introduced when developing any model to represent real-world conditions as numerical approaches may not accurately capture the full range of variability or interactions between different physical processes. These uncertainties are amplified when modelling multi-fraction sediment transport under flood conditions that includes diversion of flow and sediment where there is little or no field based data to constrain the model, specifically for sediment transport. Although some of the complex interactions between hydrodynamics, sediment mobilization and deposition during floods can be reasonably approximated in a model, not all can. For example, the effect of imbrication over time in increasing localized bed resistance, changes in suspended sediment concentrations due to source variability, and the role of LWD in changing local hydraulic and sedimentation patterns. The model results, therefore, provide a reasonable approximation of how the hydrology and sediment transport in Elbow Bow River and low-level outlet channel respond to operation of the Project. However, there are the following uncertainties:

- suspended sediment concentration estimates depend on discharge rating curves that assume concentrations scale at a constant rate with discharge. The performance of this relationship is typically confounded as suspended sediment transport is a function of discharge and sediment supply. Variation in sediment supply within a watershed, including the channel and banks, as well as during a flood, introduces hysteresis to the suspended sediment–discharge relationship. Hysteresis effects are not able to be captured using rating curves. As a result, suspended sediment concentrations, and resulting suspended sediment loads, are often overestimated. However, the rating curve approach remains the primary, practical method for determining concentrations and resulting sediment loads (Araujo et al. 2012).
- Suspended sediment concentrations are estimated based on power curve suspended sediment-discharge rating curves. These relationships are assumed to be maintained up to an order of magnitude higher than the maximum recorded measurements. A lack of suspended sediment concentration data from high magnitude floods means that values estimated for extreme flows are speculative and are presented under the assumption of unlimited sediment supply.
- The locations of bed degradation and aggradation are driven by the model domain DEMs. The DEMs have varying spatial resolutions and as a result, the accuracy of aggradation/degradation magnitude will partially reflect the source DEM resolution.

- Field surveyed bathymetric cross-sectional data post-2013 was not available for the LAA. As a result, the lack of bathymetric cross-sectional data may bias where the model determines channel aggradation/degradation as the DEM presents the active channel as a planar surface. However, the LiDAR data used to generate the DEMs was flown in late fall with water levels close to their minimum. As bedload transport has been shown to be typically occur on bar surfaces in the Elbow River rather than the thalweg (Hudson 1983), these areas would have been characterized by the LiDAR imaging. This spatial characterization reduces the effect of not be able to incorporate bathymetric cross-sections in to the model.
- The subsurface grain size distribution (GSD) for the Elbow River was assumed to be uniform from Bragg Creek to Sarcee Bridge, based on field data. Although this assumption is reasonable given the lack of variation in the field data, under flood conditions, GSD will likely vary because of new sources being accessed as well as spatio-temporal variation in deposition and remobilization during the rising and falling limb of the flood. This variability will affect sediment transport rates and amounts which the model is unable to account for.
- Bedload transport rates are based on application of the Meyer-Peter Müller bedload transport equation. As with all bedload transport equations, limitations are introduced through the association of a transport rate with discharge, shear stress or stream power and a limited understanding of sediment entrainment, transport, and deposition (Martin 2003). For example, although bed sediment characteristics are typically described using the D_{50}, bed structure is typically not incorporated (Martin 2003). Bed structure has been demonstrated to significantly affect sediment transport rates in cobble-gravel bed rivers, like the Elbow River, by promoting stability (Church et al. 1998). Furthermore, there is a lack of data on spatio-temporal bedload transport variability. These limitations often result in unreliable prediction of transport rates predicted by transport formulae (Martin 2003). However, despite these limitations and considering the difficulties in collecting field measurements, the Meyer-Peter Müller formula, which includes a form resistance term, has been found to perform reasonably well in predicting bedload motion and transport rates in rivers such as the Elbow (Gomez and Church 1989). As with the suspended sediment analysis, bedload transport rates estimated for extreme flows and associated areas of degradation/aggradation are speculative and may not reflect reality.
- The MT and ST modules were modeled separately due to computational complexity, run times and maintaining model stability. Maintenance of model stability was required due to the size of the modeling domains and the timescale of the modeling periods. This separation may introduce some error to the aggradation/degradation ranges as the ST model does not account for finer bedload components (e.g., sand) and was run based on a single D_{50} value to characterize the entire Elbow River. However, the overall pattern of degradation/aggradation

3.0 RESULTS

3.1 GEOLOGICAL SETTING

The Elbow River watershed, and subsequent runoff regime and fluvial sediment supply, is strongly influenced by its geological structure and glacial history. Three structural provinces comprise the underlying geology and include: 1) the Front Ranges; 2) the Foothills of the eastern margin of the Cordillera and 3) the Plains of the Alberta syncline (Hudson 1983). The Project area lies within the eastern portion of the 40 km wide Foothills Belt that marks the transition between the Rocky Mountains and the Plains (Osborn et al. 2006).

The Front Ranges and Foothills are underlain by marine limestone and dolomite rock of Paleozoic origin that are thrust northeast to produce a series of imbricated, northwest striking, southwest dipping locally folded and faulted thrust sheets. These thrust sheets are typically steep to near vertical where they daylight (Hudson 1983). As a result, the mountains and foothills area of the Elbow River watershed have structurally determined high relief, ridge, and valley topography. Valleys are typically U-shaped with cirques and horns reflecting erosional modification by multiple periods of glacial activity.

Wisconsin related glacial erosion and deposition have resulted in extensive deposits of colluvium over bedrock where this material is dominated by gravel sized material (Hudson 1983). The bedrock units are subject to failure from mechanical weathering and mass movement which provides both fine and coarse grained material (Hudson 1983). Tills and alluvial material in the Front Ranges predominantly originate from the Wisconsin Glaciation and reworking during subsequent advances (Jackson 1980; Moran 1986). Alluvial deposits in the Front Ranges are dominated by gravel sized material deposited in alluvial fans and fluvial and glaciofluvial plains and terraces in valley bottoms (Hudson 1983).

The Foothills are dominated by colluvium but with less prominent bedrock outcrops (Hudson 1983). The underlying bedrock reflects six different Mesozoic shale and sandstone formations that underlay the Elbow River from the confluence of the Elbow and Little Elbow to the Highway 22 bridge and are highly erodible (Hudson 1983). The Bow Valley till is the major till unit in this area along with significant alluvial deposits along valley bottoms. The mid- and lower-Foothills are dominated by thick deposits of colluvial and morainic material with valleys infilled with glaciolacustrine deposits or alluvium.

Downstream of Highway 22, the Plains zone is characterized by highly erodible Pleistocene glaciolacustrine material overlying the folded Tertiary quartz, feldspar and chert/calcareous matrix of the Paskapoo Formation (Moran 1986). The glaciolacustrine material was deposited in Glacial Lake Bragg during the retreat of ice in the Elbow and Bow Valleys at the end of the

Erratics Train Glaciation (Jackson 1980). Upon draining of the Glacial Lake Bragg and Glacial Lake Calgary, the Elbow River likely began flowing in its present course (Hudson 1983).

3.2 CLIMATE

The Elbow River watershed has a continental climate with long summer days and short winter days. Environment Canada climate normal data for Springbank Airport (ID 303F0PP), approximately 9 km north of the Project Area for period 1981 to 2010 indicate an average annual air temperature of 3.1 °C. The warmest month is July with an average temperature of 14.8 °C and the coldest is January with a mean temperature of -8.2 °C. The average annual precipitation is 469 mm of which 366 is rainfall. June has the highest rainfall of 106.7 mm. Evaporation data is not available for Springbank Airport. However, data for Calgary International Airport suggests that shallow lake evaporation and potential evaporation average 728 mm and 992 mm annually, respectively (AESRD 2013). Highest evaporation occurs in July with a shallow lake evaporation of 154 mm and 197 mm for potential evaporation (AESRD 2013) (Figure 3-1).

Although the Springbank Airport is suitable for characterizing the immediate Project Area, the values do not reflect the entire Elbow River watershed. There are significant differences in climate introduced by changes in elevation and orographic uplift effects on precipitation patterns (Flesch and Reuter 2012). To account for this difference, the Elbow River watershed was divided into an upper and lower watershed, reflecting differences between the high gradients of the Front Ranges and the low gradient of the Plains. The demarcation between the two zones is approximately at Maclean Creek where gradients start to increase rapidly. The upper watershed has an area of approximately 812 km^2 and the lower watershed, 425 km^2. Climate normal values for 1981-2010 were calculate based on the gridded, elevation adjusted, ClimateWNA dataset (Wang et al. 2006; Wang et al. 2012; Hamann et al. 2013).

The climate normal between the upper and lower watersheds exhibit clear differences in climate. Elevation influenced decreases in air temperature and increases in snow water equivalent and rainfall result in an annual average precipitation of approximately 762 mm, of which approximately 45% is attributed to snow (Figure 3-2). Maximum snow water equivalents occurring in April and maximum rainfall in June (Figure 3-2). In contrast, mean annual precipitation in the lower watershed is approximately 473 mm of which 19% is attributed to snow (Figure 3-2). Maximum snow water equivalents occurring in March and maximum rainfall in June. The earlier maximum snow water equivalent occurs earlier in the lower watershed due to snow melt occurring progressively from lower to higher elevations (Hudson 1983). As a result, winter conditions typically persist in the upper watershed until May or June. In contrast, proportionally more runoff is generated in the lower watershed in early spring. These differences in climate and resulting runoff magnitude and timing is strongly modulated by watershed characteristics in the two zones.

Daily evaporation rates were calculated as a function of the volume diverted and length of retention in the reservoir and release for each flood. These results are presented in Volume 3B, Section 6.0.

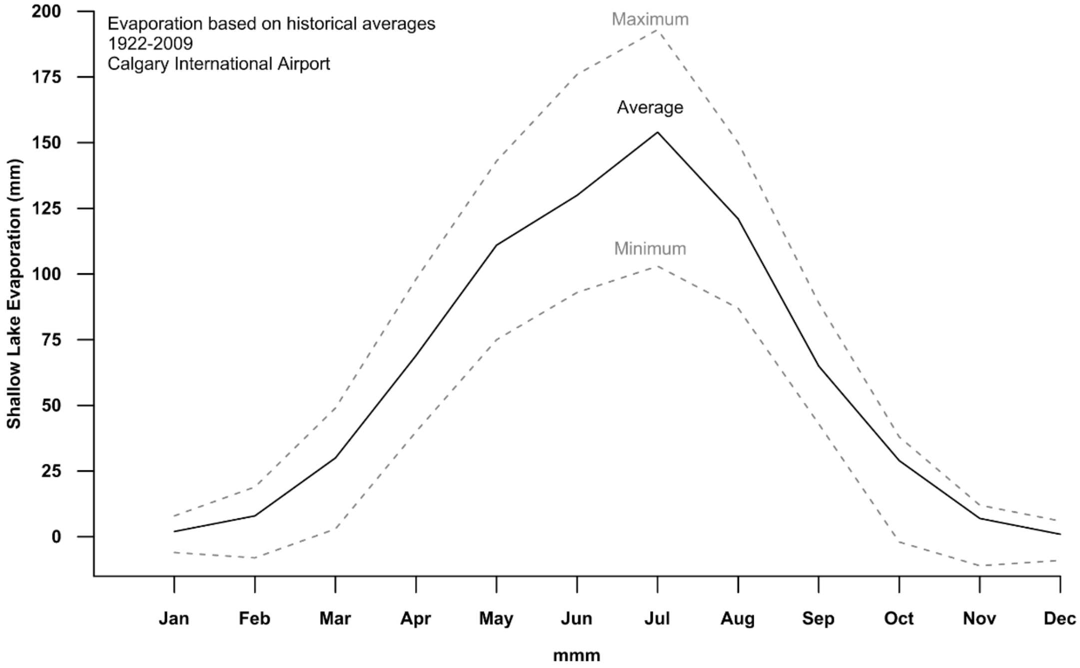

Figure 3-1 **Historical Shallow Lake Evaporation Estimates from Calgary International Airport Data**

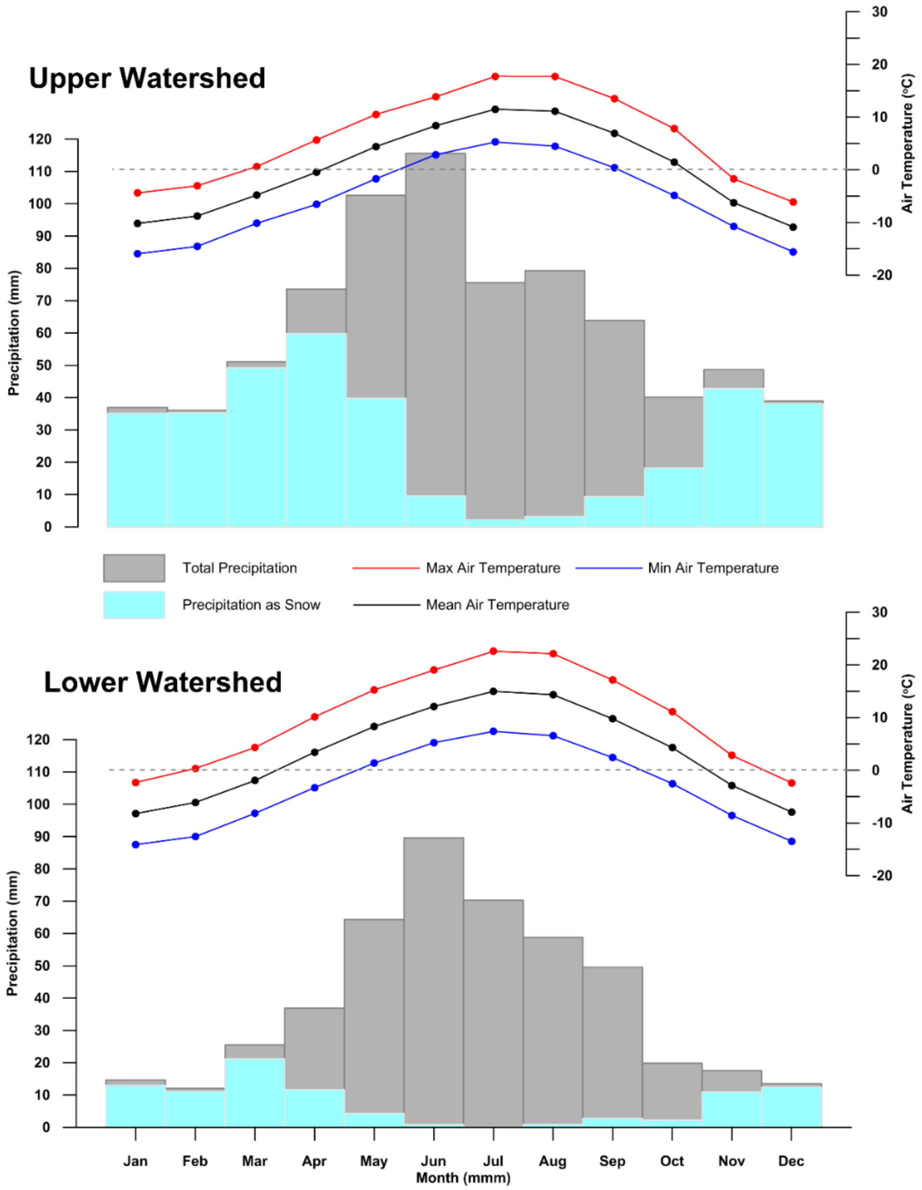

Figure 3-2 **1981-2010 Climate Normals for Upper and Lower Elbow River Watershed**

3.3 BASIN CHARACTERISTICS

The Elbow River and its tributaries have a total watershed area of approximately 1238 km^2 (Figure 2-2). From its source in the Front Ranges of the Rocky Mountains, Elbow Lake, at an elevation of 2,085 m above sea level (m asl), the river flows approximately 113 km through foothills and plains to the inlet to Glenmore Reservoir in the City of Calgary at an elevation of 1,080 m asl (Beers and Sosiak 1993). The Elbow River flows through the City of Calgary downstream of the Glenmore Reservoir dam to its confluence with the Bow River at an elevation of 1,000 m asl (Figure 2-2). The upper watershed has a minimum elevation of 1,282 m asl and a maxim of 3,212 m asl, a range of 1,929 m. Mean elevation is 1,923 m asl. The minimum elevation in the lower watershed range is 1,026 m asl, the maximum 1,461 m asl for a range of 434 m. Mean elevation is 1,199 m asl. The wide range in elevations results in a large gradient variation between the upper and lower watersheds.

The Elbow River is one of the steepest rivers in Alberta (Kellerhals et al. 1972). The overall gradient is approximately 0.9% (Figure 3-3). However, gradients in the headwaters upstream from Elbow Falls are considerably higher at approximately 1.54%. Gradients of the Elbow Rivers two main headwater tributaries, the Little Elbow and Canyon Creeks are also steep with headwater gradients of 5.42% and 4.11%, respectively. Between Elbow Falls and Bragg Creek the Elbow River gradient reduces to less than 0.8%. Where the Elbow River transitions to the Alberta Plains, gradients reduce to 0.4% and further reduce to approximately 0.2% where the Elbow River enters Glenmore Reservoir (Figure 3-3).

In contrast to headwater tributaries, tributaries in the Project area tend to have much lower gradients for most their lengths. Gradients typically increase as tributary channels incise through glaciolacustrine/till terraces to their confluence with the Elbow River. For example, the unnamed tributary that will function as the low-level outlet has a small gradient of 0.2% for the majority of its 19 km length (Figure 3-4). The channel planform in the upper reaches is sinuous and the channel is diffuse in places. Where channelization exists, widths and depths and typically less than 1.0 m. However, the gradient steepens at approximately 17 km where the channel drops approximately 20 m in 2 km to its confluence with the Elbow River, a gradient of 0.81%. This increase in gradient and associated stream power has resulted in the channel being confined to a single channel with incision of up to 3.0 m through the overlying glaciolacustrine material. This incision pattern is observed for all tributaries in the Project LAA.

Because of these marked gradient changes, the Elbow River and its tributaries transition from a steep, generally single channel mountain stream with pool-riffle sequences to a weakly braided/wandering pattern contained within broad floodplain with low gradient, typically poorly defined tributaries as the Elbow flows towards Glenmore Reservoir. The river is occasionally confined by limited bedrock canyons in reaches in the foothills and flows predominantly over gravel and cobble size alluvium for its entire length (Hudson 1983). These gradient changes also reflect the physical characteristics of the Elbow River watershed. These physical characteristics are assessed here using a HRU approach applied to the Elbow River watershed.

An HRU analysis provides context for understanding the relative influence of catchment structure on runoff response as well as sediment supply (Buttle 2006; Jensco and McGlynn 2011). HRUs are landscape units that can be defined as having a similar hydrological response to a climatic input, for example, a rainfall event (Devito et al. 2005). These landscape units are commonly defined as a combination of slope, surficial geology, and land cover as these components largely determine the magnitude and timing of the hydrological response of a watershed to precipitation or snow (Devito et al. 2005; Jensco and McGlynn 2011). The HRU classifications are presented here solely as a mechanism to identify potential first order controls on runoff controls in the Elbow River watershed. The HRU results are summarized in Table 3-1 and in Figure 3-5.

Table 3-1 Landcover, Landuse and Surficial Geology of the Elbow River Watershed

		Upper Watershed		Lower Watershed		Combined Area (km^2)
		Area (km^2)	**%**	**Area (km^2)**	**%**	
SURFICIAL GEOLOGY	Bedrock/Glacier	138.8	17	0.0	0	138.8
	Coarse material[1]	654.3	81	264.0	62	918.3
	Fine material[2]	18.5	2	160.8	38	179.2
	Total	811.5	100	424.8	100	1236.3
SLOPE	Greater than 10%	696.7	86	48.3	11	744.9
	Less than 10%	114.8	14	376.6	89	491.4
	Total	811.5	100	424.8	100	1236.3
LANDCOVER	Alpine	239.8	30	0.0	0	239.8
	Anthropogenic	22.7	3	98.4	23	121.1
	Barren Land or Water	8.5	1	12.5	3	21.1
	Cultivation (Crop/Pasture)	5.5	1	151.2	36	156.7
	Cut Blocks	31.0	4	0.6	0	31.6
	Forest	429.7	53	81.3	19	511.0
	Grassland/Shrubland	73.7	9	77.0	18	150.7
	Marsh	0.6	0	3.9	1	4.4
	Total	811.5	100	424.8	100	1236.3

NOTES:

[1] colluvial deposits; fluvial deposits; fluted moraine; glaciofluvial deposits; ice-thrust moraine; preglacial fluvial deposits; stagnant ice moraine

[2] eolian deposits; glaciolacustrine deposits; lacustrine deposits; organic deposits

The HRU results show clear differences in surficial geology, slope and landcover between the upper and lower watersheds. The upper watershed is dominated by slope gradients greater than 10% combined with bedrock and coarse grained surficial material and with a high percentage of alpine landcover. This combination suggests that runoff response to precipitation is rapid in areas with significant areas of bedrock but less in areas with coarse surficial material and forest cover. The high slope gradients also suggest that gravitational and cryogenic processes dominate sediment generation and transport (Church and Ryder 2010). Gravitational processes include rock avalanches and debris flows, all of which deliver large quantities of sediment to valley bottoms for transport. These processes suggest that the mountain sediment yields contribute sediment from surface wash of colluvium within tributary basins, with occasional inputs from mass movement where they intersect with the active channel (Hudson 1983). However, sediment derived from channel and riparian erosion of colluvium and till in both the tributaries and the Elbow River dominates suspended sediment sources, with considerable spatial variation (Hudson 1983).

In contrast, HRUs in the lower watershed are dominated by slope gradients less than 10%, a higher percentage of fine grained surficial material and cultivated/anthropogenic landcover classes. In the lower watershed, sediment sources for the Elbow River are dominated by channel and riparian erosion with silt, clays and gravels laterally eroded from valley walls where there is contact and flow levels are high enough to access the walls (Hudson 1983). Sediment sources in the tributaries are limited to channel and riparian areas with occasional inputs from minor rilling and gullying of limited areas (Hudson 1983). Runoff in these tributaries is largely intermittent in often poorly organized channels on low gradient surfaces. Generation of runoff is primarily generated during either prolonged rainfall events or early spring rainfall on partially frozen ground (See Section 3.3.1.2).

In summary, the modulation of climatic inputs by surficial geology, landcover and watershed physiography in the Elbow River watershed results in a distinct change in hydrology between the upper and lower watersheds. These differences are primarily driven by elevation effects on precipitation.

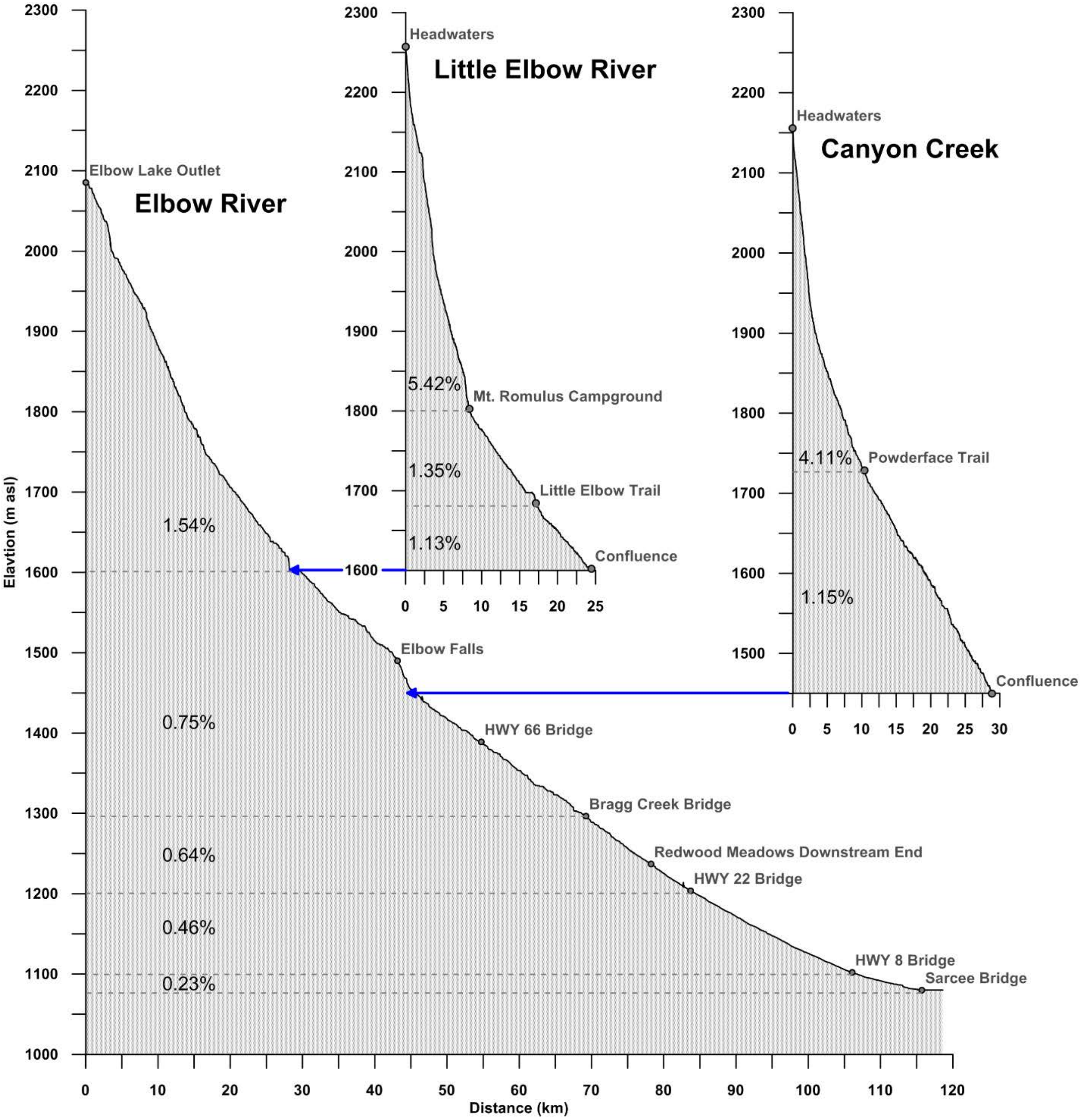

Figure 3-3 Longitudinal 3D Gradients of Elbow River and Selected Tributaries

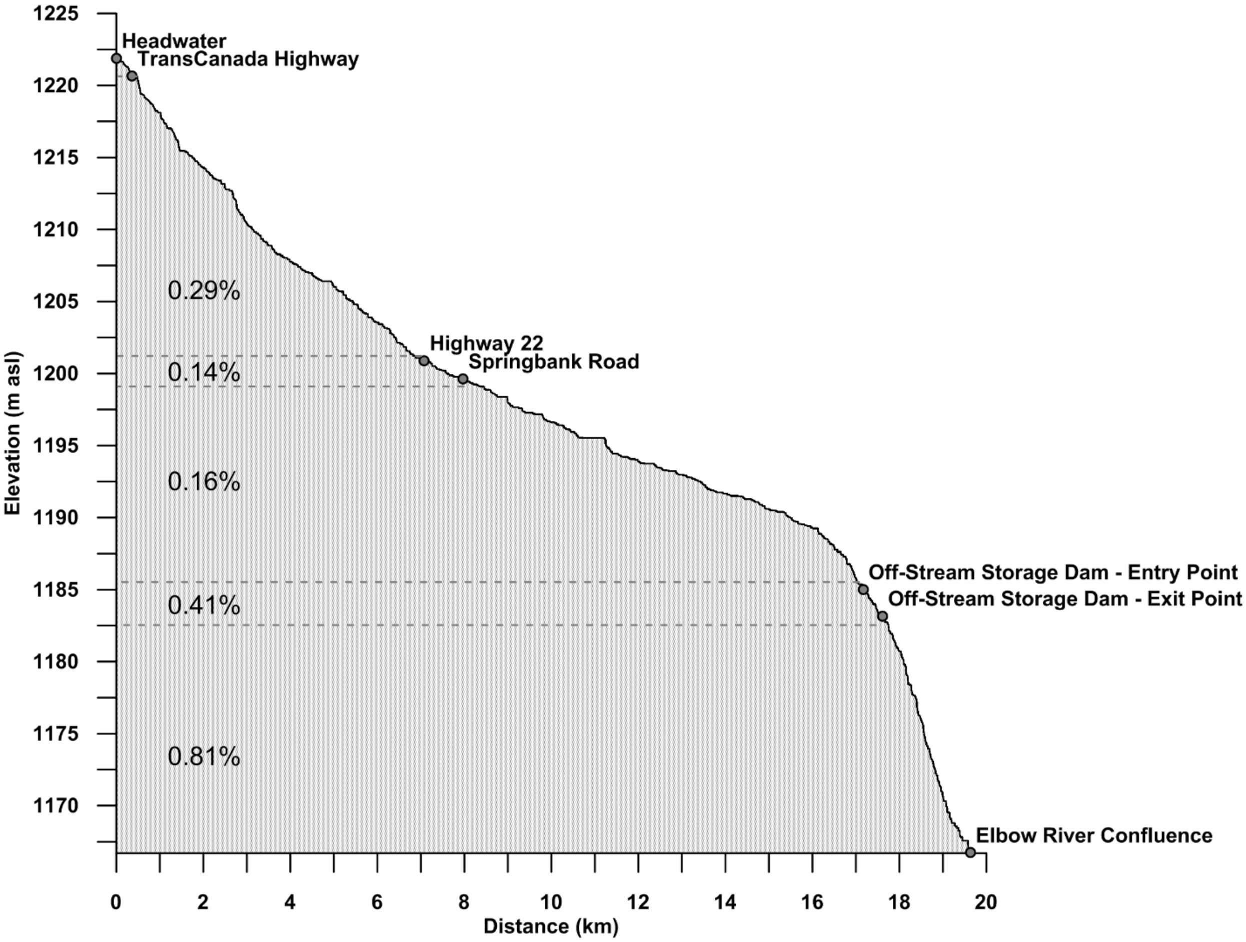

Figure 3-4 Longitudinal 3D Gradient of the Unnamed Tributary

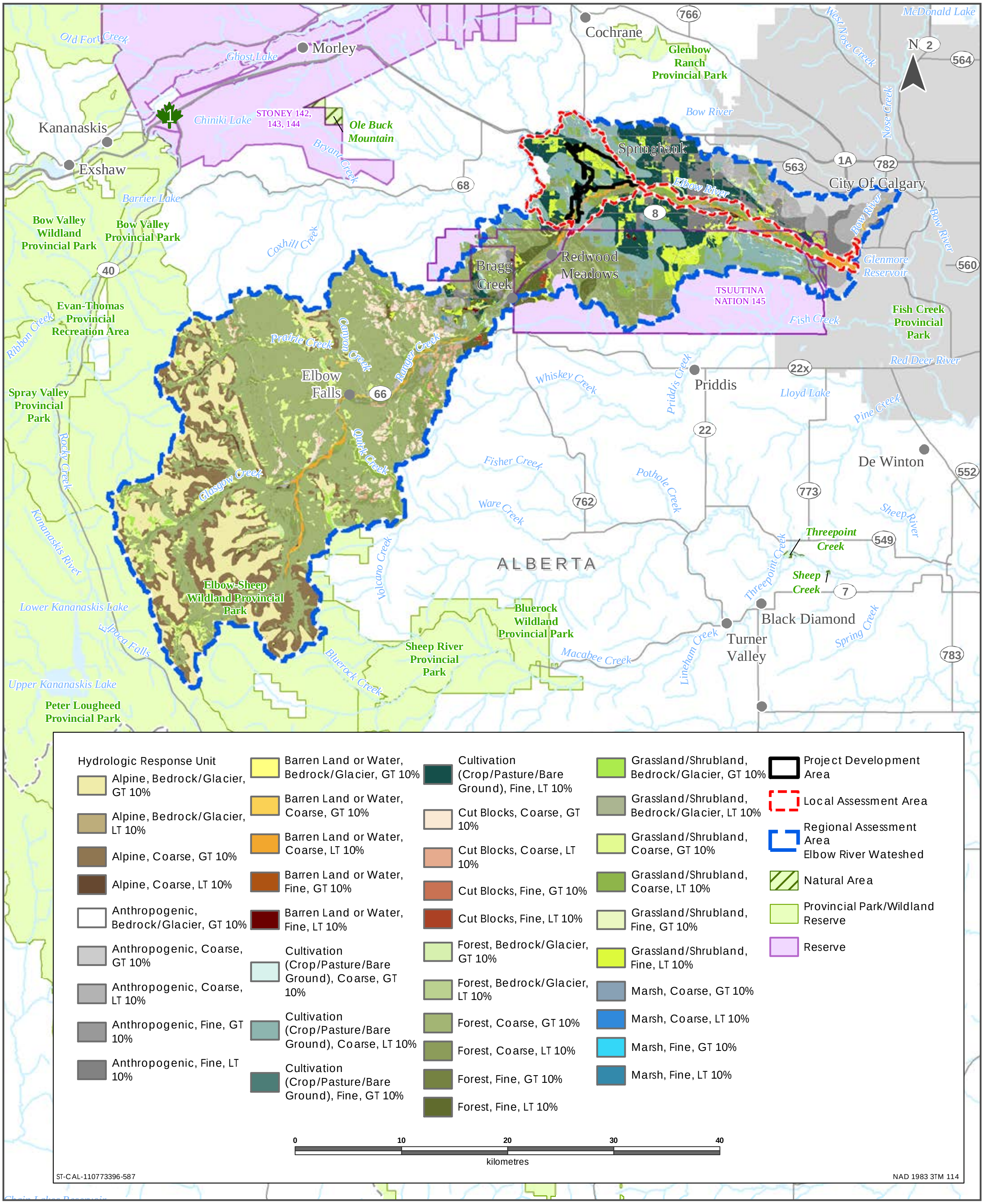

Sources: Base Data - ESRI, Natural Earth, Government of Alberta, Government of Canada
Thematic Data - ERBC, Government of Alberta, Stantec Ltd

Hydrological Response Unit Distribution in the Elbow River Watershed

Stantec

ALBERTA TRANSPORTATION SPRINGBANK OFF-STREAM RESERVOIR PROJECT ENVIRONMENTAL IMPACT ASSESSMENT

Figure 3-5

3.3.1 Hydrology

3.3.1.1 Elbow River

Two Water Survey of Canada stations on the Elbow River provide long-term flow data relevant to this assessment. These two stations are Elbow River at Bragg Creek (ID 05BJ004) upstream of the Project and Elbow River at Sarcee Bridge (ID05BJ010), downstream of the Project. The attributes of these stations are summarized in Table 3-2.

Table 3-2 Relevant Hydrometric Stations Historical Data

Station ID	Watershed Area (km^2)	Mean Daily Flow Record		Instantaneous Peak Flow Record		Hourly Flow/Stage Record		15-min Flow/Stage Record		Record
		From	To	From	To	From	To	From	To	
05BJ004 Elbow River at Bragg Creek	790.8	May 1935	Dec 2016[1]	June 1950	June 2012	Jan 1999	Oct 2016[1]	Jan 2013[1]	Dec 2013[1]	Partial
05BJ004 Elbow River at Bragg Creek	1189.3	April 1979	Dec 2016[1]	May 1979	June 2012	Mar 2006	Oct 2016[1]	-	-	Partial

NOTE:

[1] Discharge and stage data is provisional for 2014, 2015 and 2016 and subject to change

The Elbow River has a typical high-latitude runoff regime with low winter discharges and the majority of runoff derived from snowmelt (Church 1974). However, mean monthly flows for the period 1979 to 2014 for Bragg Creek and Sarcee Bridge show distinct patterns that reflect their position in the Elbow River watershed (Figure 3-6, Table 3-3). At both stations, winter flows are low in response to below freezing air temperatures and precipitation falling predominantly as snow. The slightly higher flows and standard deviations for the Sarcee station during January and February likely reflect periods of warm temperatures and enhanced melt on the Plains associated with orographically reinforced chinook (foëhn) winds that are common during winter (Hudson 1983). Spring flows increase first at Sarcee Bridge in March/April reflecting local inputs of runoff over partially frozen ground with snow melt occurring at progressively higher elevations in the upper basin as spring progresses. This pattern results in the plains snowpack being removed before the influx of the majority of the annual flow from the upper watershed in May, June and July.

Approximately 54% of the annual flow volume occurs during May, June and July in the Elbow River watershed. Of this percentage, 25% of the annual flow typically occurs in June alone. Proportionally, approximately 94% of the annual runoff is sourced from the watershed upstream of Bragg Creek with 6% contributed from the Plains over the year (Figure 3-7). In some months, there is a net loss of up to 1.0% between Bragg Creek and Sarcee Bridge, as also noted by Hudson (1983) (Figure 3-7). This loss is likely due to infiltration into the alluvium of the Elbow River valley floor (Hudson 1983). Summer recession begins in June with a rapid decline towards October and November. Over the long term, the increase in discharge between Bragg Creek and Sarcee Bridge during the summer recession is likely a result of groundwater inflows, rather the rainfall inputs on the plains (Hudson 1983).

However, sustained rainfall from stationary frontal systems over the foothills and plains can markedly increase runoff during the summer months. For example, field data collected from the Elbow River at Highway 22 during 2015 and 2016 showed marked differences in flow volumes between the two years, as a function of snowpack and rainfall differences (Figure 3-8). In 2015, the flow volume for May and June were 17% and 23% of the total annual flow, with July at 13%. Flow volumes in 2016 were 17% of the total annual flow in May, 15% in June and 24% in July. The increase in flow during July 2016 was a result of approximately 206 mm of rain falling over the month, as recorded at Calgary International Airport. This rainfall amount represents a 208% increase over the 1981-2010 climate normal rainfall of 66.9 mm. This example illustrates that the timing, and generating mechanism of flows in the Elbow River can be quite variable.

Although intra- and inter-annual flows can vary considerably depending on driving mechanisms, FDC for Bragg Creek and Sarcee Bridge show that the Elbow River is typically a low flow system for most the year (Figure 3-9). Based on the FDCs, Bragg Creek and Sarcee Bridge have median discharges of 6.3 m^3/s and 7.5 m^3/s, respectively (Figure 3-9). The bankfull discharge (recurrence interval of 1.54 years) for Bragg Creek is estimated at approximately 47 m^3/s and the mean annual flood (recurrence interval of 2.33 years) is estimated at 80 m^3/s (Stantec 2015a). These two flows, which are important for downstream sediment transport and fish habitat maintenance are only equaled or exceeded 1.4% and 0.3% of the time, respectively. These percentages equate to these flow levels occurring approximately 5 days and 1 day per year, on average.

Table 3-3 Summary of Mean Monthly Flows for Bragg Creek and Sarcee Bridge 1979-2016

Station	Jan	Feb	Mar	Apr	May	Jun	Jul	Aug	Sep	Oct	Nov	Dec
	Mean flow (m^3/s) (standard deviation in brackets)											
05BJ004 Elbow River at Bragg Creek	3.0 (0.7)	2.9 (0.5)	3.2 (0.7)	4.7 (1.2)	14.5 (7.1)	25.8 (13.1)	15.4 (7.4)	9.4 (3.5)	8.1 (3.7)	6.6 (2.1)	4.8 (1.1)	3.8 (0.9)
05BJ004 Elbow River at Sarcee Bridge	3.7 (0.4)	3.6 (0.3)	4.2 (0.8)	5.4 (1.5)	14.8 (8.7)	29.5 (19.4)	15.5 (7.2)	9.7 (3.8)	8.5 (3.9)	6.7 (2.1)	5.4 (0.6)	4.2 (0.5)

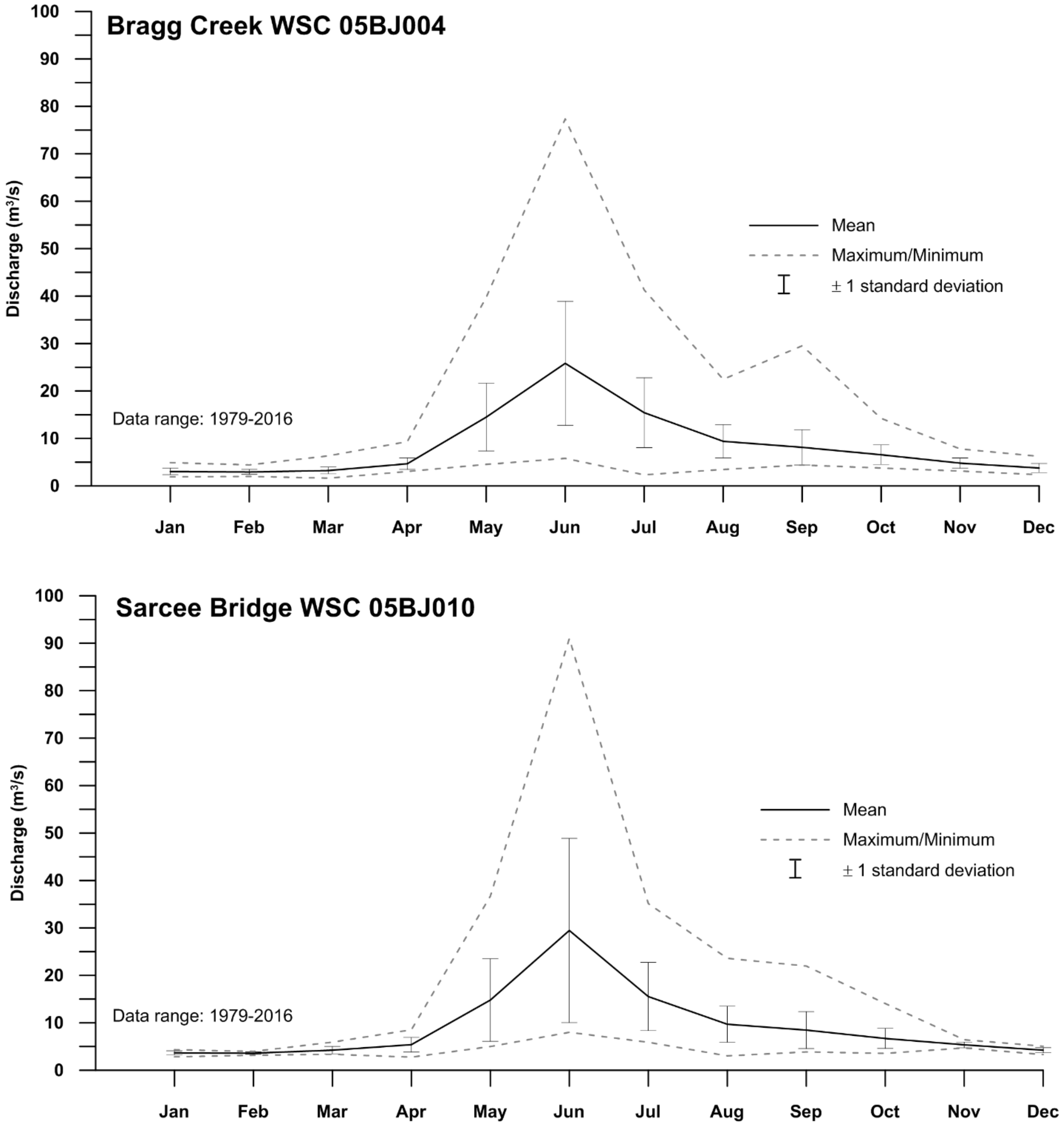

Figure 3-6 Mean, Minimum and Maximum Monthly Flows at Bragg Creek and Sarcee Bridge Stations

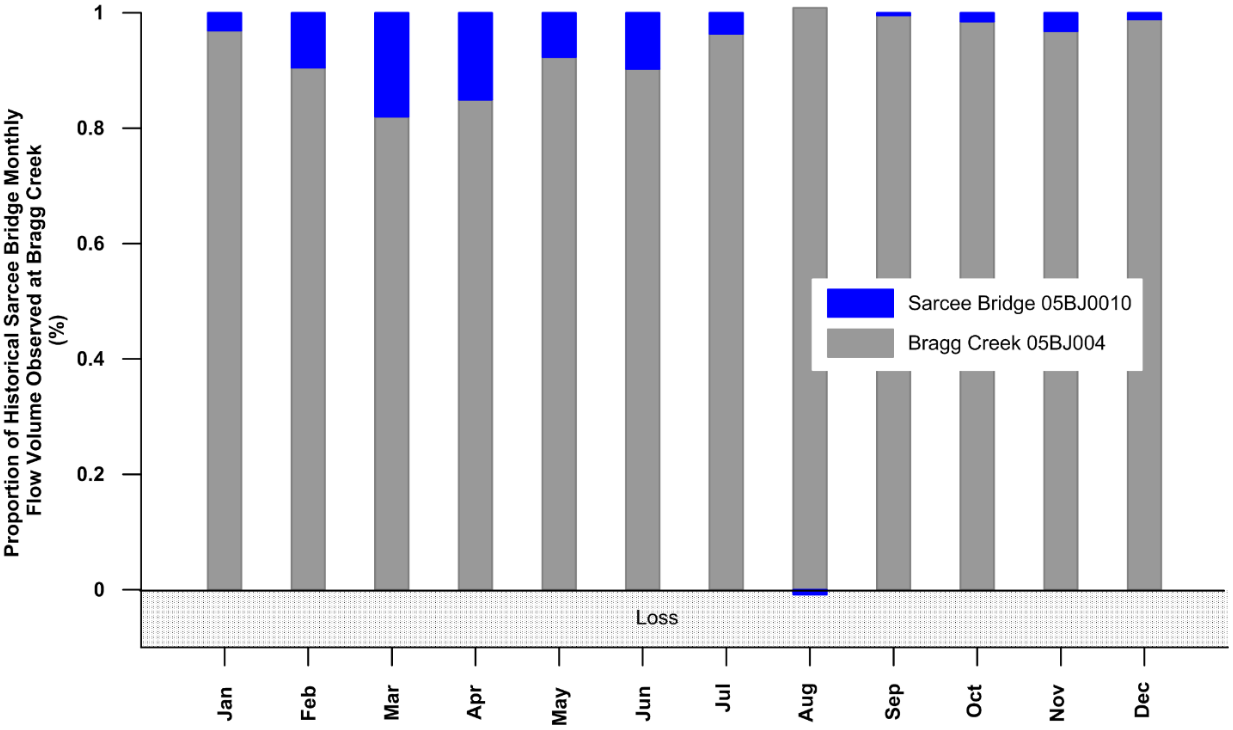

Figure 3-7 Proportion of Sarcee Bridge Monthly Flow Observed at Bragg Creek

Generation of high flows in the Elbow River Basin are complex with changes in magnitude reflecting different combinations of driving mechanisms. Early spring floods driven by snowmelt alone are typically small and occur soon after ice break-up (Hudson 1983). Increasing flood magnitudes reflect an increasing rainfall contribution in the upper watershed with additional inputs from the lower watershed (Hudson 1983). High magnitude floods occur when substantial rainfall occurs during spring melt when higher elevation snowpack are isothermal, or close to isothermal. For example, in June 2013, heavy rainfall and rapidly melting snowpack in the Front Ranges of the Canadian Rocky Mountains resulted in widespread flooding in multiple watersheds, including the Elbow River. Over 200 mm and as much as 350 mm of precipitation fell in watershed headwaters between June 19th and June 22nd (Pomeroy et al. 2016).

The intensity of the 2013 storm was the result of coupling between upper and lower circulation systems. This coupling resulted in upslope winds from the east that were warm and moist, raising the freezing level and resulting in rainfall rather than snowfall at high elevations (Pomeroy et al. 2013). Snowmelt over partially frozen soil at higher elevations may have increased runoff by up to 30%, in some areas (Pomeroy et al. 2016). The system persisted for over 36 h (Pomeroy et al. 2016). Localized pockets of high intensity convection driven rainfall over the foothills and plains as well as in the upper Elbow River watershed also contributed to extreme runoff conditions. As a result, flood generation and frequency in the Elbow River watershed reflects a range of processes that change with increasing magnitude.

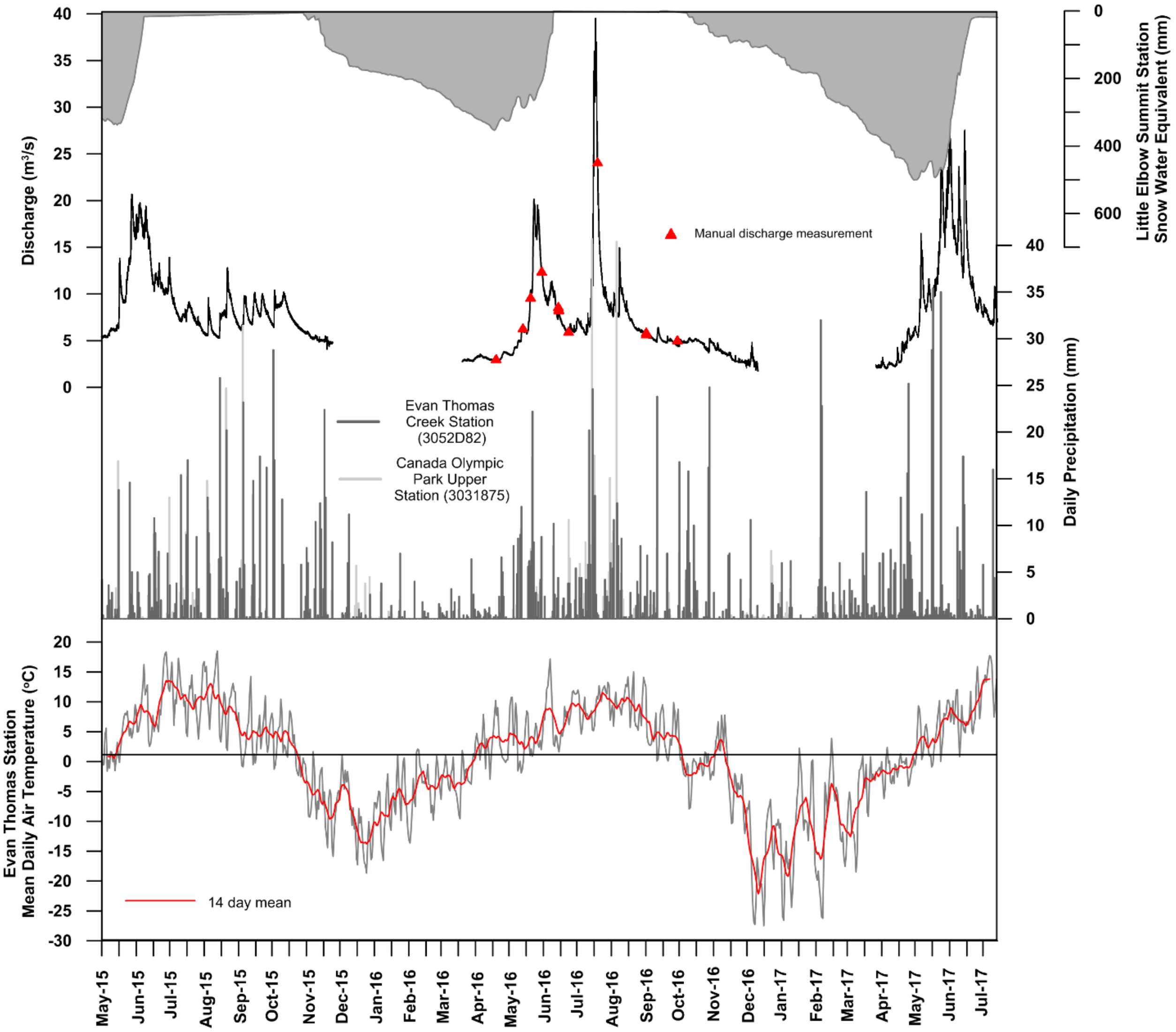

Figure 3-8 Hydrometeorology of Elbow River at Highway 22, 2015 - 2017

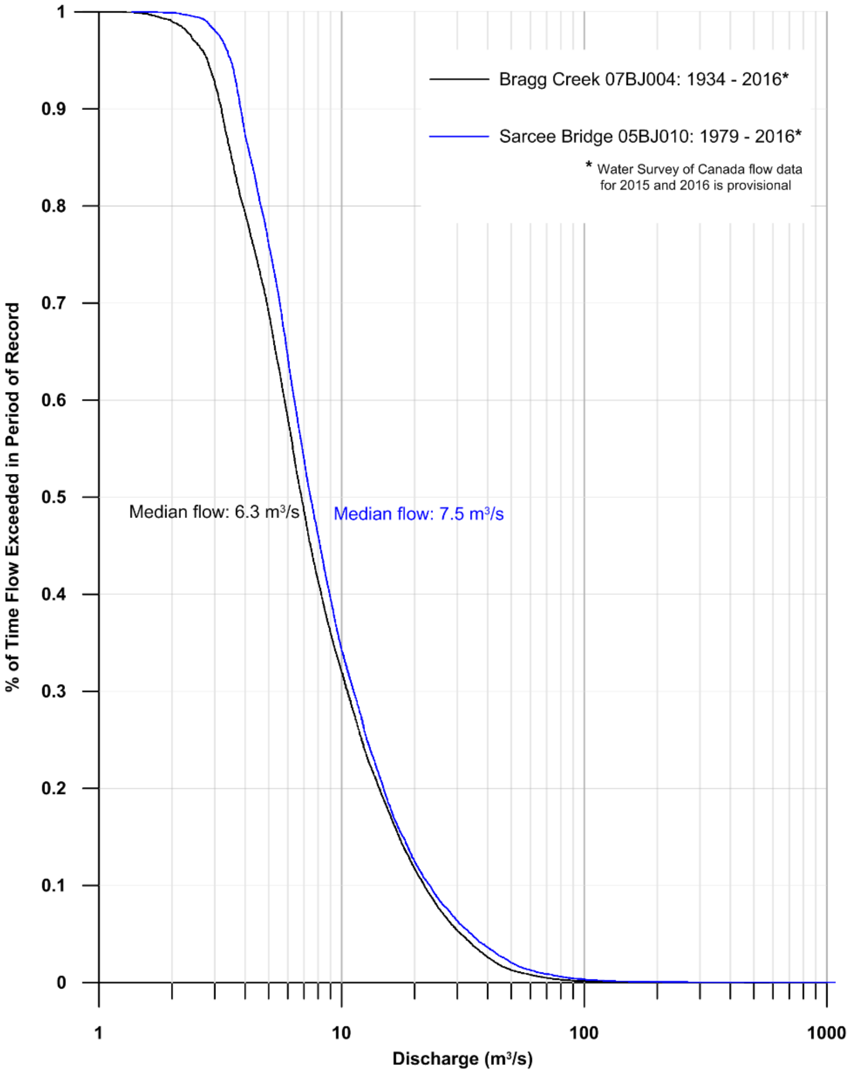

Figure 3-9 Flow Duration Curves at Bragg Creek and Sarcee Bridge

A detailed flood frequency analysis was undertaken using peak instantaneous flows at the Bragg Creek Station for the period 1934 to 2013 and for the period 1908 to 2013 for downstream stations by Stantec (2015). Data from the downstream stations was amalgamated into a Combined Station on the basis of minor differences in watershed area and distances between stations (Stantec 2015).

Initial flood peak and volumetric analyses on the data for Bragg Creek and the Combined Station followed the frequency analysis procedure for stormwater design developed by the City of Calgary (AMEC 2014). Analyses were done using 10 different probability distributions fitted using the HYFRAN+ software with statistical testing for randomness, stationarity, homogeneity, independence, and outliers performs using the City of Calgary procedure (Stantec 2015b). Plotting of the instantaneous peak, 7-day and 56-day flow volumes on log-log paper with best fit lines fitted showed that for recurrence intervals of less than 10 years, a logarithmic equation provided the best fit and for greater than 10 years, a power curve.

Because floods in the Elbow River are generated from a mixed population of snowmelt, rain-on-snow and rainfall only drivers, fitting standard curves at higher recurrence intervals can be problematic. Given that the data set includes the 2013 flood, which was anomalous in the historical record in terms of peak discharge, volume, and hydrograph shape, the unbiased plotting position formulae for historical floods (Guo 1990) was used to calculate plotting positions (Stantec 2015b). The combined logarithmic and power curves are used to estimate recurrence intervals for instantaneous peak, 7-day and 56-day flow volumes, summarized in Table 3-4.

Table 3-4 Estimated Flood Frequencies for Elbow River at the Diversion Structure

Recurrence Interval (years)	Instantaneous Peak Discharge (m^3/s)	7-Day Volume (dam^3)	56-Day Volume (dam^3)
500	1,800	174,000	371,000
200	1,110	132,000	322,000
100	765	107,000	290,000
50	530	86,600	260,000
20	330	65,600	226,000
10	200	53,100	203,000
5	140	38,100	172,000
2	70	20,000	105,000

Flows in the Elbow River are typically at their lowest in February. Mean monthly flow data shows a steady recession from fall flows into winter with a consistent low variance of 0.5 m^3/s around the mean values over the majority of the winter period (November to February) (Table 3-3 and Figure 3-6). The majority of the low flow during winter is sourced from the watershed upstream of Bragg Creek with between 2 and 5% of the mean monthly flow supplied by the lower watershed. As noted by Hudson (1983), winter discharge at Bragg Creek is primarily sourced from the upper Elbow River watershed upstream of Elbow Falls. Lows in discharge correspond to prolonged periods of cold temperatures with higher low flows corresponding to increases in air temperature above freezing during, for example, chinook events (Hudson 1983). Seven day average low flows (7Q) estimated for various recurrence intervals for Bragg Creek and Sarcee Bridge are summarized in Table 3-5. Low flow estimates are shown for the open water season (March to October) and winter (November to April).

Table 3-5 Estimated 7-day Low Flows for Elbow River at Bragg Creek and Sarcee Bridge

Season		$7Q_2$ (m^3/s)	$7Q_{10}$ (m^3/s)	$7Q_{20}$ (m^3/s)	$7Q_{100}$ (m^3/s)
BRAGG CREEK	Open Water	3.40	2.35	2.04	1.48
	Winter	2.26	1.61	1.41	1.05
SARCEE BRIDGE	Open Water	3.88	2.80	2.48	1.87
	Winter[1]	2.68	2.28	2.15	1.87

NOTE:

[1] Sarcee Bridge winter values are based on only eight years of data and should be treated with caution

3.3.1.2 Tributaries

The LAA contains several tributaries to the Elbow River that contribute flow from the plains. Based on field collected data from the 36.4 km^2 watershed of the unnamed tributary that will form the low-level outlet channel, the hydrological regime of small tributaries in the Project area is typically intermittent (Figure 3-10).

Although limited to one year of continuous observation, mean flow in the unnamed tributary is approximately 30 L/s or 0.83 L/s/km^2, when flow is present. The peak flow recorded was 791 L/s after a period of prolonged rainfall in July 2016 (Figure 3-10). Based on visual observations during this peak flood, bankfull discharge is in the order of 1.0 m^3/s. The field data collected to date suggests that surface flow is only initiated in tributaries after either prolonged rainfall resulting in high antecedent moisture conditions or when rain falls on partially frozen ground, enhancing runoff during early spring precipitation events. Rainfall events in late spring do not appear to result in similar magnitude runoff responses suggesting that increased ground infiltration and spring vegetation growth significantly attenuates runoff (Figure 3-10). Snowmelt does not appear play a significant role in runoff generation for the data record presented. During winter and for periods during the summer months, there is no surface flow. However, specific electrical conductivity values of 1.2 to 1.7 mS/cm (1200 to1700 µS/cm) and significant dilution of electrical conductivity during rainfall events suggests that baseflow in the unnamed tributary is, in part, maintained by springs (Figure 3-11). Other tributaries in the area surrounding the Project have been observed to be spring fed and to maintain flow year-round.

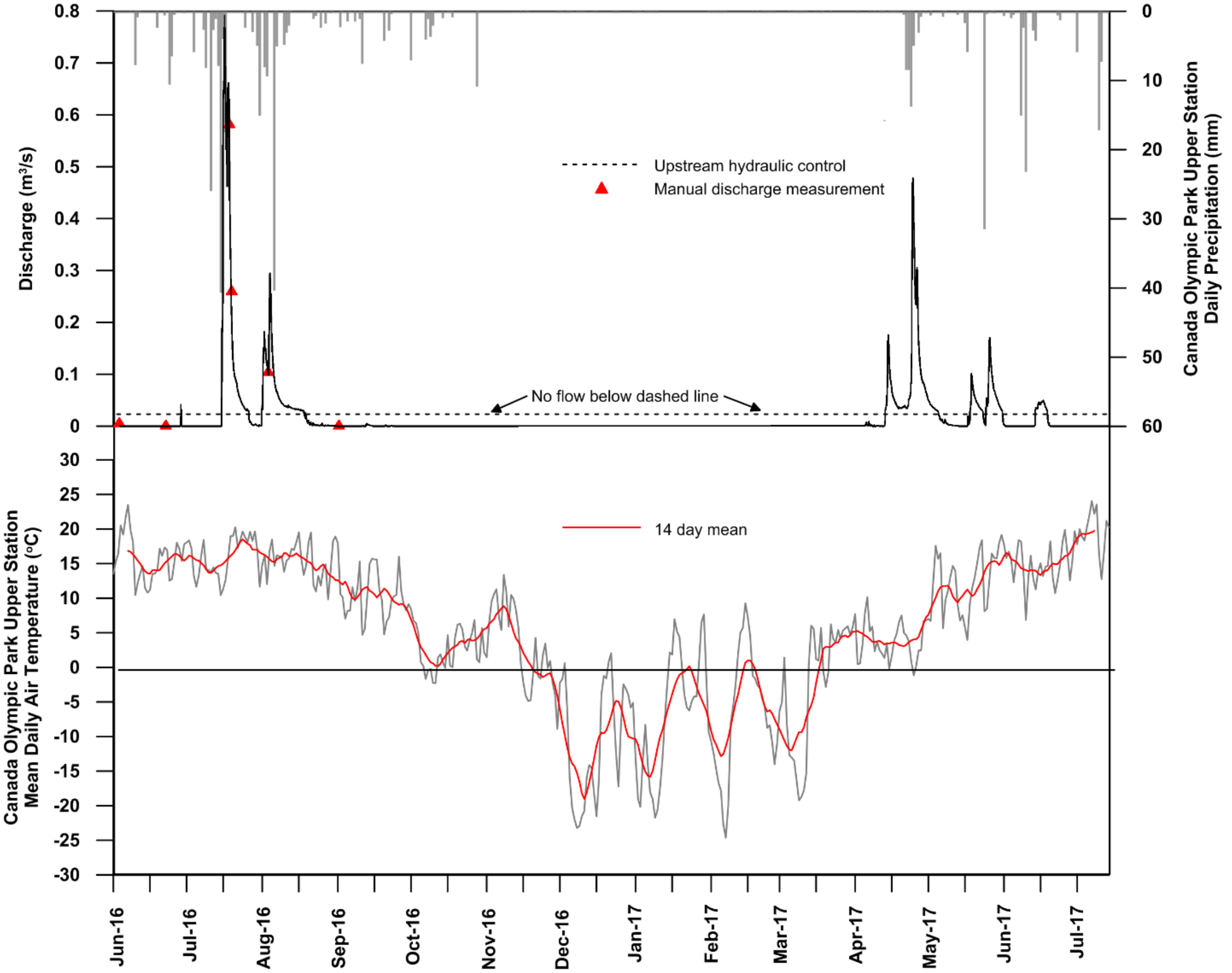

Figure 3-10 Hydrometeorology of the Unnamed Tributary, 2016- 2017

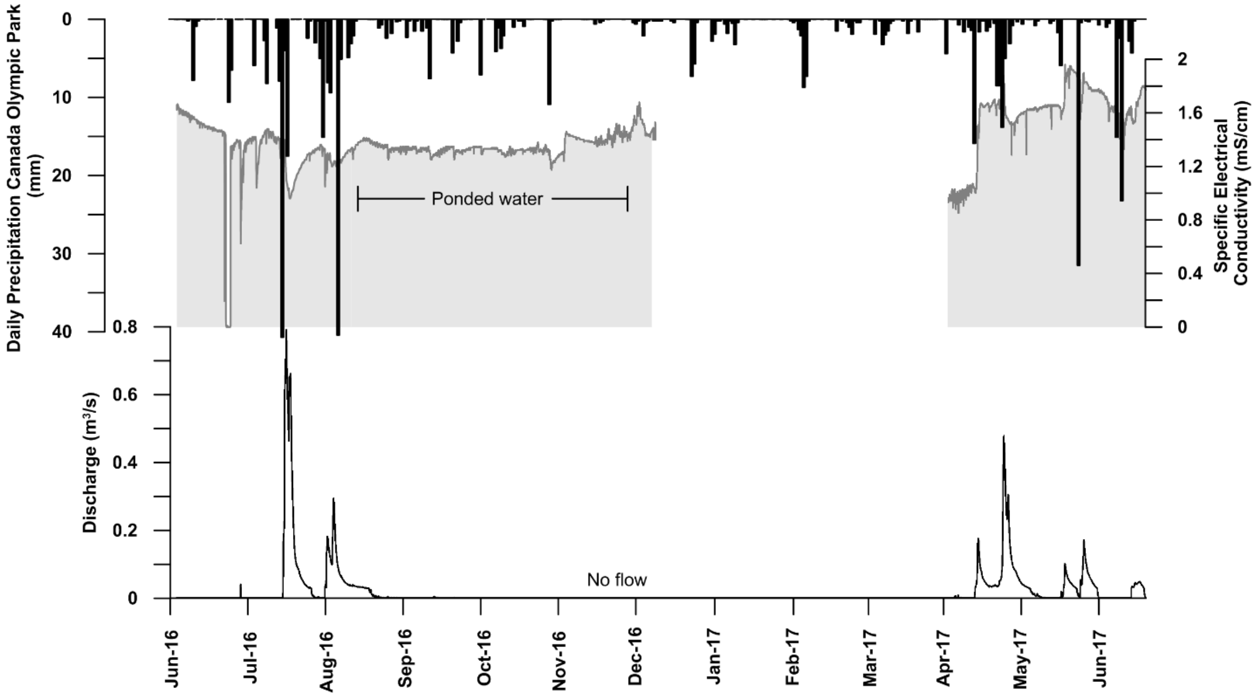

Figure 3-11 Response of Electrical Conductivity to Rainfall Events in the Unnamed Tributary

3.3.1.3 Waterbodies

There are several small, naturally co-occurring waterbodies within the project development area (PDA). As a result, runoff contributions will be intermittent and result in fluctuating water levels.

3.3.2 Water Quality

3.3.2.1 Total Suspended Sediment Concentrations

The rating curves generated for Bragg Creek, Highway 22, Twin Bridges and Sarcee Bridge show a positive relationship between TSS concentrations and discharge (Figure 3-12). Samples of TSS at discharge less than 10 m³/s dominate the data set with the maximum discharge sampled at approximately 100 m³/s. As expected, there is considerable variability around the fitted curves. Increased variability is present at the lower end of the TSS concentration/discharge pairs with less scatter at the higher end. Although the reduction in variability may reflect a stronger relationship between discharge and TSS at higher flows, it also reflects a lower sample size. As a result, the fitted curves and associated parameter values are sensitive to the number of samples contained within each bin. However, the slope values fit within the expected range of between 1 and 2 (Knighton 1998).

Although the slope values fit within the expected range, the values show a clear decrease in slope from 2.078 at Bragg Creek to 1.311 at Sarcee Bridge. Sites with high slope values have been interpreted as indicating that most sediment transport occurs with high discharge, as a function of sediment availability and higher erosive power for transport (Asselman 2000). As a result, large parts of the annual load is transported during high discharge. However, the decrease in slope values downstream in the Elbow River suggest that TSS concentrations decline with higher discharge downstream.

The decrease in slope values offers some insight into how the suspended sediment regime changes downstream in the Elbow River watershed. The slope value decrease can be interpreted as indicating that a significant proportion of fine sediment goes into storage between Bragg Creek and Sarcee Bridge during high flows. This storage may play a significant role in lowering downstream concentrations, and thus suspended sediment yields, during high flows as well as providing a sediment source during non-flood flow periods in the lower reaches. The remobilization of stored sediment likely explains why the rating curve parameters suggest that TSS concentrations at Sarcee Bridge are higher at low flows than at Bragg Creek. As low to medium flows dominate the Elbow River hydrological regime (Section 3.3.1.1), remobilization or winnowing of fine sediment deposited during high flows and inputs from sources within or near the City of Calgary likely control the overall TSS concentrations, and thus suspended sediment yields, of the Elbow River. This control within the lower reaches of the Elbow River has also demonstrated by Sosiak and Dixon (2006).

The dominance of low flows and associated TSS samples has implications for the estimation of TSS at flood flow levels. The maximum TSS recorded at Bragg Creek and Highway 22 for the period 1999 to 2016 was 3187 mg/L and 3570 mg/L for flows of 100 m^3/s and 71 m^3/s, respectively. As a result, no measured data exists to constrain possible TSS concentrations at flows over an order of magnitude higher than the maximum measured. In the absence of constraining data, the TSS-discharge relationships shown in Figure 3-12 were assumed to be applicable up to 1,000 m^3/s. This extension assumes that no curvature effects occur at high concentrations (Asselman 2000; Warrick 2015). A 1,000 m^3/s cutoff was used as it is an order of magnitude higher than the maximum discharge that TSS has been measured at and has only been exceeded in the instrumental record during the 2013 flood. This exceedance peaked at 1,170 m^3/s with flows above 1,000 m^3/s for a total of four hours.

Maintenance of the fitted relationships up to 1000 m^3/s generates peak TSS concentrations for the Design Flood of approximately 140,000 mg/L at Bragg Creek. This concentration equates to approximately 14% by weight and assuming a density of 2,650 kg/m^3, approximately 5% by volume. Although the validity of this estimate is unknown and is speculative, the concentration weight and volume percentages fall within the range of sediment concentrations associated with high magnitude floods.

High discharge flows of water and sediment in open channels during floods exhibit a wide range of sediment concentrations and sizes (Costa 1988; Knighton 1998; Pierson 2005). However, as sediment concentrations increase, the behaviour of the fluid shifts from Newtonian to non-Newtonian to viscoplastic. These transitions mark the boundaries between a water flood, hyperconcentrated flow and debris flows (Costa 1988). Although there is debate over the assigning of boundaries, water floods typically have sediment concentrations ranging from 1 - 40% by weight and 0.4 – 20% by volume (Scott 1988; Costa 1988). Although the estimated peak concentrations at Bragg Creek are well within this range, a limiting factor in generating such high concentrations in the Elbow River is sediment supply.

Sediment concentrations in the upper Elbow River watershed are typically supply limited (Hudson 1983). This supply is dominated by surface wash with occasional inputs from mass movement that connect with tributary channels as well as from river channel and valley wall erosion where toes are not protected by lag deposits or forest (Hudson 1983). However, the heavy rainfall and snow melt that produced the Design Flood resulted in widespread channel avulsions, debris flows and debris torrents that introduced significant amounts of sediment to the fluvial system in this area (Pomeroy et al. 2016). As a result, sediment transport during the Design Flood upstream of Bragg Creek was unlikely to be supply limited. Thus, the high suspended sediment concentrations indicated by the rating curve relationship coupled with high discharge may have been possible. However, recognizing the uncertainties surrounding the estimates of suspended concentrations at high discharges in the Elbow River, the values and data generated from them likely represent the upper envelope of reality and should be interpreted as hypothetical rather than absolute. As a result, TSS values generated for 2013 are only used in the modelling and are not used in any long-term metric analysis, unless noted otherwise.

Estimates of mean monthly along with maximum and minimum mean monthly TSS concentrations are summarized in Figure 3-13. As would be expected based on the hydrological regime, the data shows that the highest mean monthly concentrations, and associated variability, occur during the high flow period of June. Concentrations are higher at Bragg Creek and Highway 22, and then decline by approximately 30% downstream (Table 3-6). In contrast, downstream concentrations for the remaining open water months are typically between 100% and 400% higher (Table 3-6).

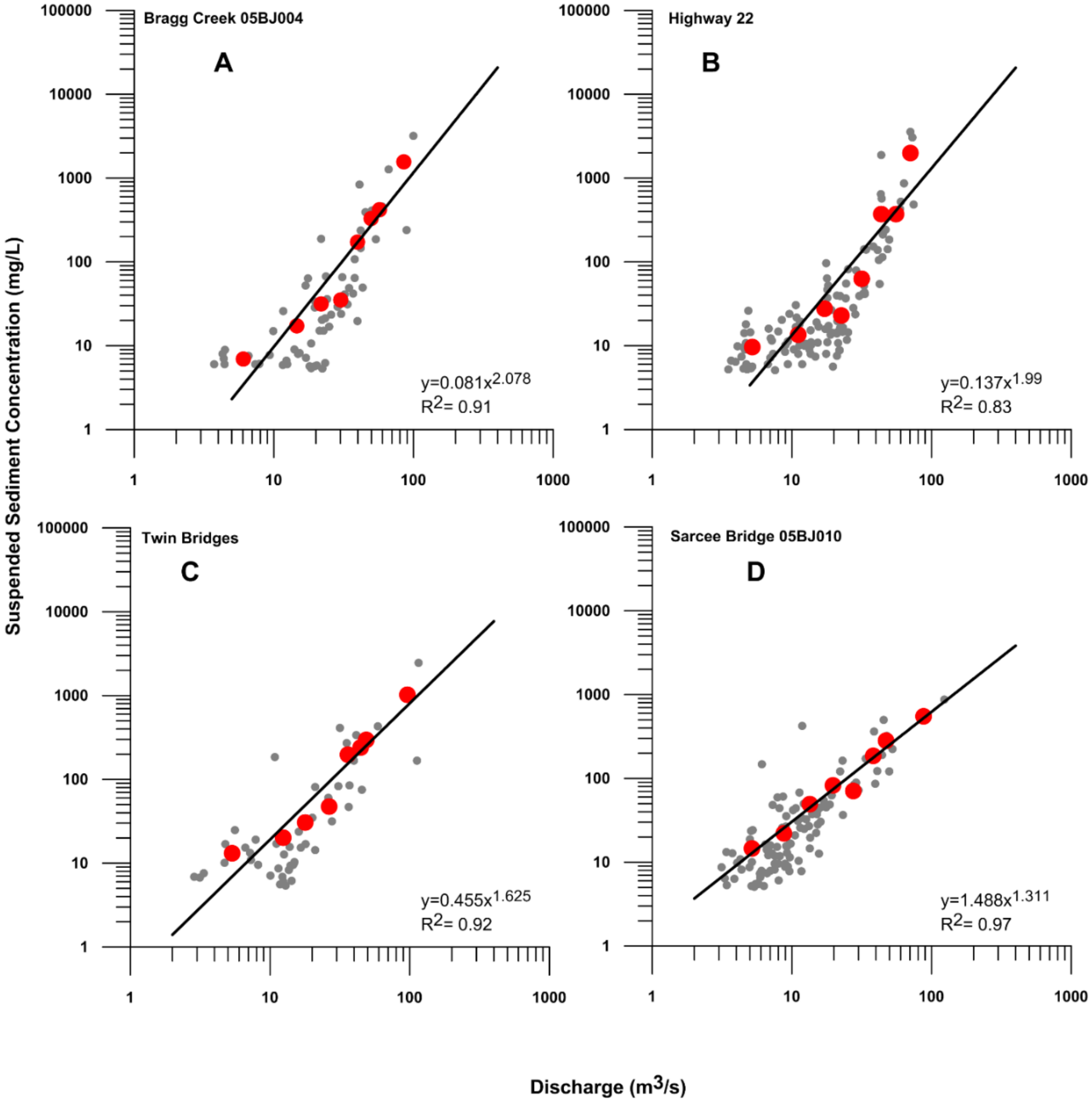

Figure 3-12 Suspended Sediment Concentration, Discharge Rating Curves

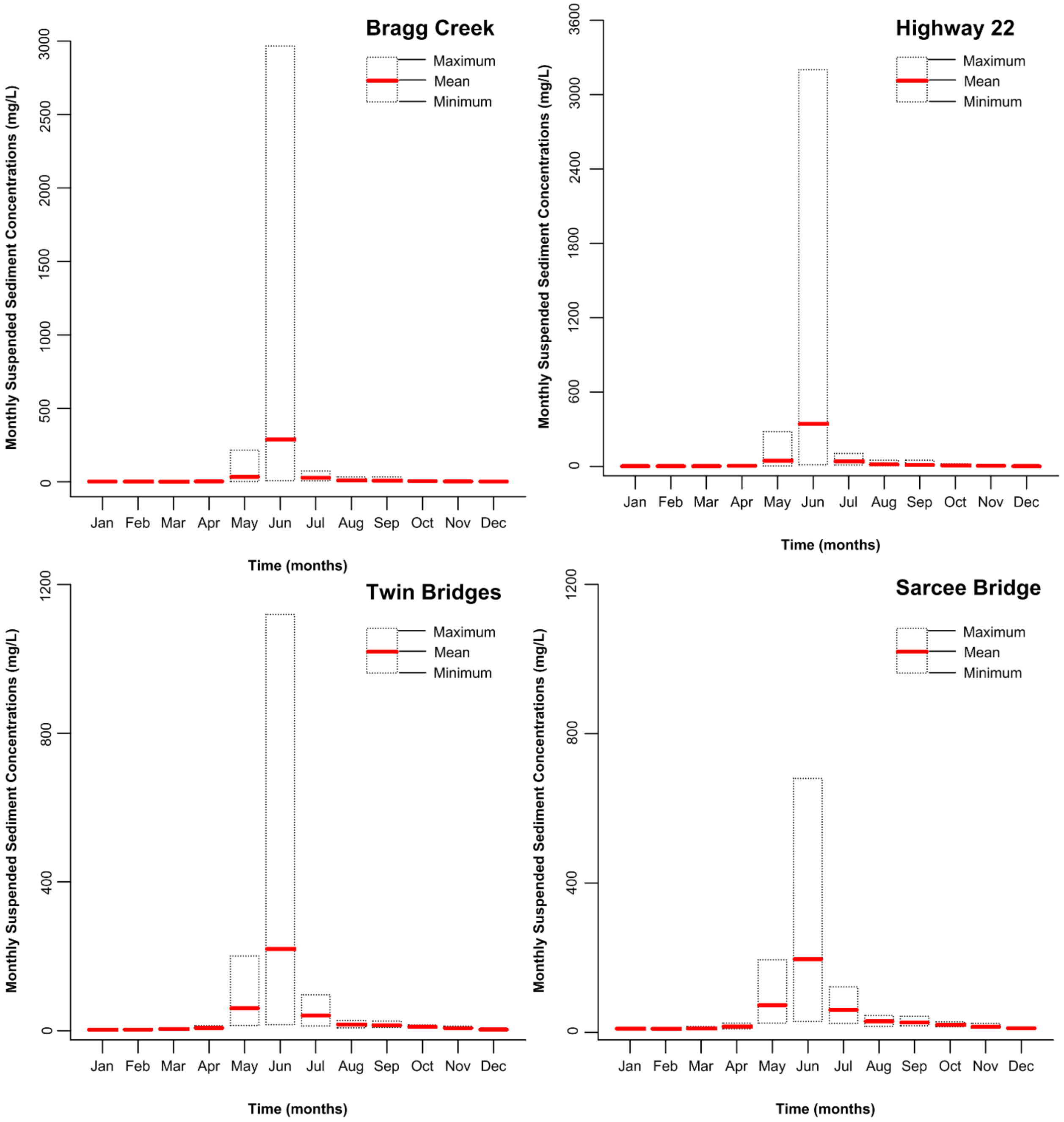

Figure 3-13 Historical Monthly Suspended Sediment Concentrations

Table 3-6 Estimated Mean Monthly Total Suspended Sediment Concentrations

	Jan	Feb	Mar	Apr	May	Jun	Jul	Aug	Sep	Oct	Nov	Dec
Bragg Creek (mg/L)	2	2	1	3	33	288	28	10	8	5	3	2
Highway 22 (mg/L)	3	3	4	7	60	219	41	16	14	10	7	3
Twin Bridges (mg/L)	3	3	4	7	60	219	41	16	14	10	7	3
Sarcee Bridge (mg/L)	10	10	10	15	72	196	60	30	26	20	15	11
Bragg Creek/Sarcee Bridge Difference (%)	400	400	900	400	118	-32	114	200	225	300	400	450

Conversion of the continuously measured turbidity to TSS was based on 11 grab samples. The range of concentrations represented by the grab samples is low, ranging from 1.5 to approximately 70 mg/L. As a result, higher TSS concentrations should be treated with caution. However, the dynamics of TSS as recorded by the turbidimeter at the project site is likely accurate. The TSS time series shows a clear pattern of TSS concentrations peaking on the discharge rising limb

3.3.2.2 Total Dissolved Solids Concentrations

The TDS rating curves generated for Highway 22 and Twin Bridges show a slightly negative relationship between TDS concentrations and discharge (Figure 3-14). The power curve parameters are similar for both Highway 22 and Twin Bridges with intercepts of 298 and 282 and slopes of -0.168 and –0.144, respectively. These values are similar to those presented by Hudson (1983) who found an intercept of 320 and a slope of -0.189 at Bragg Creek. However, the values presented here for Twin Bridges differs from Hudson’s (1983) relationship for Sarcee Bridge. His data suggests an intercept of 405 and a slope of -0.238. He attributed the increase in slope steepness to increasing influence of groundwater downstream. However, as stated by Hudson (1983), the inclusion of more summer samples would flatten the rating relationship. As the data used here was sampled primarily during the open water period and the reduction in slope is reflected in the slope value for Sarcee Bridge.

The negative slope values show that concentrations decrease with increasing discharge because of dilution. Monthly variability in TDS concentrations shows this effect at both sites (Figure 3-15). Concentrations are highest during the winter month reflecting the dominance of groundwater maintaining baseflow which has a longer residence time and thus solute uptake (Knighton 1998). In contrast, the onset of spring melt dilutes TDS concentrations to their lowest point in May with a general increasing trend during June and July (Figure 3-15). This pattern is most evident at Twin Bridges.

The differences in TDS concentrations between Bragg Creek and Twin bridges likely reflects shifts in groundwater sources throughout the year. For example, borehole TDS data from within the PDA suggests that bedrock sourced groundwater has lower TDS concentrations than shallow groundwater contained within unconsolidated surficial deposits (see Volume 4, Section 5 Hydrogeology for more detail). This pattern suggests that TDS concentrations will vary throughout the year depending on relative contributions from each source and the sub-surface residence time (Grasby et al. 1999). Periods of high runoff would likely result in quicker pathways to the Elbow River through the upper unconsolidated surficial deposits. As these deposits contain higher TDS concentrations, they may explain the higher TDS concentrations and variability during spring and summer at Highway 22 as compared to Twin Bridges. Although the TDS concentrations at both sites show dilution with increasing flow, the only slightly negative slopes will result in increasing TDS loads with increasing discharge.

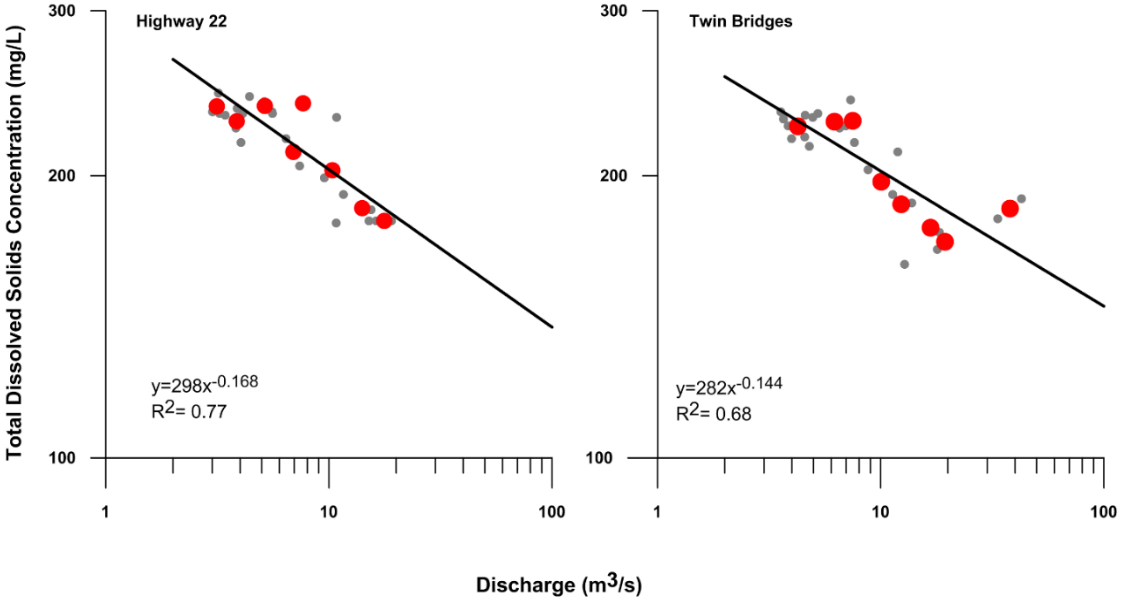

Figure 3-14 Total Dissolved Sediment Concentration, Discharge Rating Curves

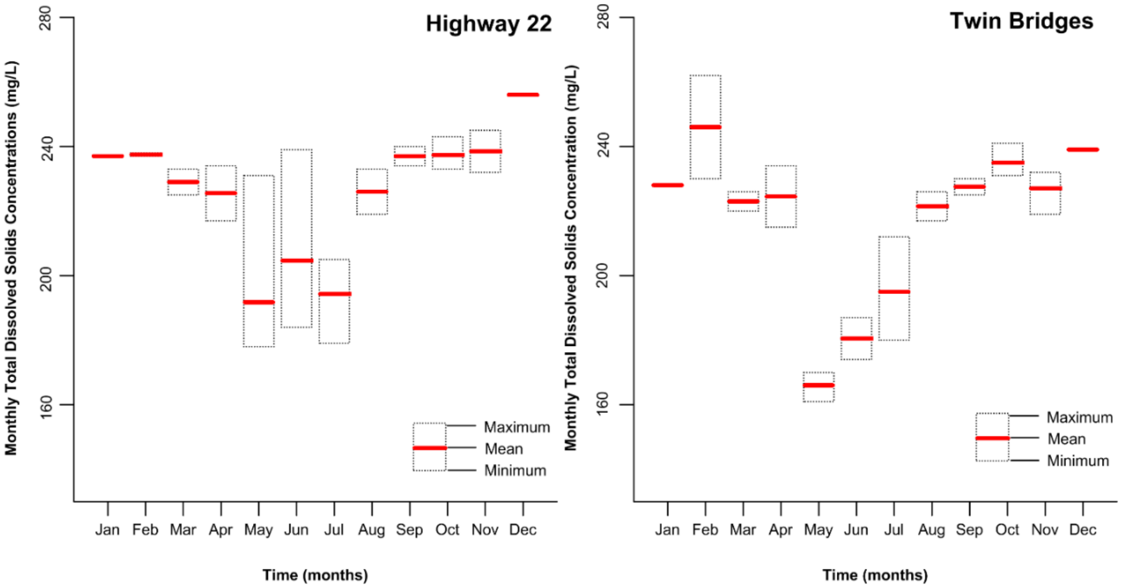

Figure 3-15 Historical Monthly Total Dissolved Solids Concentrations

Estimated TDS data based on electrical conductivity collected from the Elbow River at Highway 22 during 2015 – 2017 at 15-minute resolution have a similar value range and concentration pattern to that shown in Figure 3-16. TDS values in 2015 and 2016 clearly show the dilution effect of snowmelt in the upper watershed reducing concentrations in June. Concentrations then increase to peak in August in 2015. In contrast, prolonged rainfall in July 2016 had a significant dilution effect on TDS in the Elbow River which then resulted in an increase and maintenance of TDS concentrations at approximately 190 mg/L before a rapid decline in October to values less than 140 mg/L. In both years, TDS concentrations decline throughout September to November, in contrast to the pattern shown in Figure 3-15. Concentrations are also lower at around the 150 mg/L level as opposed to approximately 240 mg/L suggested by the long-term data for spring and fall. These discrepancies likely reflect the inability of the rating curve approach to capturing the detail of intra- and inter-annual variability.

TDS data from the Unnamed Tributary show a similar pattern of dilution with rainfall (Figure 3-17). However, TDS values are significantly higher than those measured in the Elbow River suggesting that there is significant groundwater contribution to the flow regime. Evidence of this groundwater contribution can be seen in the maintenance of high TDS values in the absence of flow. Field observations suggest that near surface groundwater flow was maintained for prolonged periods after rainfall events, resulting in the maintenance of steady, high TDS values (Figure 3-17). This near surface groundwater resulted in no measurable flow, but could maintain pooling in channel bed gravel depressions. If extended dry periods were experienced, eventually this near surface water table would decrease to below the channel surface with resulting zeroing of TDS values (Figure 3-17).

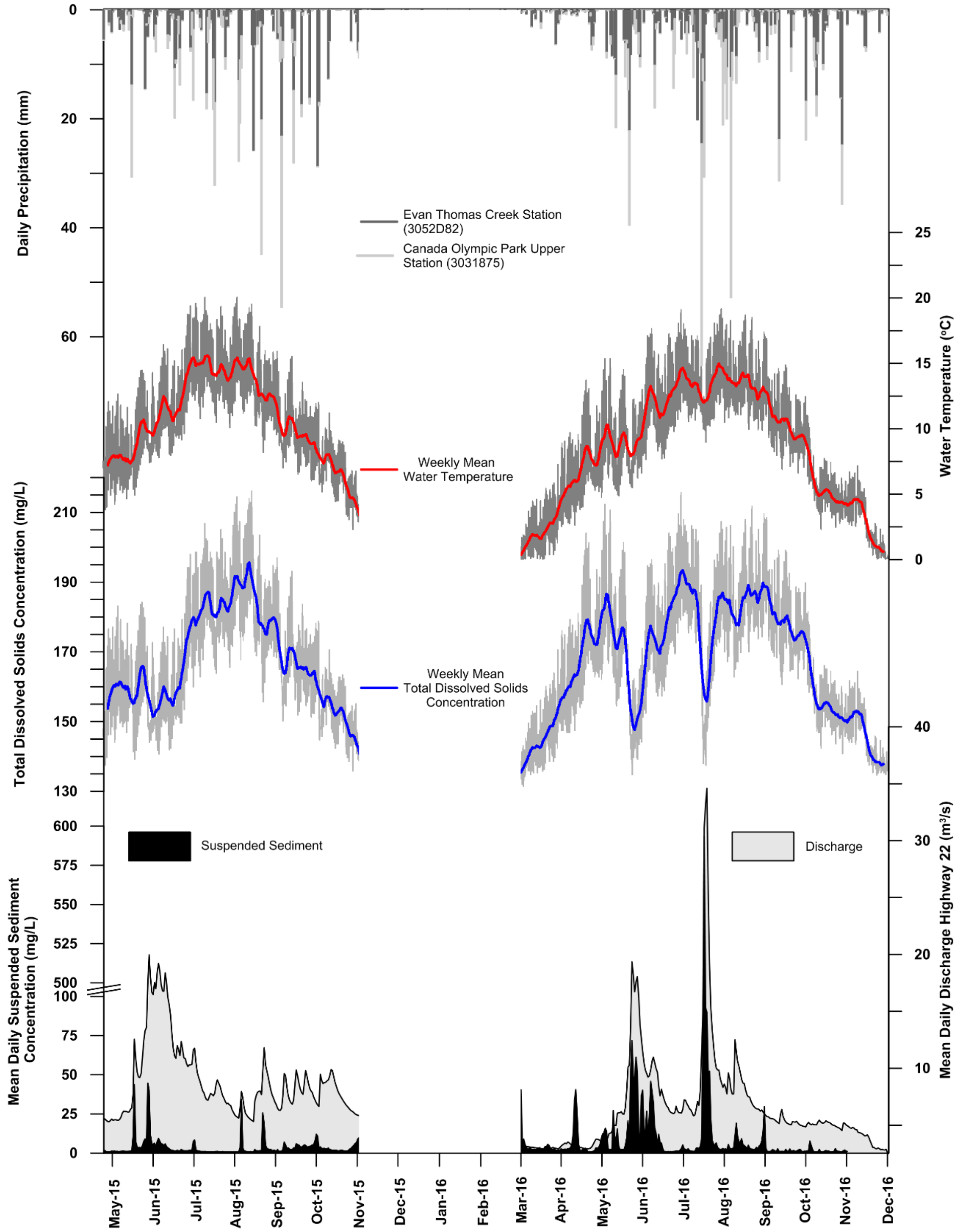

Figure 3-16 Continuous, 15-min Resolution Suspended Sediment and Total Dissolved Solids Concentrations at Highway 22, 2015-2016

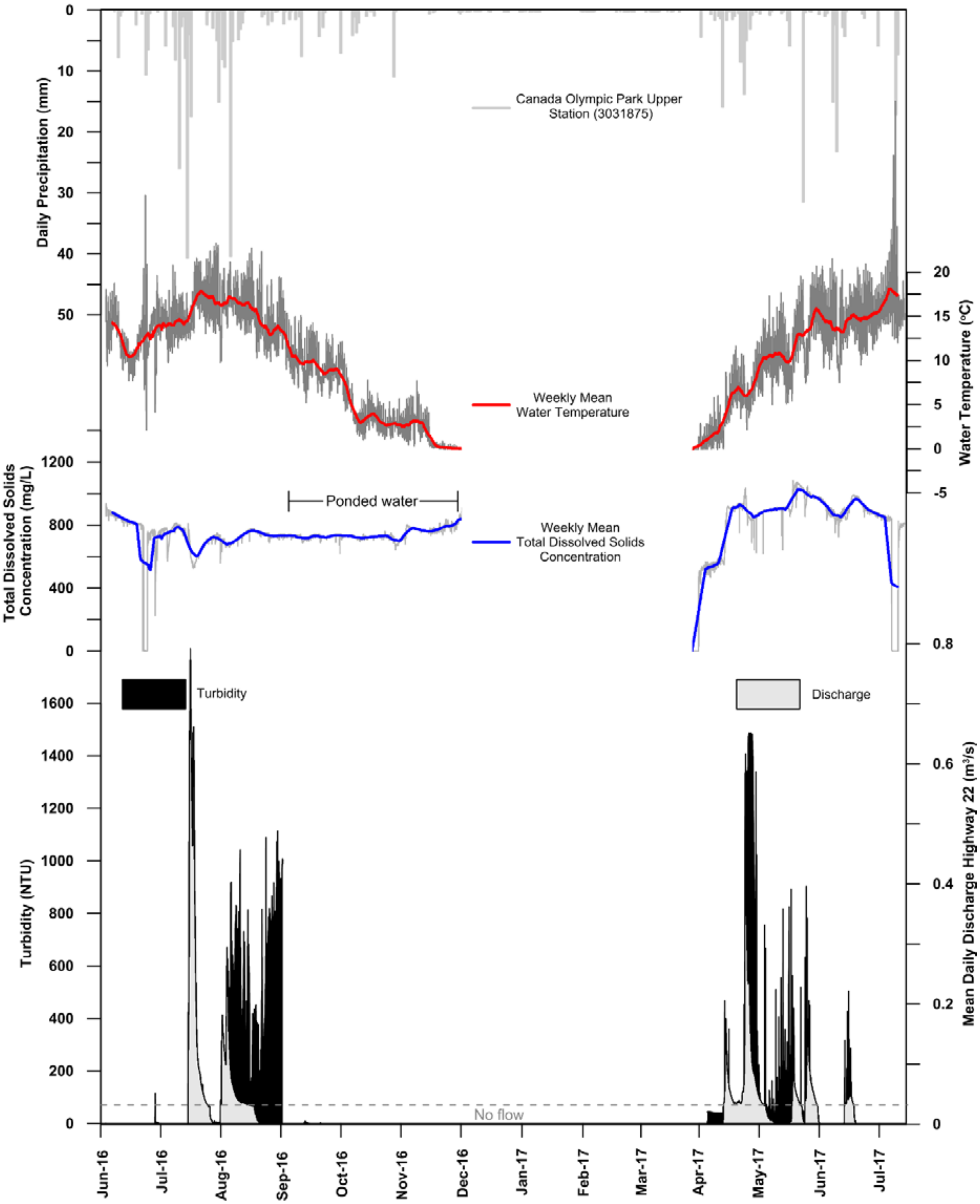

Figure 3-17 Continuous, 15-min Resolution Suspended Sediment and Total Dissolved Solids Concentrations at the Unnamed Tributary, 2016-2017

3.3.3 Grain Size Distribution of Surface and Shallow Sub-Surface Sediment in the Elbow River

Sediment characteristics play a critical role in the ability of a given flow to mobilize, transport and deposit bed sediment. Although surface GSD give valuable information, for example, on the degree of armouring in a river system and an indication of the coarser range of material transported during floods, the shallow subsurface GSD better reflects the sediment likely to be actively transported as a stream's bedload (Parker et al. 1982; Dietrich et al. 1989).

Surface and shallow subsurface particle size analysis results were run on sediment samples from 14 bar sites located between Redwood Meadows and Glenmore Reservoir (Figure 2-2). Particle size distributions were estimated using a combination of field based and lab based sieving with additional data provided by photo sieving of high resolution digital images using BaseGrain, a MATLAB based automatic object detection software tool (Detert and Weitbrecht 2013). A total of 14 sites were physically sampled for surface and sub-surface particle size distributions. A total of 14 sites were physically sampled for surface and shallow sub-surface particle size distributions. A further 36 surface sites were sampled using photo sieving. Approximately 1,100 kg were sieved on-site for the surface particle size analysis; 822 kg sieved on-site for the shallow subsurface analysis with 236 kg of the on-site subsurface sample removed to the laboratory for fine fraction analysis using a combination of sieve and hydrometer analysis. Shallow subsurface samples were taken down to an average depth of approximately 0.3 m. Compliance with ASTM C136-71 minimum sample masses at each site are summarized in Table 3-7.

Table 3-7 Sediment Sample Minimum Mass Compliance

Sample Name	Surface Sample Weight (kg)	D_{max} (D_{90}) (m)	Sample Mass Required ASTM C136-71) (kg)	Compliant	Shallow Sub-Surface Sample Weight (kg)	D_{max} (D_{90}) (m)	Sample Mass Required ASTM C136-71) (kg)	Compliant
ER100	98.8	0.101	84	✓	90.3	0.060	38	✓
ER101	53.8	0.058	36	✓	59.6	0.056	34	✓
ER102	88.1	0.060	38	✓	75.2	0.057	35	✓
ER103	89.6	0.055	34	✓	62.3	0.052	30	✓
ER104	84.6	0.133	127	✗	68.2	0.063	41	✓
ER105	85.3	0.092	73	✓	64.5	0.075	54	✓
ER106	97.6	0.098	80	✓	31.8	0.061	39	✗
ER107	59.4	0.054	32	✓	44.3	0.046	26	✓
ER108	93.5	0.124	113	✗	63.1	0.073	51	✓
ER109	87	0.060	38	✓	62.6	0.048	27	✓
ER110	89.3	0.063	41	✓	65.8	0.093	74	✗
ER111	81.2	0.065	43	✓	60.7	0.063	41	✓
ER112	76.1	0.058	37	✓	63.1	0.042	22	✓
ER113	14	0.049	28	✗	10	0.028	12	✗
Total	1098.3	-	803	-	821.5	-	525	-

The surface D_{50} from Redwood Meadows to the Weaselhead averaged approximately 37 mm and 29 mm (standard deviations of 15 mm and 10 mm, respectively) for field sampled and photo sieved samples, respectively (Table 3-8). These overall D_{50} values align closely with an average surface D_{50} of 34 mm (pebble count) and 33 mm (photo sieving) presented by Klohn Crippen Berger (2016) in for three sites downstream of Twin Bridges. The D_{50} sampled here downstream of Twin bridges indicate an average of 32 mm and 29 mm for field sampled and photo sieved, respectively (Table 3-8).

The sub-surface D_{50} from Redwood Meadows to the Weaselhead averaged approximately 20 mm (standard deviation of 7 mm) (Table 3-8). Downstream of Twin Bridges, the average subsurface D_{50} was 17 mm with a standard deviation of 10 mm (Table 3-8). Similar to the surface averages, this data is in close accordance with that from Klohn Crippen Berger (2016). Their sampling suggests a subsurface D_{50} of 22 mm with a minimum of 19 mm and a maximum of 24 mm for their sites.

The surface particle size results suggest that there is considerable variability in particle sizes along the length of the Elbow River with no evidence of a clear trend in either D_{30}, D_{50} or D_{90} from section to section (Table 3-8 and Figure 3-18). Although the surface data suggests that there is currently no clear trend in particle size down the Elbow River, the D_{30}, D_{50} and D_{90} results for the subsurface samples suggest that there is a downstream fining trend. However, the variation in all shallow subsurface particle diameters also increases downstream, offsetting the apparent pattern of downstream fining.

Based on the surface and shallow subsurface GSD, the Elbow River is dominated by gravel sized material (2 – 64 mm) and coarse silt/sand (0.063 – 2 mm). For the subsurface GSD, gravels account for, on average, 77% and coarse silt/sand, 13% of the GSD. Fines account for 3%. Bore hole data collected by Stantec from the Elbow River floodplain near the diversion structure at depths of between 1.8 and 4.0 m show a similar GSD. Gravel sized fractions from the bore holes account for between 53% and 79% and sand sized fractions, 17% to 36% of the GSD. Fines accounted for less than 10% and are silt sized. The borehole suggests that the GSD percentages measured in on the active floodplain are maintained at depth, except for a slight increase in the percentage of fine particles.

The low percentage of shallow subsurface particles less than 0.063 mm suggests that most sub-0.063 m particles have been winnowed leaving a censored layer of coarse gravel with voids free of fines (Carling and Reader 1982; Bundt and Abt 2001). This type of bed stratification results in a higher proportion of fine in voids beneath the censored surficial layer, resulting in a fining of the subsurface material in comparison to the surface GSD, as typical of many gravel bed rivers. Although not strong, this pattern is observed for the Elbow River subsurface GSD data (Figure 3-18) and supported by the borehole data.

The ratio between the surface and shallow subsurface D_{50} can be used to indicate the degree of armouring in a river system and as a result, indicate sediment supply (Bundt and Abt 2001). Where the ratio is close to 1, rivers typically have a high sediment supply in contrast to ratios closer to 2, which indicates lower sediment supply. Analysis of the $D_{50\ \mathrm{surface}}/D_{50\ \mathrm{subsurface}}$ for the Elbow River suggests that surface armouring increases downstream and coarse sediment transport becomes increasing supply limited (Table 3-9 and Figure 3-18) (Dietrich et al. 1989).

Table 3-8 Elbow River Surface and Shallow Sub-Surface Particle Size Summary

Location		Surface – Field Sieved (mm)			Surface – Photo Sieved (mm)			Shallow Subsurface (mm)		
		D_{30}	D_{50}	D_{90}	D_{30}	D_{50}	D_{90}	D_{30}	D_{50}	D_{90}
Redwood Meadows to Highway 22 Bridge	ER100	40	54	101	24	36	75	12	25	60
	ER101	23	30	58	17	23	51	15	24	56
	ER102	22	30	60	20	29	64	12	22	57
	ER103	15	23	55	17	24	54	6	15	52
	ER104	37	56	133	23	37	107	12	24	63
	Avg.	**28**	**38**	**81**	**20**	**30**	**70**	**12**	**22**	**57**
	Std. Dev.	**11**	**15**	**35**	**3**	**6**	**23**	**3**	**4**	**4**
Highway 22 Bridge to Twin Bridges	ER105	41	56	92	24	35	96	16	30	75
	ER106	46	60	98	23	37	83	11	27	61
	ER107[1]	11	21	54	-[2]	-	-	7	13	46
	ER108	47	62	124	31	48	105	12	25	73
	ER109	12	24	60	14	22	54	4	13	48
	ER110	17	27	63	18	27	58	11	20	73
	Avg.	**29**	**42**	**82**	**22**	**34**	**79**	**10**	**21**	**63**
	Std. Dev.	**17**	**20**	**28**	**7**	**10**	**22**	**4**	**7**	**13**
Twin Bridges to Weaselhead	ER111	31	44	65	25	37	75	16	28	63
	ER112	19	28	58	20	30	62	8	15	42
	ER113	13	24	49	13	20	48	4	9	28
	Avg.	**21**	**32**	**57**	**19**	**29**	**61**	**9**	**17**	**44**
	Std. Dev.	**9**	**11**	**8**	**6**	**9**	**14**	**6**	**10**	**17**
Overall Average		26	37	71	20	29	67	10	20	54
Overall Standard Deviation		12	15	28	6	10	24	4	7	18

NOTES:

[1] ER107 represents the particle size distribution from the low-level outlet channel and is included in the Elbow River particle size data because sediment mobilized and transported from the low-level outlet channel is a sediment source for Elbow River.

[2] No appropriate photo sieving sites were identified for the low-level outlet.

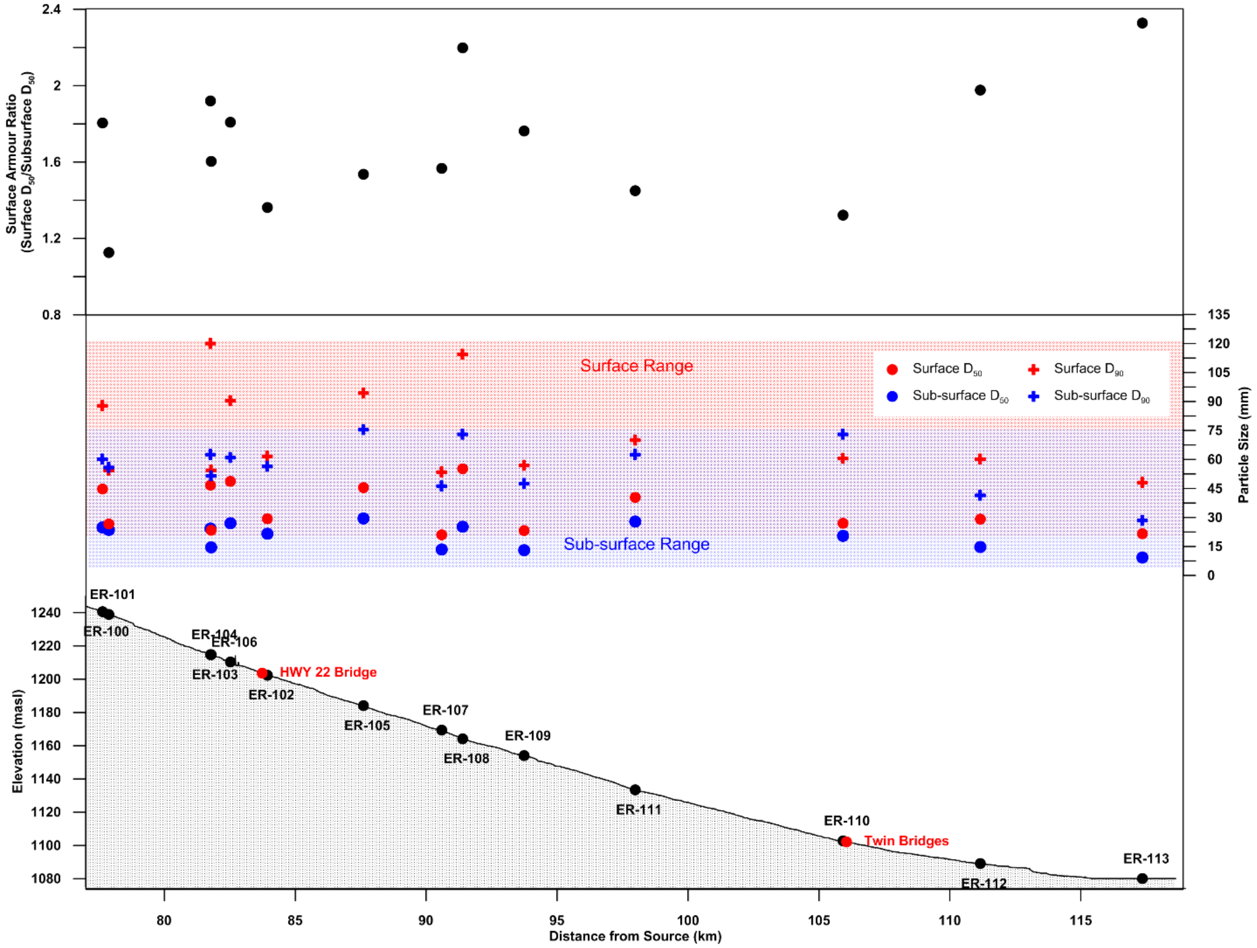

Figure 3-18 Surface and Shallow Sub-Surface Grainsize Distributions for Elbow River

Table 3-9 Degree of Bed Armouring in Elbow River

Location		Armour Ratio $D_{50\ surface}/D_{50\ subsurface}$
Redwood Meadows to Highway 22 Bridge	ER100	1.80
	ER101	1.13
	ER102	1.36
	ER103	1.60
	ER104	1.92
	Avg.	**1.56**
	Std. Dev.	**0.32**
Highway 22 Bridge to Twin Bridges	ER105	1.54
	ER106	1.81
	ER107	1.57
	ER108	2.20
	ER109	1.76
	ER111	1.45
	Avg.	**1.72**
	Std. Dev.	**0.27**
Twin Bridges to Weaselhead	ER110	1.32
	ER112	1.98
	ER113	2.33
	Avg.	**1.51**
	Std. Dev.	**0.71**

3.3.4 Sediment Yield

3.3.4.1 Total Suspended Sediment and Total Dissolved Solids

Total suspended sediment concentration (TSS) data for the Elbow River, was sourced from two datasets, one long-term and one site specific to the Project. The long-term data sets were sourced from Alberta Environment and Parks and the City of Calgary water quality data bases (see Appendix D4 for detail). This data set represents 12 sampling sites that have been combined into four locations, Bragg Creek, Highway 22, Twin Bridges (Highway 8) and Sarcee Bridge and consists of discrete samples of TSS. Although data has been collected some sites since 1979, a common period of 1999-2015 was used in this analysis. Site specific data was collected on Elbow River at Highway 22. Data from this site consists of continuous TSS for the period 2015 to 2017 and 2016 to 2017, respectively.

Longer-term suspended sediment yields were estimated for Bragg Creek, Highway 22, Twin Bridges and Sarcee Bridge using site specific TSS-discharge rating curves. These curves were generated using measured hourly discharge values for the Bragg Creek station obtained from the WSC for the period January 1999 to December 2016 and for March 2006 to December 2016 for the Sarcee Bridge station (Lazowski 2016, pers. comm.). Flow and stage data for 2014, 2015 and 2016 is provisional and subject to change. Data from 2013 was not included (see Section 3.3.2). Hourly flow records are not available for Highway 22 and Site Twin Bridges. As a result, hourly discharge was estimated by scaling from Bragg Creek and Sarcee Bridge stations, respectively. Scaling was applied using the single station method of Watt et al. (1989) with an exponent of 0.8, calibrated to flows measured at Highway 22. The resulting TSS-discharge rating curves were defined using a group averaging approach. These averaged curves were then applied to mean daily flows for the period 1979 to 2016 to estimate daily suspended sediment yields as a function of mean daily flow.

The estimated monthly, long-term, suspended sediment yields for Bragg Creek, Highway 22, Twin Bridges, and Sarcee Bridge are summarized in Figure 3-19 and Figure 3-20. These data suggest that there is considerable variation in both mean monthly flow volumes and mean monthly suspended sediment yields throughout the Elbow River system. However, as expected, the months with the highest mean flow volumes and yields, and highest variability, coincide with May and June. This timing suggests that most of the annual suspended sediment yield is transported during spring rainfall and snowmelt driven hydrographs.

Using the longer-term data, mean annual suspended sediment yields for Bragg Creek is estimated here as 28,684 t per year (36 t/km^2/a) for the period 1979 to 2016. The mean annual suspended sediment yield estimate for Bragg Creek is close to the estimate of 23,300 t per year for the period 1968-1969 and 1971-1975 by Ashmore and Day (1988a). Hudson (1983) estimated the long term annual yield for Bragg Creek as 18,200 t per year, based on estimated data for 1935 to 1979 with an average unit term of approximately 34 t/km^2/a. McPherson (1975) estimated the average suspended sediment yield for Bragg Creek as 26 t/km^2/a. The coefficient of variance for Bragg Creek suspended sediment yield is high at 197%, indicating considerable variability in suspended sediment yield from year to year.

Annual average suspended sediment yield is estimated at 33,974 t per year (29 t/km^2/a) for Sarcee Bridge (Figure 3-21). This contrasts with estimates of 75, 600 t per year estimated by Hudson (1983). However, Hudson's (1983) estimates had a significant variation of between 35,000 and 105, 000 t per year resulting in a unit term of between 29.6 and 88.9 t/km^2/a. This variability partially reflects the ratio methods and short record length used by Hudson (1983) and the inherent variance of suspended sediment yields within the Elbow River system. The coefficient of variance for Sarcee Bridge suspended sediment yield based on the data used in this study is reduced from that observed for Bragg Creek but is still high at 138%. Overall, the annual load data for 1979 to 2016 indicates that there is considerable variability in yields within the Elbow River and it is likely that this variability is largely a function of sediment source variation.

Suspended sediment sources in the Elbow River vary (Hudson 1983). However, Hudson (1983) notes that higher flows typically produce the greatest SSC values, and therefore sediment yields (Figure 3-19 and Figure 3-20). He attributed this to higher stages accessing the toes of banks and cliffs above any coarse lag toe protection at the base of banks, rather than sediment sourced in-channel or from upstream inputs. This process was estimated as occurring at flows higher than between 20 and 30 m^3/s, with recurrence intervals between 1.05 and 1.25 years (Hudson 1983). Field observations in 2015 and 2016 support this discharge range (Figure 3-22). Flows in June 2015 were generally below 20 m^3/s with suspended sediment concentrations typically below 50 mg/L. In contrast, flows greater the 20 m^3/s in July of 2016 resulted in suspended sediment concentrations of up to 600 mg/L (Figure 3-22). Closer examination of suspended sediment–discharge hysteresis in June and July 2016 also supports Hudson's (1983) hypothesis of suspended sediment sources.

Plots of suspended sediment concentration versus discharge typically show two types of hysteresis, clockwise and anti-clockwise. Clockwise hysteresis occurs when the concentration on the ascending discharge limb is higher than for the same discharge on the descending limb. Anti-clockwise is the opposite. Clockwise hysteresis has been used to infer near field sediment sources where there is rapid depletion of sediment stored in the channel (Beel et al. 2011) or sediment mobilized from sources close to channel banks (. Navratil et al. 2010). Anti-clockwise has commonly been interpreted as indicating delayed sediment input from upstream slopes (McDonald and Lamoureux 2009; Duvert et al. 2010; Beel et al. 2011). More complex hysteresis loops in a "figure-of-eight" are related to initial exhaustion followed be renewed supply later in the flood.

Hysteresis values during snowmelt driven flows in June 2016 show low SSC and weak clockwise hysteresis index values of between 0.11 and 0.16. Discharge peaked at less than 7 m^3/s in the example period (Figure 3-23). In contrast, SSC during the July 2016 high flow peaked at around 40 m^3/s with strong clockwise hysteresis Indexes of between 1.97 and 7.32 indicated. The peak flow of around 40 m^3/s is close to the bankfull discharge of approximately 47 m^3/s (recurrence interval of 1.54 years). The presence of strong clockwise hysteresis supports Hudson's (1983) hypothesis that although suspended sediment sources are varied in the Elbow River, higher concentrations are associated with near field erosion of channel banks and cliffs under higher stages, particularly downstream of Bragg Creek, rather than from upper watershed sources.

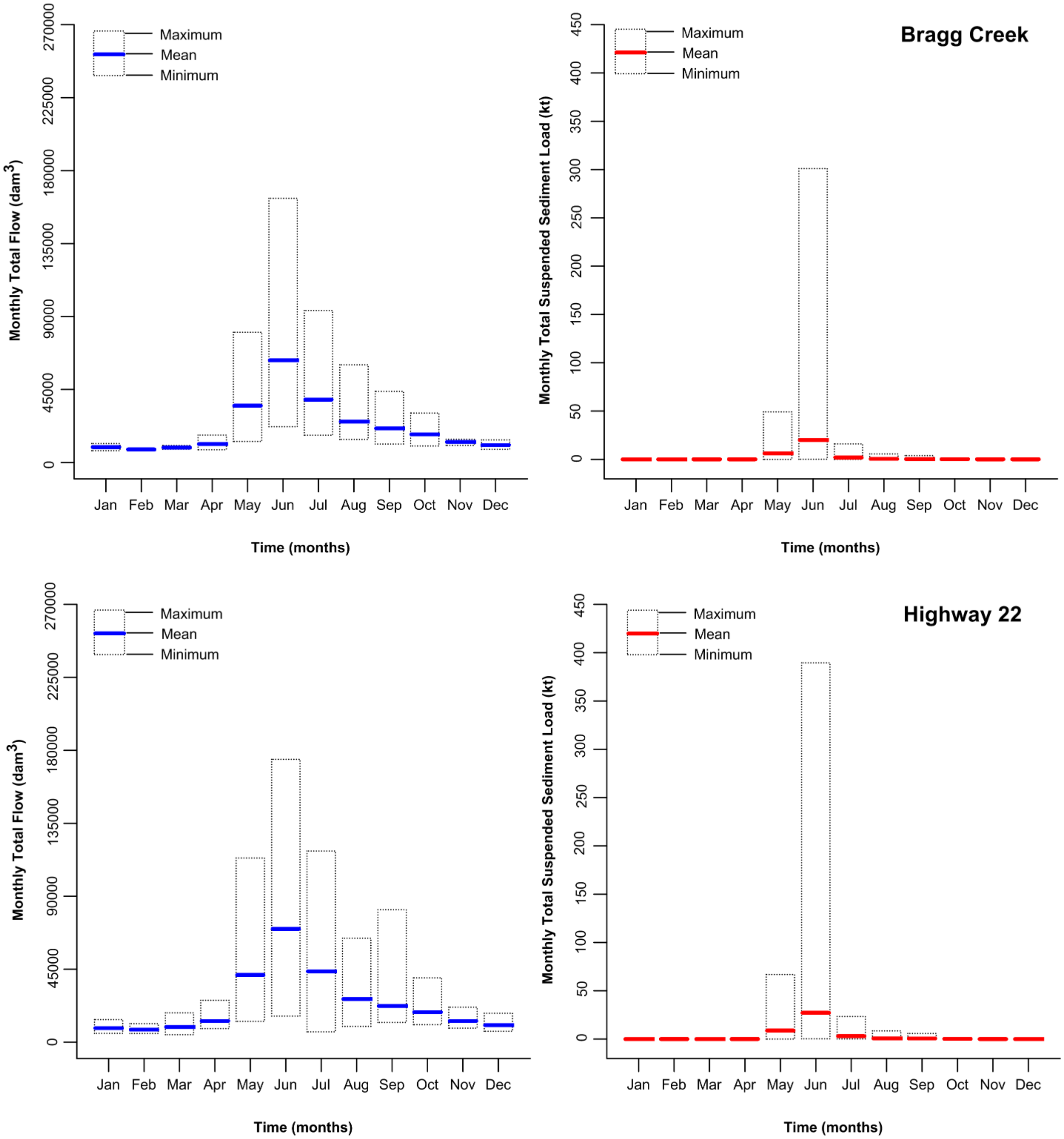

Figure 3-19 Historical Average Monthly Flow Volume and Suspended Sediment Yield at Bragg Creek and Highway 22, 1979 - 2016

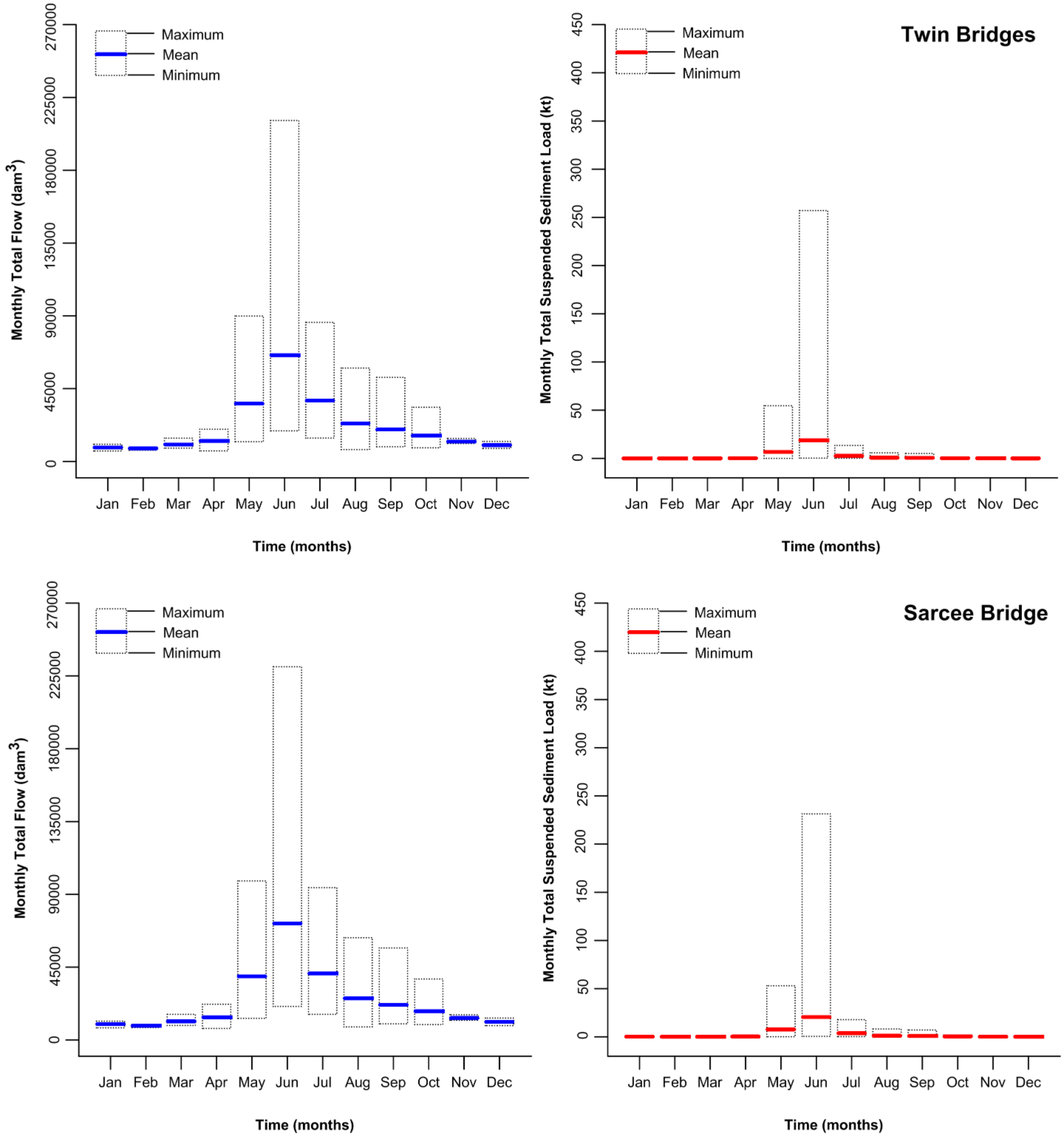

Figure 3-20 Historical Average Monthly Flow Volume and Suspended Sediment Yield at Twin Bridges and Sarcee Bridge, 1979 – 2016

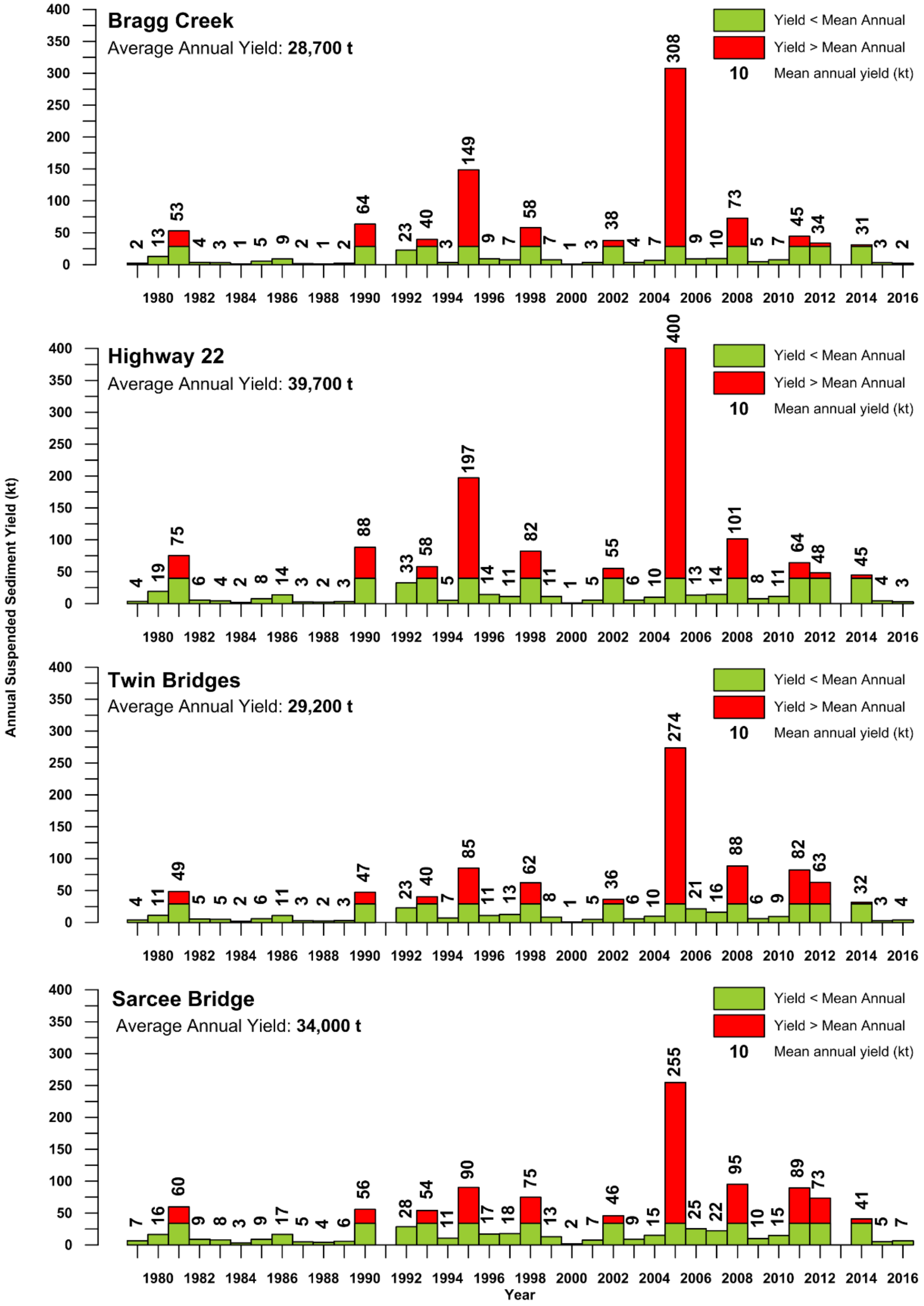

Figure 3-21 Elbow River Annual Suspended Sediment Yields, 1979-2016

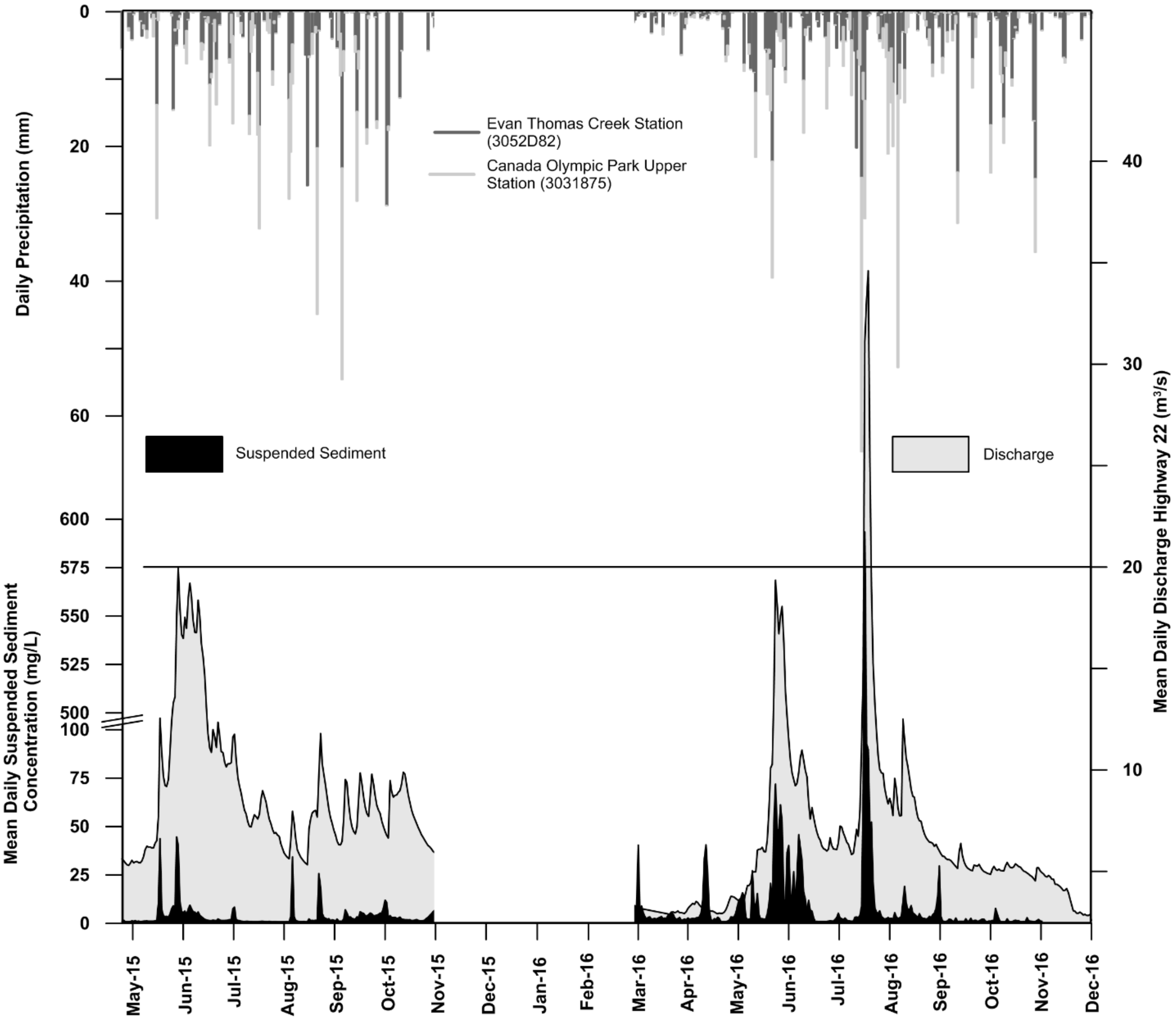

Figure 3-22 Mean Daily Suspended Sediment Concentrations and Flow at Highway 22, 2015 and 2016

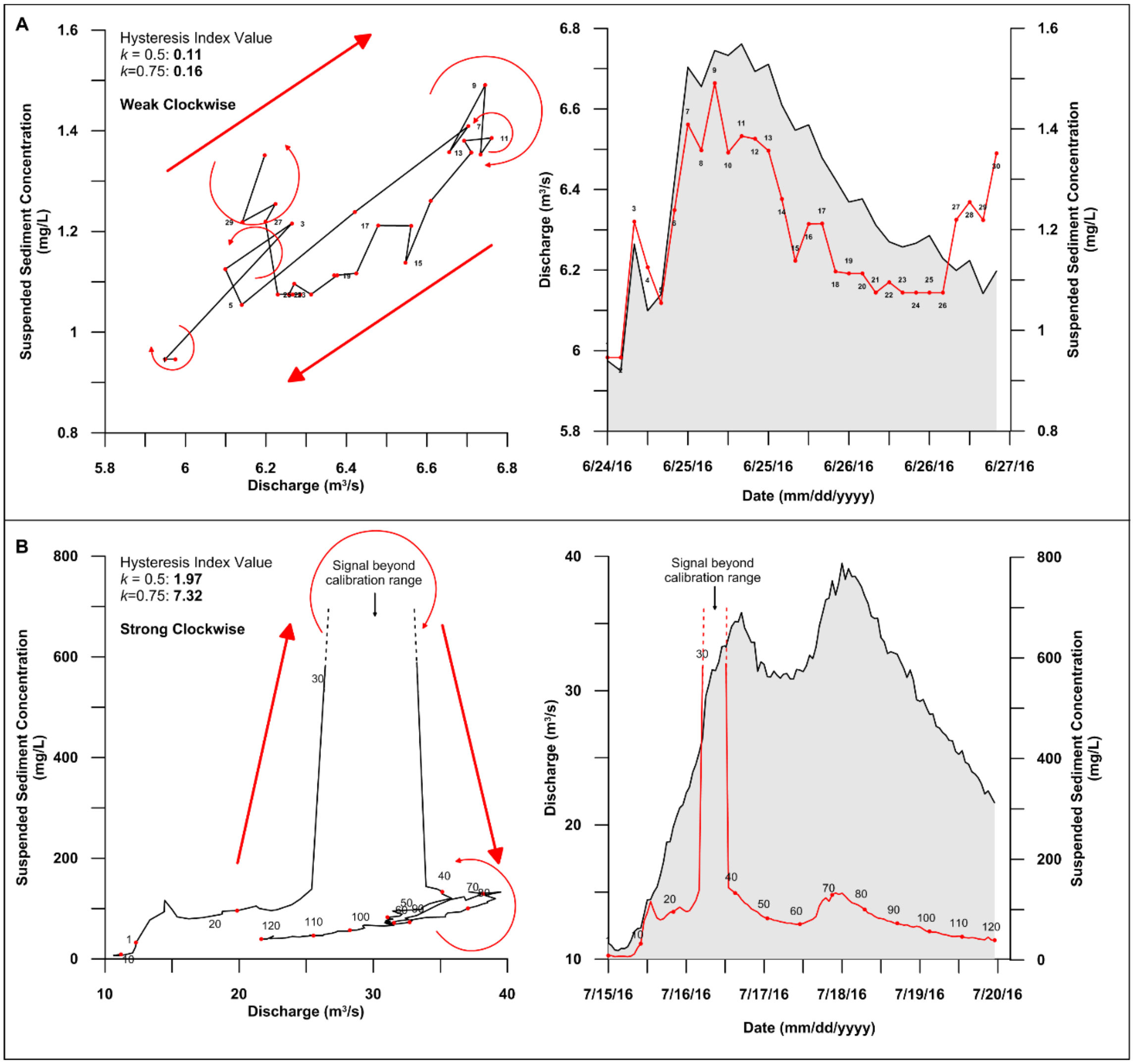

Figure 3-23 Suspended Sediment Concentration and Discharge Hysteresis at Highway 22, June and July 2016

Annual TDS yields show that yields are relatively even between years and locations (Figure 3-24). The average annual yield for Highway 22 is estimated as 54,600 t and for Twin Bridges, 54,400 t. These values are similar to those estimated by Hudson (1983) of 54,628 t for Bragg Creek (based on data from 1935-1979) and 65,925 t for Sarcee Bridge (based on data from 1935-1979). As noted by Hudson (1983), average monthly TDS yields are relatively even between months with the exception of May, June and July, reflecting the influence of spring runoff (Figure 3-25). As a result, the distribution of TDS yields closely mirrors the runoff regime. TDS concentrations also appear to increase downstream, specifically during May and June, paralleling discharge increases. However, on a per unit area basis, yields decrease from approximately 64 t/km^2/a to 51 t/km^2/a. A similar pattern was noted by Hudson (1983).

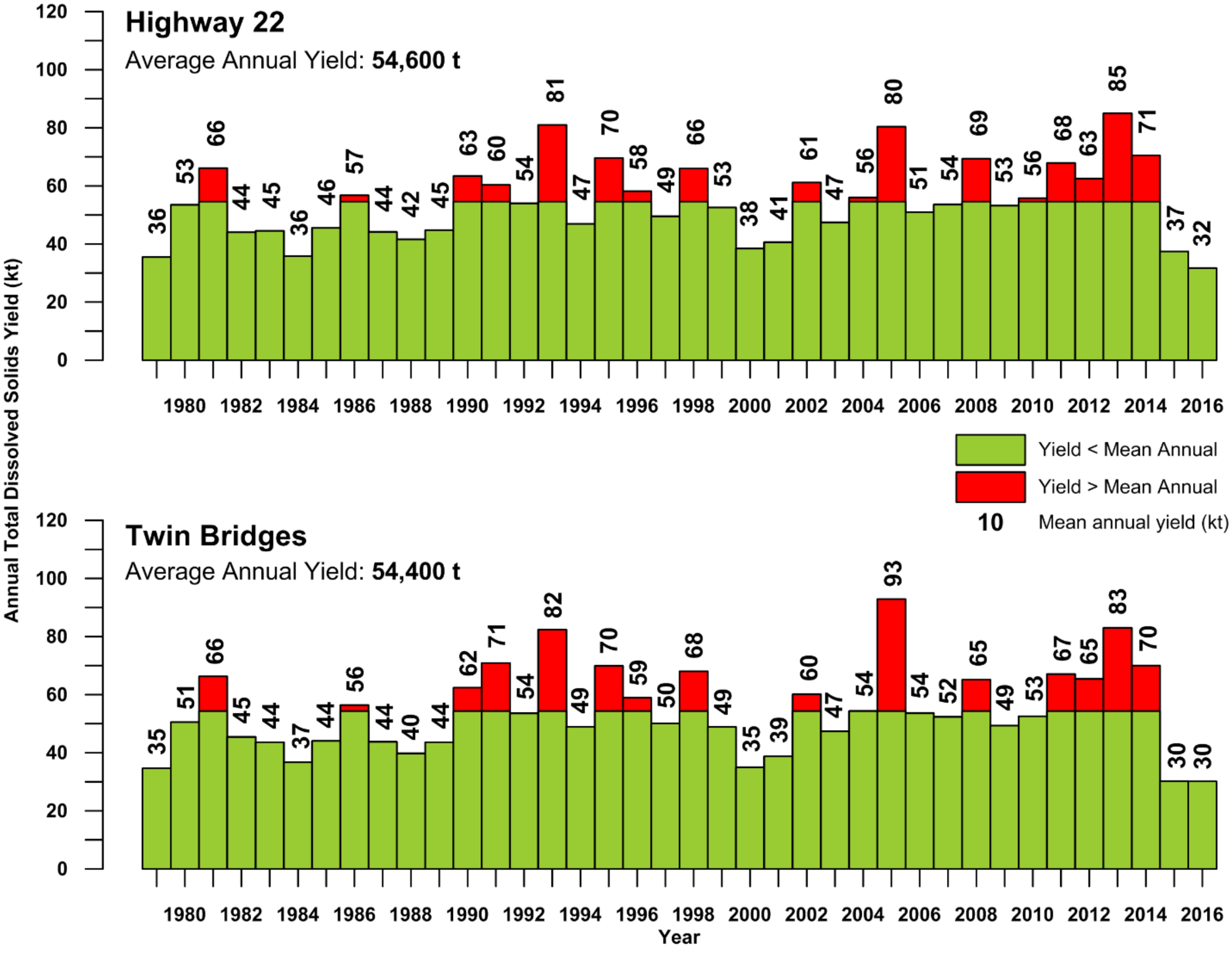

Figure 3-24 Elbow River Annual Total Dissolved Solids Yields, 1979-2016

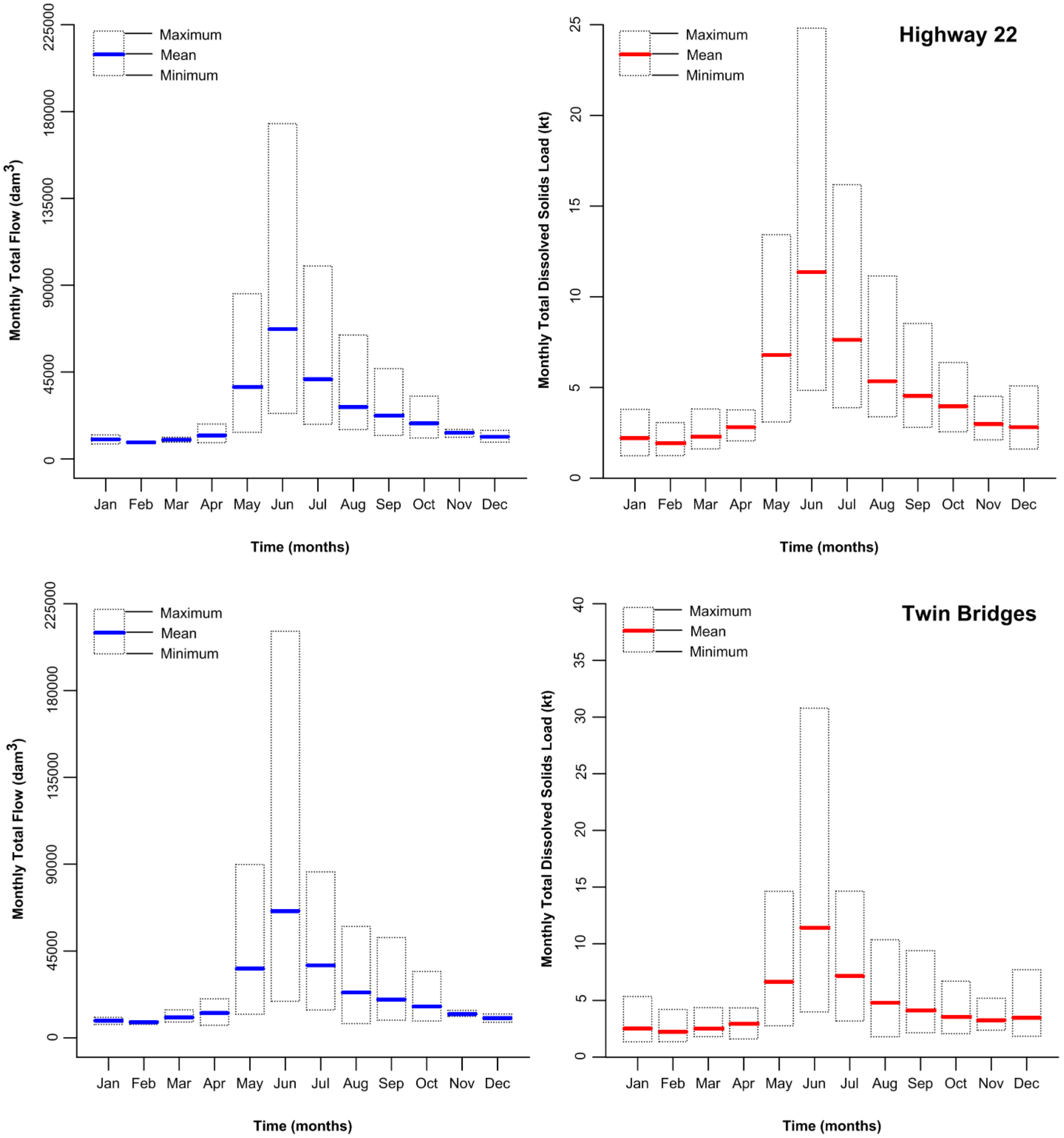

Figure 3-25 Historical Average Monthly Flow Volume and Total Dissolved Solids Loads at Highway 22 and Twin Bridges, 1979 – 2016

3.3.4.2 Bedload

There is limited field measured data on bedload transport rates in the Elbow River. However, in-river measurements using basket samplers by Hollingshead (1971) and Hudson (1983) suggest that bedload transport in the Elbow River varies considerably in space and time. Based on actual sampling of bedload at Bragg Creek, Hollingshead (1971) suggested that the bed is at the point of incipient motion at around 23 m^3/s. Hudson's (1983) measurements suggest that the relationship between discharge and bedload transport is proportional to approximately the 4th to 5th power of discharge. However, large variations in load have been reported for similar hydraulic conditions, primarily as a function of sediment-supply limited transport and spatial variability at both micro- and meso-scales (Hudson 1983).

Based on field measurements at Bragg Creek, Hudson (1983) noted that the shear stress required to mobilize thalweg deposits was approximate 146 N/m^2 which corresponds to a discharge of approximately 500 m^3/s. In contrast, the critical shear stress to mobilize bar deposits was approximately 56 N/m^2 (Hudson 1983). These differences suggest that bedload transport is primarily occurring over bars during high flows until boundary shear stresses exceed the critical shear stress for the armoured thalweg deposits. Based on Hudson (1983) mean annual bedload transport over a 15-year period are 13, 453 t at Bragg Creek and 1013 t at Sarcee Bridge. These differences reflect, in part, that there is significant bedload storage in sediment sinks through the course of the Elbow River, particularly where there are major changes in gradient (Figure 3-3). As noted by Hudson (1983), sediment is stored in slow moving waves which control local bedload sediment supply rates.

3.3.4.3 Effective Discharge

Analysis of suspended sediment loads and discharge at sites upstream and downstream of the diversion structures suggest that the effective discharge range, based on mean daily flows, for suspended sediment is between 35 and 50 m^3/s for all sites except Sarcee Bridge, which is between 15 and 29 m^3/s (Figure 3-26). The effective discharge is the flow that transports the most sediment. The Bragg Creek flows are equaled or exceeded between 3.4% and 1.2% of the time (12 days and 4 days per year, on average), respectively. At Sarcee Bridge, the effective discharge range is equaled or exceeded 19.7% and 6.8% of the time (72 days and 25 days per year, on average), respectively.

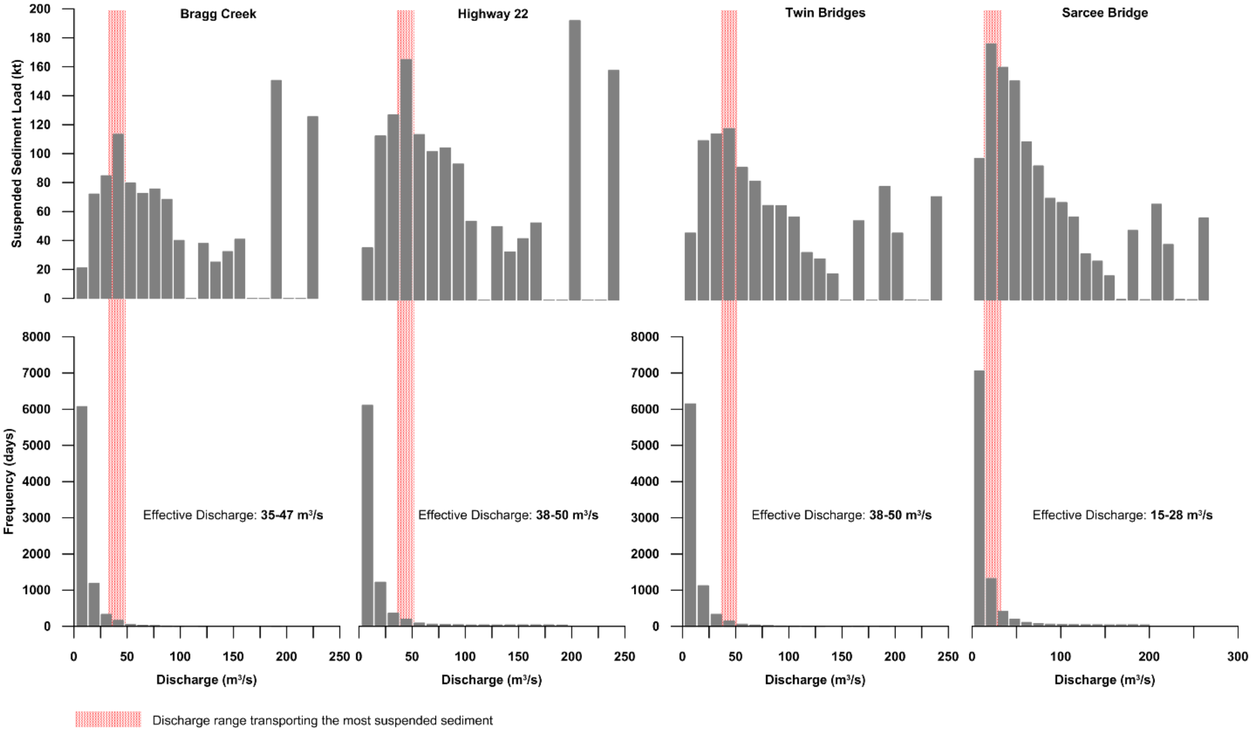

Figure 3-26 Effective Discharge for Suspended Sediment Transport

3.3.5 Ice Dynamics

Semi-quantitative observations of ice build-up and decay on the Elbow River near the Highway 22 bridge are used as an analog for ice dynamics in the vicinity of the Project diversion structures. Remote camera and continuous water level data show that freeze-up was rapid and occurred in less than 24 hours (Figure 3-27). Available field evidence suggests that anchor ice on the channel bottom combined with frazil ice likely resulted in a small ice jam across a riffle zone immediately downstream of the Highway 22 bridge. This jam caused water to back up behind the jam which then froze due to overnight temperatures on December 10th into December 11th falling to -21 °C. This ice layer remained in place until the start of in situ thermal degradation in March 2017, prior to the spring freshet (Figure 3-28). The thermal degradation took approximately 14 days from March 15 – 29. Minor water flow on the top of the ice sheet was observed from March 15 to 22. Complete collapse of the ice cover over the active channel occurred on March 23. No backwater effects due to ice jamming were observed during this thermal degradation.

December 10, 2016 16:00:00 h

December 11, 2016 16:00:00 h

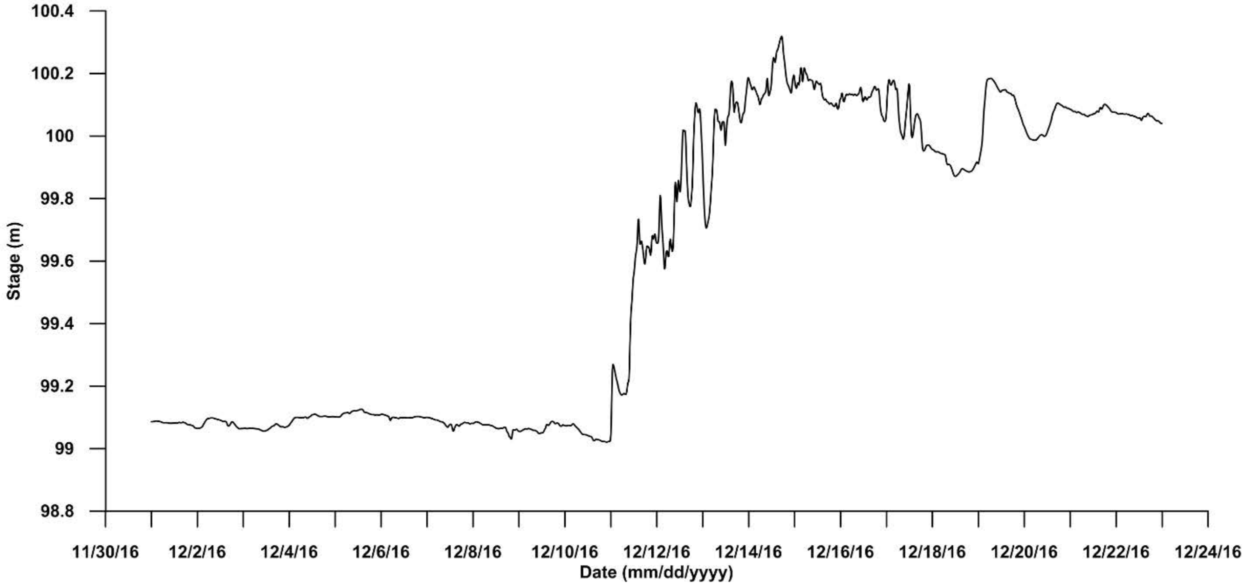

Figure 3-27 Ice Freeze up at Highway 22 Bridge, December 10-11 (2016)

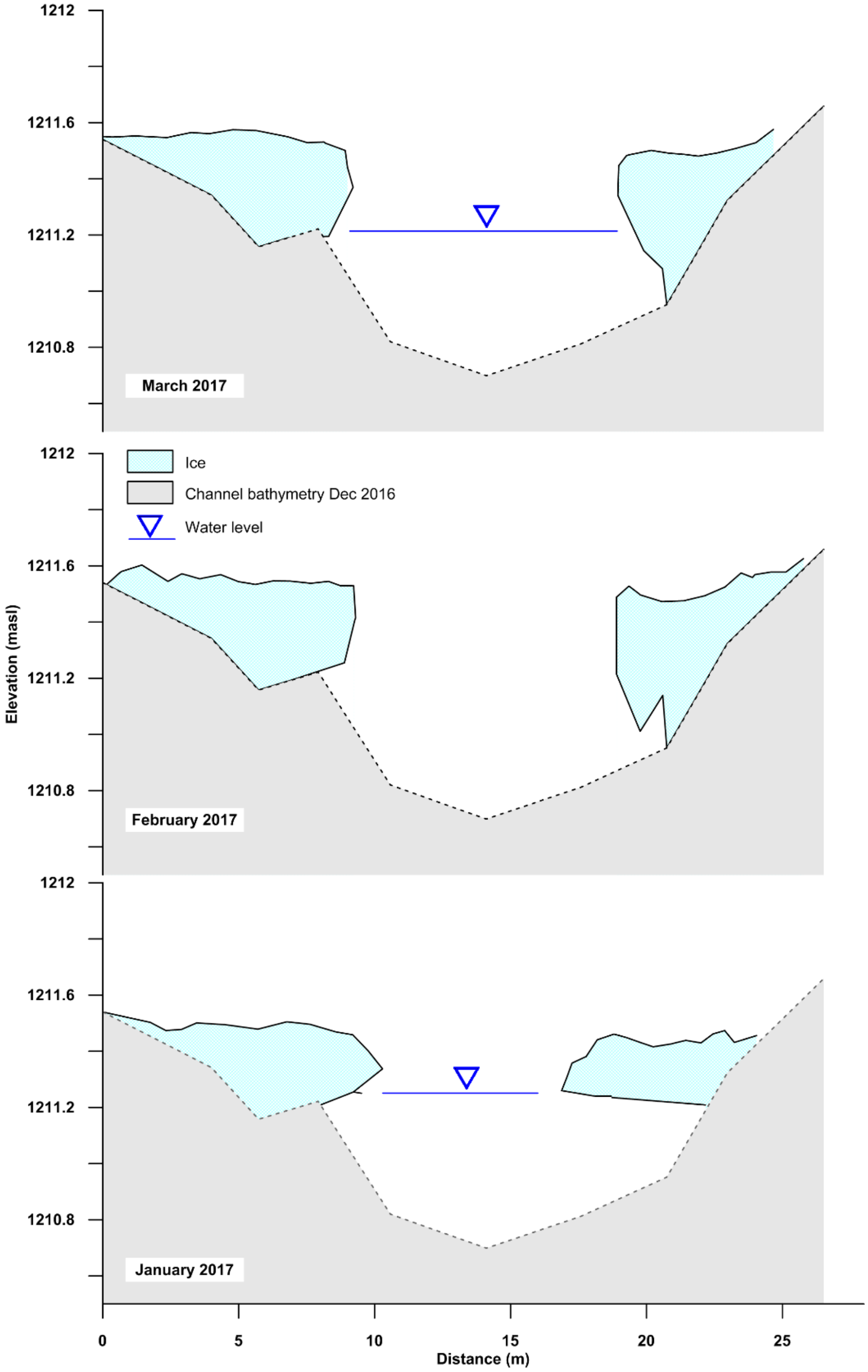

Figure 3-28 Ice Thickness Change at Cross Section 1, Winter 2016-2017

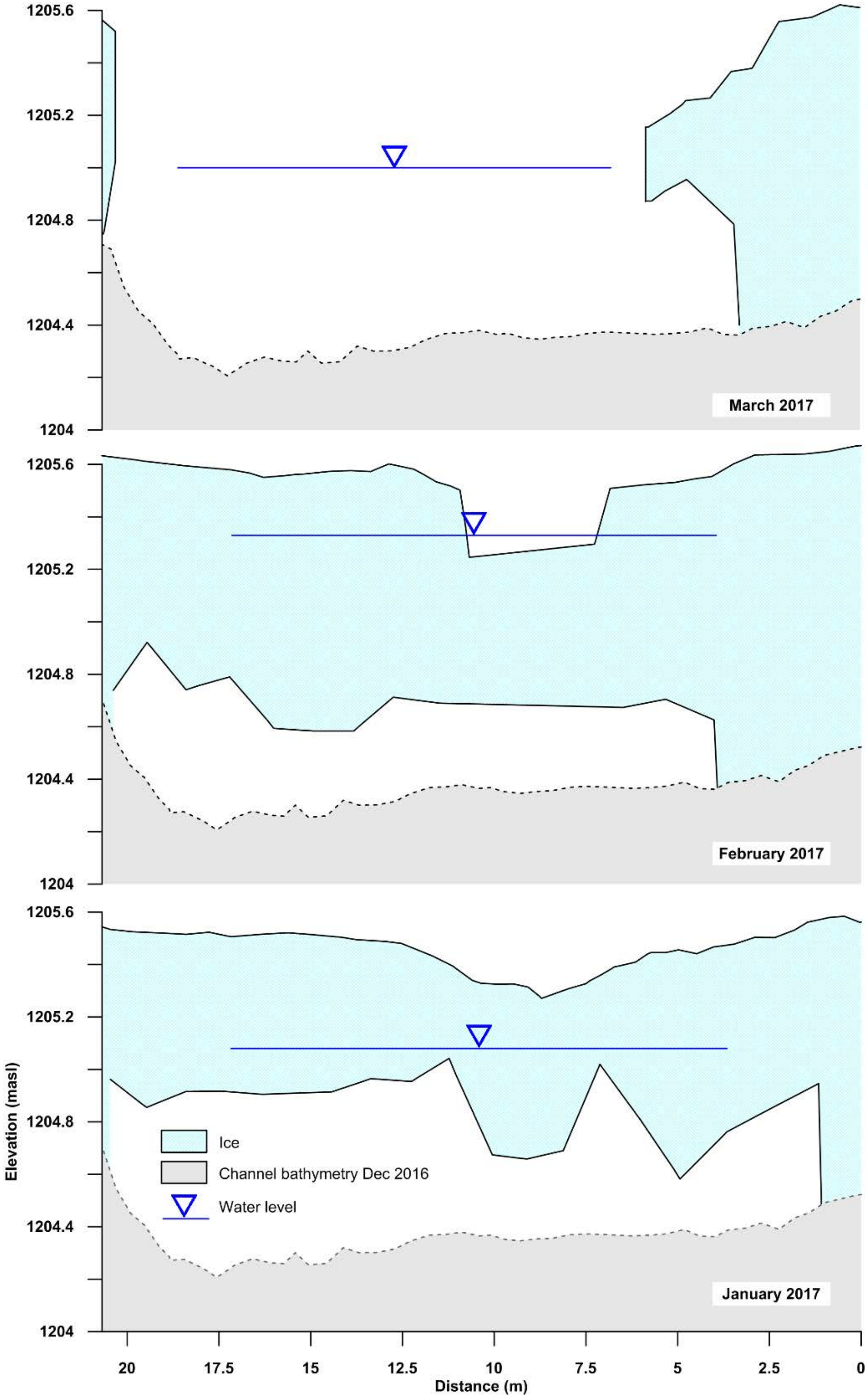

Figure 3-29 Ice Thickness Change at Cross Section 2, Winter 2016-2017

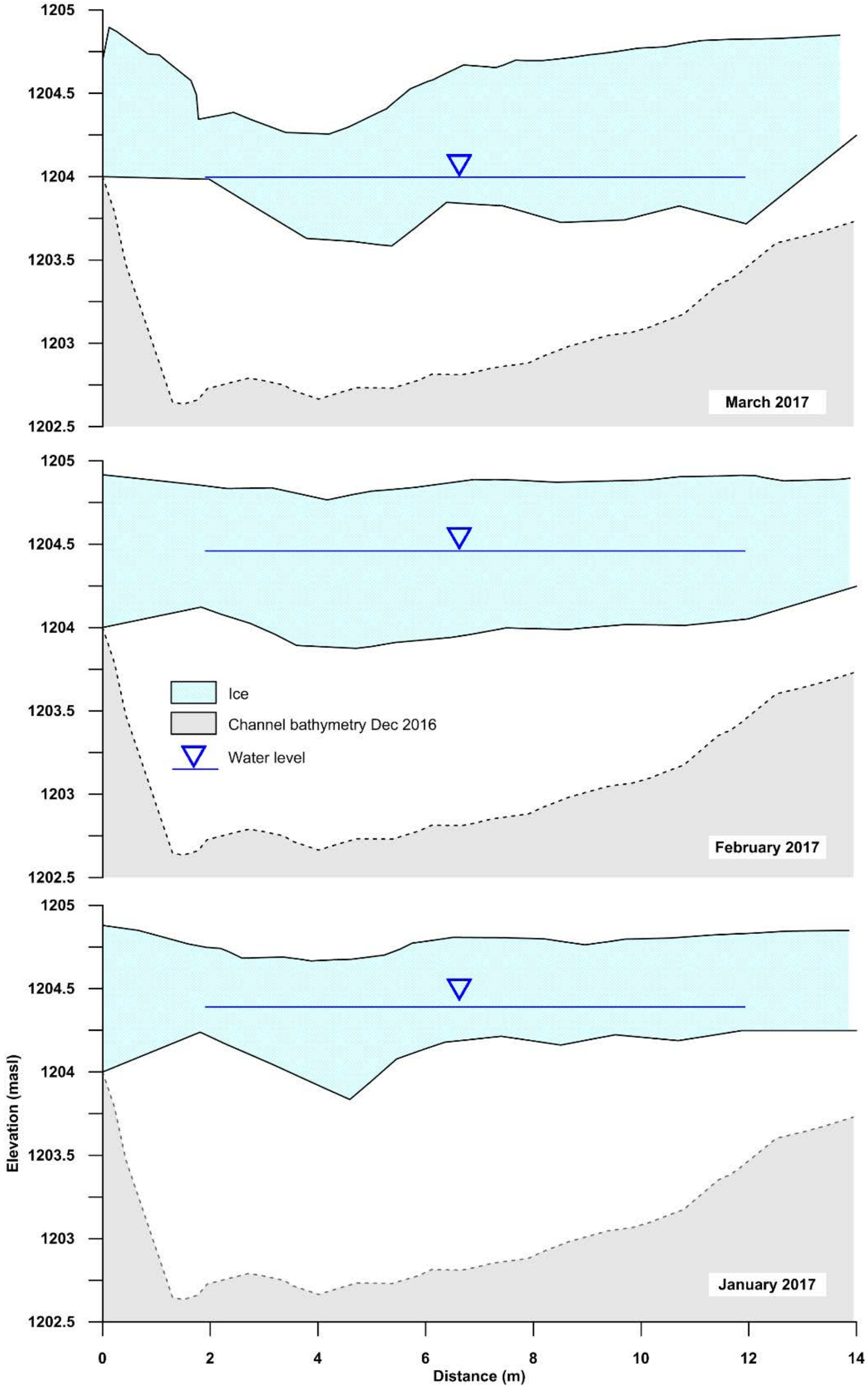

Figure 3-30 Ice Thickness Change at Cross Section 3, Winter 2016-2017

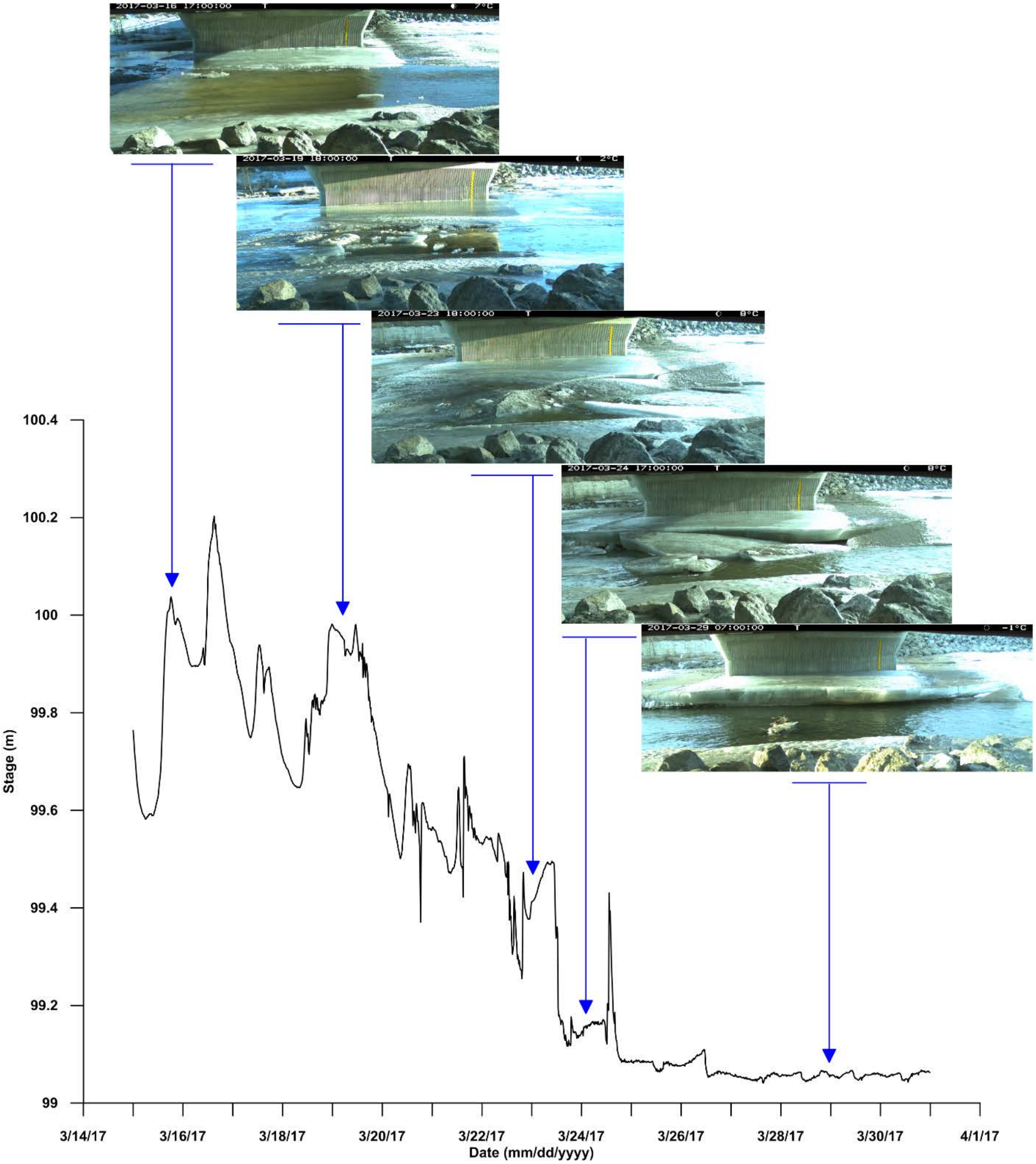

Figure 3-31 Ice Break Up at Highway 22 Bridge, March 16 – 29 (2017)

3.4 HYDRODYNAMIC MODEL

3.4.1 Calibration

The Mike 21 coupled model of HD and MT modules were calibrated using the water levels and suspended sediment concentration (SSC) measured at WSC stations in the model domain. The boundary conditions were defined by hourly discharges at Bragg Creek and daily water levels at Glenmore Reservoir dam. The following key parameters were calibrated:

- The choice of time step requires consideration of numerical stability and solution accuracy. Sensitivity model runs were conducted with various time steps 30 to 300 seconds. A time step of 60 seconds was then chosen for all model runs.
- The bed resistance value of Manning's roughness was varied from 10 $m^{1/3}/s$ to 45 $m^{1/3}/s$ in the model domain.
- Based on a Smagorinsky formulation, the eddy viscosity was set to a coefficient of 0.28.
- The bed critical shear stress was set to 23 N/m^2.

3.4.2 Sediment Transport and Geomorphology

The model results produced expected patterns of suspended sediment concentrations without diversion and with diversion under each of the three floods. As a result, these results are presented in Volume 3b, Section 6.0 and are not discussed here. The model results for degradation and aggradation suggest that the model is representing degradation/aggradation patterns in the Elbow River reasonably well. For example, degradation is shown as typically occurring on bar heads with aggradation downstream, as would be expected (Figure 3-32). The figure also shows that zones of aggradation and degradation reflect the underlying morphology shown in the satellite imagery. The results specific to each flood are presented in Volume 3B, Section 6.0 and are not discussed here.

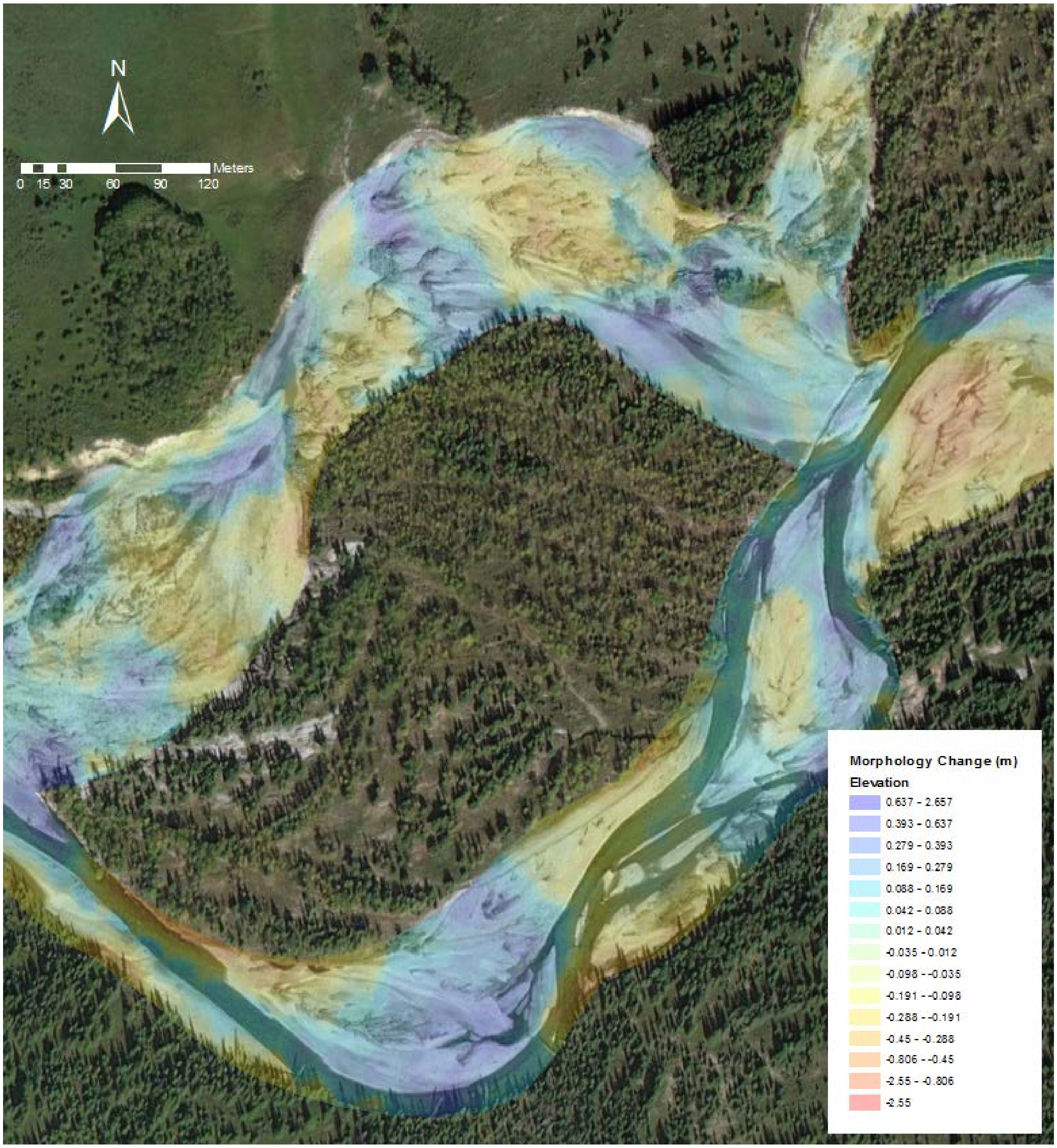

Figure 3-32 Example Aggradation and Degradation Changes in Elbow River

4.0 REFERENCES

Alberta Environment (AENV). 2006. Guidelines for quality assurance and quality control in surface water quality programs in Alberta. Environmental Monitoring and Evaluation Branch. Edmonton, Alberta.

AESRD (Alberta Environment and Sustainable Resource Development). 2012. Alberta Canadian Wetland Classification System (CWCS) Merged Wetland Inventory. Available online at: http://www.envinfo.gov.ab.ca/arcgis/services/wms/Water/MapServer/WMSServer.

AESRD. 2013. Evaporation and Evapotranspiration in Alberta 1912-2009. 282 pp.

Alberta Boreal Monitoring Institute (ABMI). 2012. Human Footprint (2012). Alberta Boreal Monitoring Institute. Edmonton, Alberta.

Alberta Boreal Monitoring Institute (ABMI). 2010. Wall-to-Wall Landcover (2010). Alberta Boreal Monitoring Institute. Edmonton, Alberta.

Alberta Government. 2013. Evaporation and Evapotranspiration in Alberta. Government of Alberta.

AMEC. 2014. Frequency analysis procedures for stormwater design manual. City of Calgary, Calgary, Alberta.

Andrews, E.D. 1980. Effective and bankfull discharges of streams in the Yampa River basin, Colorado and Wyoming. Journal of Hydrology 46: 311-330.

Araujo, H.A., A.B. Cooper, M.A. Hassan, and J. Venditti. 2012. Estimating suspended sediment concentrations in areas with limited hydrological data using a mixed-effects model. Hydrological Processes 26: 3678-3688.

Ashmore, P.E., and T.J. Day. 1988a. Spatial and temporal patterns of suspended-sediment yield in the Saskatchewan River basin. Canadian Journal of Earth Sciences 25: 1450-1463.

Ashmore, P., and T.J. Day. 1988b. Effective discharge for suspended sediment transport in streams of the Saskatchewan River Basin. Water Resources Research 24: 864-870.

Asselman, N.E.M. 2000. Fitting and interpretation of sediment rating curves. Journal of Hydrology 234: 228-248.

BC MoE (British Columbia Ministry of Environment). 2009. Manual of British Columbia Hydrometric Standards. Resources Information Standards Committee Report: 204 pp.

Beel, C.R., J.F. Orwin, and P.G. Holland. 2011. Controls on slope-to-channel fine sediment connectivity in a largely ice-free valley, Hoophorn Stream, Southern Alps, New Zealand. Earth Surface Processes and Landforms 36: 981-994.

Beers, C., and A. Sosiak. 1993. Water quality of the Elbow River. Environmental Quality Monitoring Branch, Environmental Assessment Division, Alberta Environmental Protection W92-04: 148 pp.

Benda, L., M.A. Hassan, M. Church, and C.L. May. 2005. Geomorphology of steepland headwaters: the transition from hillslopes to channels. Journal of the American Water Resources Association 41: 835-851.

Benjankar, R., D. Tonina, and J. McKean. 2015. One-dimensional and two-dimensional hydrodynamic modeling derived flow properties: impacts on aquatic habitat quality predictions. Earth Surface Processes and Landforms 40: 340-356.

Bunte, K, and SR. Abt. 2001. Sampling Surface and Subsurface Particle-size Distributions in Wadable Gravel- and Cobble-bed Streams for Analysis in Sediment Transport, Hydraulics, and Streambed Moni-toring, RMRS-GTR-74. US Department of Agriculture, Forest Service, Rocky Mountain Research Station: Fort Collins, CO.

Bunte, K., S.R. Abt, K.W. Swingle, and D.A. Cenderelli. 2014. Effective discharge in Rocky Mountain headwater streams. Journal of Hydrology 519: 2136-2147.

Buttle, J. 2006. Mapping first-order controls on streamflow from drainage basins: the T^3 template. Hydrological Processes 20: 3415-3422.

Caissie, D. and S. Robichaud. 2009. Towards a better understanding of the natural flow regimes and streamflow characteristics of rivers of the Maritime Provinces. Canadian Technical Report of Fisheries and Aquatic Sciences 2843: 53p.

Carling, P.A., and N.A. Reader. 1982. Structure, composition and bulk properties of upland stream gravels. Earth Surface Processes and Landforms 7: 349-365.

Church, M., and J.M. Ryder. 1972. Paraglacial sedimentation: a consideration of fluvial processes conditioned by glaciation. GSA Bulletin. 83(10): 3059-3072.

Church, M. 1974. Hydrology and permafrost with reference to Northern North America. Permafrost Hydrology. Proceedings of Workshop Seminar 1974. Canadian National Committee for the International Hydrological Decade, Ottawa Ontario. 7:7-20.

Church, M.A., D.G. Mclean, and J.F. Wolcott. 1987. River bed gravels: sampling and analysis. Gravel-bed Rivers. John Wiley and Sons, New York, New York.

Church, M., M.A. Hassan, J.F. Wolcott, 1998. Stabilizing self-organizing structures in gravel-bed stream channels: field and experimental observations. Erosion, Sedimentation, and Geomorphology. 34(11):3169-3179.

Church, M and JM. Ryder. 2010. Physiography of British Columbia in Pike, R.G., T.E. Redding, R.D. Moore, R.D. Winker and K.D. Bladon (editors). 2010. Compendium of forest hydrology and geomorphology in British Columbia. B.C. Min. For. Range, For. Sci. Prog., Victoria, B.C. and FORREX Forum for Research and Extension in Natural Resources, Kamloops, B.C. Land Manag. Handb. 66: 17-44.

Cohen, S.J., L.E. Welsh, and P.Y.T. Louie. 1989. Possible impacts of climate warming scenarios on water resources in the Saskatchewan River sub-basin. National Hydrology Research Centre, Saskatoon, Saskatchewan.

Costa, J.E. 1988. Rheologic, geomorphic, and sedimentologic differentiation of water floods, hyperconcentrated flows, and debris flows. In: Baker, V.R., Kochel, R.C., Patton, P.C. (Eds.) *Flood Geomorphology*. Wiley: 113-122.

Daly, C., M. Halbleib, J.I. Smith, W.P. Gibson, M.K. Doggett, G.H. Taylor, J. Curtis, and P.P. Pasteris. 2008. Photographically sensitive mapping of climatological temperature and precipitation across the conterminous United States. International Journal of Climatology. 28(15):2031-2064.

Detert, M., and V. Weitbrecht. 2012. Automatic object detection to analyze the geometry of gravel grains – a free stand alone tool. IN. Munos, R.M. (ed), River Flows 2012, Taylor and Francis, London. p 595-600.

Detert, M., and V. Weitbrecht. 2013. User guide to gravelometric image analysis by BASEGRAIN. In, Fukuoka et al. (eds.). Advances in River Sediment Research. Taylor and Francis, London. p 1789-1796.

Devito K, I. Creed, T. Gan, C. Mendoza, R. Petrone, U. Silins, and B. Smerdon. 2005. A framework for broad-scale classification of hydrologic response units on the Boreal Plain: is topography the last thing to consider? Hydrological Processes 19: 1705-1714.

DHI. 2005. MIKE 21, Inland, Coastal Waters and Seas in 2D. Danish Hydraulic Institute.

DHI. 2007. MIKE 21 ST, Non-cohesive sediment transport module: user guide. Danish Hydraulic Institute. 56 pp.

Dietrich, W.E., J.W. Kirchner, H. Ikeda, and F. Iseya. 1989. Sediment supply and the development of the coarse surface layer in gravel-bedload rivers. Nature 340: 215-217.

Downing, J.P. 1991. Instruction manual: OBS-1 and 3 suspended solids and turbidity monitor. D&A Instrument. Washington State, USA.

Duvert C., N. Gratiot, O. Evrard, O. Navratil, J. Némery, C. Prat, and M. Esteves. 2010. Drivers of erosion and suspended sediment transport in three headwater catchments of the Mexican Central Highlands. Geomorphology 123: 243–256.

FAO (Food and Agriculture Organization of the United Nations). 1998. Crop evapotranspiration - Guidelines for computing crop water requirements - FAO Irrigation and drainage paper 56.

Faustini, J.M., and J.A. Jones. 2003. Influence of large woody debris on channel morphology and dynamics in steep, boulder-rich mountain streams, western Cascades, Oregon. Geomorphology 51: 187-205.

Fehr, R. 1987. Simple detection of grain size distribution of sediment material using line-count analysis. Schweizer Ingenieur und Architekt 105. 1104-1109 (in German).

Ferguson, RI. 1986. River loads underestimated by rating curves. Water Resources Research 22: 74-76.

Ferguson RI. 1987. Accuracy and precision of methods for estimating river loads. Earth Surface Processes and Landforms 12:95–104.

Flesch, T.K., and G.W. Reuter. WRF model simulation of two Alberta flooding events and the impact of topography. Journal of Hydrometerology. 13(2):695-708.

Glysson, D.G. 1987. Sediment-transport curves. U.S. Geological Survey. Reston, Virginia.

Gomez, B., and M. Church. 1989. An assessment of bed load sediment transport formulae for gravel bed rivers. Water Resources Research 25: 1161-1186.

Graham, D.J.; S.P. Rice, and I. Reid. 2005. A transferable method for the automated grain sizing of river gravels. Water Resources Research 41: W07020.

Graham, D.J., A.J. Rollet, H. Piégay, and S.P. Rice. 2010. Maximizing the accuracy of image-based surface sediment sampling techniques. Water Resources Research 46: W02508.

Grasby, S.E., I. Hutcheon, and L. McFarland. 1999. Surface-water-groundwater interaction and the influence of ion exchange reactions on river chemistry. Geology 27: 223-226.

Gray, J.R., and F.J.M. Simões. 2008. Estimating sediment discharge: Appendix D. Sedimentatoin engineering: processes, measurements, modeling, and practice. American Society of Civil Engineers. Park Ridge, Illinois.

Guo, S.L. 1990. A discussion on unbiased plotting positions for the general extreme value distribution. Journal of Hydrology. 121(1-4):33-44.

Gurnell, A.M. 1987. Suspended sediment. In Glacio-fluvial Sediment Transfer – an Alpine Perspective, Gurnell, A.M., Clark, M.J. (eds). Wiley, Chichester: 305-354.

Gurnell, A.M., and J. Warbuton. 1990. The significance of suspended sediment pulses for estimating suspended sediment load an identifying suspended sediment sources in alpine glacier basins. International Association of Hydrological Sciences Publication 193: 563-470.

Hamann, A., T. Wang, D.L. Spittlehouse, and T.Q. Murdock. 2013. A comprehensive, high-resolution database of historical and projected climate surfaces for Western North America. Bulletin of the American Meteorological Society 94: 1307-1309.

Hollingshead, A.B. 1971. Sediment transport measurements in gravel river. Journal of Hydraulics Division, ASCE 97, HY11: 1817-1834.

Hudson, H.R. 1983. Hydrology and sediment transport in the Elbow River basin, SW Alberta. Unpublished PhD Thesis, The University of Alberta. 344 pp.

Hudson, J.A. 1988. The contribution of soil moisture storage to the water balances of upland forested and grassland catchments. Hydrological Sciences Journal. 33(3):2150-3435.

Jackson, L.E., Jr. 1980. Glacial history and stratigraphy of the Alberta portion of the Kananaskis Lakes map area. Canadian Journal of Earth Sciences 17: 459-477.

Jackson, L.E., G.M. MacDonald, and M.C. Wilson. 1982. Paraglacial origin for terraced river sediments in Bow Valley, Alberta. Canadian Journal of Earth Sciences 19: 2219-2231.

Jensco, K.G. and B.L. McGlynn. 2011. Hierarchial controls on runoff generation: Topographically driven hydrologic connectivity, geology and vegetation. Water Resources Research 47, W11527.

Kellerhals, R., and D.I. Bray. 1971. Sampling procedures for coarse fluvial sediments. Journal of the Hydraulics Division, ASCE 97: 1165-1180.

Kellerhals, R. C.R. Neill, D.L. Bray. 1972. Hydraulic and geomorphic characteristics of rivers in Alberta. Research Council of Alberta, River Engineering and Surface Hydrology Report. Edmonton, Alberta.

Klohn Crippen Berger. 2016. Calgary Rivers Morphology and Fish Habitat Study: Gravel Bed Sediment Sampling Program. Draft Report A03311B01 issued September 2016 to City of Calgary: 93 pp.

Knighton, D. 1998. Fluvial forms and processes. A new perspective. Arnold, London. 383 pp.

Lawler, D.M., G.E. Petts, I.D.L. Foster, and S. Harper. 2006. Turbidity dynamics during spring storm events in an urban headwater river system: the Upper Tame, West Midlands, UK. Science of the Total Environment 360: 109–126.

Maidment, D.R. 1993. Handbook of Hydrology. McGraw Hill.

Martin, Y. 2003. Evaluation of bed load transport formulae using field evidence from the Vedder River, British Columbia. Geomorphology. 53(1-2):75-95

McDonald D.M., and S.F. Lamoureux. 2009. Hydroclimatic and channel snowpack controls over suspended sediment and grain size transport in a High Arctic catchment. Earth Surface Processes and Landforms 34: 424–436.

McPherson, H.J. 1975. Sediment yields from intermediate-sized stream basins in Southern Alberta. Journal of Hydrology 25: 243-257.

Mehta, A.j., Hayter, E.J., Parker, W.R., Krone, R.B. and Teeter, A.M., 1989. Cohesive Sediment Transport. I: Process Description. Journal of Hydraulic Engineering – ASCE 115 (8), 1076 – 1093.

Meyer-Peter, E., and R. Müller. 1948. Formulas for bed-load transport. Proceedings of the 2nd Meeting, International Association for Hydraulic Structures Research, Stockholm, Sweden, Appendix, 2, pp 39–64.

Minella JPG, Merten GH, Reichert JM, Clarke RT. 2008. Estimating suspended sediment concentrations from turbidity measurements and the calibration problem. Hydrological Processes 22: 1819–1830

Moran, S. 1986. Surficial geology of the Calgary urban area. Alberta Research Council, ARC/AGS Bulletin 53: 57 pp.

Morianou, G.G., N.N. Kourgialas, and G.P. Karatzas. 2016. Comparison between curvilinear and rectilinear grid based hydraulic models for river flow simulation. Prcodeia Engineering 162: 568-575.

Navratil, O., C. Legout, D. Gateuille, M. Esteves, and F. Liebault. 2010. Assessment of intermediate fine sediment storage in a braided river reach (southern French Prealps). Hydrological Processes 24:1318–1332.

Oerung, C., S. Sauvage, and J-M. Sánchez-Pérez. 2010. Dynamics of suspended sediment transport and yield in a large agricultural catchment, southwest France. Earth Surface Processes and Landforms 35: 1289–1301.

Orwin, J.F., and C.C. Smart. 2005. An inexpensive turbidimeter for monitoring suspended sediment. Geomorphology 68: 3-15.

Orwin. J.F., S.F. Lamoureux, J. Warburton, and A. Beylich. 2010. A framework for characterizing fluvial sediment fluxes from source to sink in cold environments. Geografiska Annaler 92A: 155-176.

Orwin, J.F., and H. de Pennart. 2013. Guide for determining hydrometric, climate and water quality monitoring standards for oil and gas operators. Canadian Association of Petroleum Producers: 74 p.

Osborn, G., G. Stockmal, and R. Haspel. 2006. Emergence of the Canadian Rockies and adjacent plains: A comparison of physiography between end-of-Laramide time and the present day. Geomorphology 75: 450-477.

Papanicolaou, A.N., M. Elhakeem, G. Krallis, S. Prakash, J. Edinger. 2008. Sediment transport modeling review – current and future developments. Journal of Hydraulic Engineering 134:1-14.

Parker, G., P.C. Klingeman, and D.G. McLean. 1982. Journal of the Hydraulics Division. Journal of the Hydraulics Division. 108(4):544-571.

Pierson, T.C. 2005. Hyperconcentrated flow – transitional process between water flow and debris flow. In: Jakob, M., Hungr, O. (eds.) *Debris-flow Hazards and Related Phenomena.* Springer: 159-202.

Pomeroy, J.W., X. Fang, K. Shook, and P.H. Whitfield. 2013. Predicting in ungauged basins using physical principles obtained using the deductive inductive, and abductive reasoning approach. Canadian Water Resources Association. Waterloo, Ontario.

Pomeroy, J.W., R.E. Stewart, and P.H. Whitfield. 2015. The 2013 flood event in the South Saskatchewan and Elk River basins: causes, assessment and damages. Canadian Water Resources Journal. 14(1-2):1-13

Ryder, J.M. 1971. Some aspects of the morphometry of paraglacial alluvial fans in south-central British Columbia. Canadian Journal of Earth Sciences. 8(10):1252-1264.

Scott, K.M. 1988. Origins, behaviour, and sedimentology of lahars and lahar-runout flows in the Toutle-Cowlitz River System. US Geological Survey Professional Paper 1447A: 74 pp.

Searcy, J.K. 1959. Flow-duration curves. Manual of Hydrology: Part 2. Low-flow techniques. US Geological Survey Water-Supply Paper 1542-A. 38 pp.

Simões, F.J.M., and C.T. Yang. 2006 “Numerical Modeling for Rivers and Reservoirs,” Chapter 5 in Erosion and Sedimentation Manual (C.T. Yang, ed.), US Bureau of Reclamation, Technical Service Center, Denver, CO. 5-32 – 5-92.

Sosiak, A., and J. Dixon. 2006. Impacts on water quality in the upper Elbow River. Water Science and Technology 53: 309-316.

Stähly, S., H. Friedrich, and M. Detert. 2017. Size ration of fluvial grains’ intermediate axes assessed by image processing and square-hole sieving. Journal of Hydraulic Engineering. DOI: 10.1061.

Stantec (Stantec Consulting Ltd.). 2015a. Springbank Off-Stream Reservoir (SR1) – Conceptual Design Update. Memo, April 3, 2015. 23 pp.

Stantec. 2015b. Springbank Off-Stream Reservoir Project Hydrology Flood Frequency Analysis. Memo, Rev. 1.0, Dec 14, 2015. 55 pp.

Stantec. 2015c. Springbank Off-Stream Reservoir Project Probable Maximum Flood Analysis. Memo, Aug 7, 2015. 133 pp.

Strom, K.B., R.D. Kuhns, and H.L. Lucas. 2010. Comparison of automated photo grain sizing to standard pebble counts. Journal of Hydraulic Engineering 136: 461-473.

Vogel, R.M., and N.M. Fennessey. 1995. Flow Duration Curves II: A review of applications in water resources planning. Water Resources Bulletin 31: 1029-1039.

Walling, D.E., B.W. Webb, and J.C. Woodward. 1992. Some sampling considerations in the design of effective strategies for monitoring sediment-associated transport. Erosion and Sediment Transport Monitoring Programmes in River Basins (Proceedings of the Oslo Symposium, August 1992). IAHS Publ. no. 210: 279-288.

Wolman, M.G., and J.P. Miller. 1960. Magnitude and frequency of forces in geomorphic processes. Journal of Geology 68: 54-74.

Wang, T., A. Hamann, D.L. Spittlehouse, and S.N. Aitken. 2006. Development of scale-free climate data for western Canada for use in resource management. International Journal of Climatology, 26, 383–397.

Wang, T., A. Hamann, D. Spittlehouse, and T. Murdock. 2012. ClimateWNA-high-resolution spatial climate data for western North America; Journal of Applied Meteorology and Climatology, 51: 16-29.

Warrick, J.A. 2015. Trend analyses with river sediment rating curves. Hydrological Processes 29: 936-949.

Watt W.E., K.W. Lathem, C.R. Neill, T.L. Richards, and J. Rousselle. 1989. Hydrology of floods in Canada —a guide to planning and design. National Research Council of Canada, Ottawa, 245 pp.

Wentworth, C.K. 1922. A Scale of Grade and Class Terms for Clastic Sediments. The Journal of Geology 30: 377-392.

Wilcock, W.S.D. 2004. Physical response of mid-ocean ridge hydrothermal systems to local earthquakes. 5(11):1-26.

Wohl, E. 2017. Bridging the gaps: An overview of wood across time and space in diverse rivers. Geomorpholgy 279: 3-26.

Wolman, G.M. 1954. A method of sampling coarse river-bed material. American Geophysical Union. 35(6):951-956.